THE EFFECT OF FEEDING CONDITIONS ON THE DROP SIZE OF PICKERING EMULSIONS IN UNBAFFLED STIRRED TANKS

A THESIS SUBMITTED TO
THE GRADUATE SCHOOL OF NATURAL AND APPLIED SCIENCES
OF
MIDDLE EAST TECHNICAL UNIVERSITY

BY

MELİHA YAĞMUR ÖZDEMİR

IN PARTIAL FULFILLMENT OF THE REQUIREMENTS
FOR
THE DEGREE OF MASTER OF SCIENCE
IN
CHEMICAL ENGINEERING

SEPTEMBER 2022

Approval of the thesis:

THE EFFECT OF FEEDING CONDITIONS ON THE DROP SIZE OF PICKERING EMULSIONS IN UNBAFFLED STIRRED TANKS

submitted by **Meliha Yağmur Özdemir** in partial fulfillment of the requirements for the degree of **Master of Science** i**n Chemical Engineering, Middle East Technical University** by,

Prof. Dr. Halil Kalıpçılar
Dean, Graduate School of **Natural and Applied Sciences** _____

Prof. Dr. Pınar Çalık
Head of the Department, **Chemical Engineering** _____

Assoc. Prof. İnci Ayrancı Tansık
Supervisor, **Chemical Engineering, METU** _____

Examining Committee Members:

Assoc. Prof. Zeynep Çulfaz Emecen
Chemical Engineering, METU _____

Assoc. Prof. İnci Ayrancı Tansık
Chemical Engineering, METU _____

Assoc. Prof. Harun Koku
Chemical Engineering, METU _____

Assoc. Prof. Berna Topuz
Chemical Engineering, Ankara University _____

Assist. Prof. Gökhan Çelik
Chemical Engineering, METU _____

Date: 09.09.2022

I hereby declare that all information in this document has been obtained and presented in accordance with academic rules and ethical conduct. I also declare that, as required by these rules and conduct, I have fully cited and referenced all material and results that are not original to this work.

Name Last name : Meliha Yağmur Özdemir

Signature :

ABSTRACT

THE EFFECT OF FEEDING CONDITIONS ON THE DROP SIZE OF PICKERING EMULSIONS IN UNBAFFLED STIRRED TANKS

Özdemir, Meliha Yağmur
Master of Science, Chemical Engineering
Supervisor: Assoc. Prof. İnci Ayrancı Tansık

September 2022, 128 pages

Emulsions are systems consisting of two immiscible liquids. These immiscible liquids are generally oil and water phases. Oil and water phases are called the dispersed and continuous phases, respectively. Emulsions can be classified as single and multiple emulsions. Oil-in-water (o/w) and water-in-oil (w/o) emulsions are the examples of single emulsions, and water-in-oil-in-water (w/o/w) and oil-in-water-in-oil (o/w/o) emulsions are examples of multiple emulsions. Emulsions are an example of immiscible liquid-liquid mixing. Emulsions are thermodynamically unstable and stabilizing agents are required to obtain stable emulsions. Emulsions stabilized by solid particles are known as Pickering emulsions. Pickering emulsions have advantages over surfactant-based emulsions which are stabilized by chemical surfactants.

In this thesis, the effect of feeding conditions of the dispersed phase on the drop size of Pickering emulsions produced in an unbaffled stirred tank was investigated. Silicone oil and distilled water were selected as the dispersed and continuous phases, respectively. Hydrophilic zinc-oxide solid particles were selected as the stabilizing agent. Zinc-oxide stabilized oil-in-water (o/w) Pickering emulsions were produced. A standard six-bladed Rushton turbine (RT) with a diameter of one-third of the tank

diameter (D=T/3) was used as the impeller. The impeller shaft was positioned at three locations which are at the center, e/T=0 and at two eccentricity ratios, e/T=0.1 and e/T=0.2. Eccentricity (e) is the distance between the impeller shaft and center of the tank, and T is tank diameter. The impeller tip speeds, all corresponding to the turbulent flow regime, were selected as 1.85, 2, 2.32 m/s. To determine the effect of feeding conditions of the dispersed phase on drop size of Pickering emulsions, two feeding conditions were tested: dispersed phase was fed either from the liquid surface within 5 seconds which is referred to as surface feeding, or into the impeller zone over 900 seconds which is referred to as impeller zone feeding. The drop size and drop size distribution analysis was done using dynamic light scattering.

In conclusion, the drop sizes and drop size distributions decreased as the impeller tip speed is increased for all positions of the impeller shaft. For both feeding conditions of the dispersed phase (surface feeding and impeller zone feeding), the smallest drop size was obtained at e/T=0.1 and at the highest impeller tip speed, 2.32 m/s. The feeding of the dispersed phase into the impeller zone was found to be more effective for obtaining smaller drop sizes. The impeller discharge stream-wall interactions and the presence of vortex and its connection with impeller blades were found to cause an increase in drop size by affecting the impeller flow pattern. When the feeding condition of the dispersed phase is changed from surface feeding to impeller zone feeding, a significant effect of varying feeding conditions of the dispersed phase on drop size was found at e/T=0.2 and at an impeller tip speed, 2 m/s. It was also found that a reduction in power consumption can be achieved by changing the emulsion production process while obtaining similar drop sizes.

Keywords: Pickering Emulsions, Unbaffled Stirred Tanks, Vortex Formation, Eccentricity Ratio, Feeding Conditions.

ÖZ

BESLEME KOŞULLARININ ENGELSİZ KARIŞTIRMALI TANKLARDA PİCKERİNG EMÜLSİYONLARININ DAMLA BOYUTU ÜZERİNE ETKİSİ

Özdemir, Meliha Yağmur
Yüksek Lisans, Kimya Mühendisliği
Tez Yöneticisi: Doç. Dr. İnci Ayrancı Tansık

Eylül 2022, 128 sayfa

Emülsiyonlar birbiri içinde karışmayan iki sıvıdan oluşan sistemlerdir. Bu birbirine karışmayan sıvılar genellikle yağ ve su fazlarıdır. Yağ ve su fazları sırasıyla dağılan ve sürekli fazlar olarak adlandırılırlar. Emülsiyonlar, tekli ve çoklu emülsiyonlar olarak sınıflandırılabilirler. Su içinde yağ (s/y) ve yağ içinde su (y/s) emülsiyonları tekli emülsiyonların örnekleridir ve su içinde yağ içinde su (s/y/s) ve yağ içinde su içinde yağ (y/s/y) emülsiyonları çoklu emülsiyonların örnekleridir. Emülsiyonlar, karışmayan sıvı-sıvı karıştırmanın bir örneğidir. Emülsiyonlar termodinamik olarak kararsızdır ve kararlı bir hale gelebilmeleri için stabilize edici ajan gereklidir. Katı partiküller tarafından stabilize edilen emülsiyonlara Pickering emülsiyonları denir. Pickering emülsiyonları, kimyasal yüzey aktif maddeler tarafından stabilize edilen yüzey aktif madde bazlı emülsiyonlara göre avantajlara sahiptir.

Bu tezde, dağılan faz besleme koşullarının engelsiz karıştırmalı tanklarda üretilen Pickering emülsiyonlarının damla boyutu üzerine etkisi araştırıldı. Silikon yağı ve saf su sırasıyla dağılan faz ve sürekli faz olarak seçildi. Hidrofilik çinko-oksit katı parçacıkları stabilize edici ajan olarak seçildi. Çinko-oksit katı parçacıkları ile stabilize edilmiş su içinde yağ Pickering emülsiyonları üretildi. Karıştırıcı olarak

tank çapının üçte biri çapında (D=T/3) standart 6 bıçaklı Rushton türbini (RT) kullanıldı. Karıştırıcı şaftı merkezde, e/T=0, ve merkez dışında, e/T=0.1 ve e/T=0.2, olmak üzere üç noktada konumlandırıldı. Merkez dışı şaft, karıştırıcı şaftı ile tankın merkezi arasındaki mesafedir ve T tank çapıdır. Türbülanslı akış rejimine karşılık gelen karıştırıcı uç hızları olarak 1.85, 2 ve 2.32 m/s seçildi. Dağılan fazın besleme koşullarının Pickering emülsiyonlarının damla boyutu üzerindeki etkisini belirlemek için, iki besleme koşulu test edildi: dağılan faz, yüzey beslemesi olarak adlandırılan sıvı yüzeyinden 5 saniye içerisinde veya karıştırıcı bölgesi beslemesi olarak adlandırılan karıştırıcıya yakın bölgeye 900 saniye içerisinde beslendi. Damla boyutu ve damla boyut dağılımı analizi dinamik ışık saçılımı kullanılarak yapıldı.

Sonuç olarak, karıştırıcı şaftının bütün konumları için, karıştırıcı uç hızı arttıkça damla boyutları ve damla boyutu dağılımları azalmıştır. Dağılan fazın her iki besleme koşulu için (sıvı yüzeyinden besleme ve karıştırıcı bölgesine besleme) en küçük damla boyutu e/T=0.1'de ve en yüksek karıştırıcı uç hızı olan 2.32 m/s'de elde edilmiştir. Dağılan fazın karıştırıcıya yakın bölgeye beslenmesi, daha küçük damla boyutu elde etmek için daha etkili bulunmuştur. Karıştırıcı çıkış akımı-tank duvarı etkileşimleri ve girdabın varlığı ve girdabın karıştırıcı kanatlarının ucu ile arasındaki etkileşiminin, karıştırıcı akış düzenini etkileyerek damla boyutunda artışa neden olduğu bulunmuştur. Dağılan fazın besleme koşulu sıvı yüzey beslemesinden karıştırıcı bölgesi beslemesine değiştirildiğinde, dağılan fazın değişen besleme koşullarının damla boyutu üzerindeki önemli etkisi e/T=0.2 ve 2 m/s karıştırıcı uç hızında bulundu. Ayrıca emülsiyon üretim prosesini değiştirerek benzer damla boyutlarına daha düşük güç tüketimlerinde ulaşılabileceği bulunmuştur.

Anahtar Kelimeler: Pickering Emülsiyonları, Engelsiz Karıştırmalı Tanklar, Vortex Oluşumu, Merkez Dışı Shaft, Besleme Koşulları.

To my one and only family,

ACKNOWLEDGMENTS

Most importantly, I would like to thank to my thesis advisor Assoc. Prof. İnci Ayrancı Tansık for the guidance and understanding showed me throughout my master's education which was carried out during the majority of the Covid-19 pandemic. I am also grateful for her patience, interest, advice and encouragement at every stage of my research.

I would like to thank to members of Multiphase Mixing Research Laboratory, Ahmet Fırat Taşkın for his support and friendship and Ezgi Altıntaş for helping in the process of adaptation to the laboratory. I would also like to thank to Özge Demirdoğan and Dila Dönmez for answering my questions about their theses. I would like to thank to Seçkin Sertaç Lallı and Ata Dönmez for their help about the pump flow rate control unit.

I would like to thank to Assoc. Prof. Emre Büküşoğlu and one of his laboratory members Ali Akman for their help in obtaining the microscopic image of the emulsion drops.

I would like to thank to Berkan Atman deeply for his endless support throughout my research. It was so nice to laugh with you and feel your support on this pleasant journey.

I would like to thank to my friends Zülal Çetin, Uğur Burak Yanık, Pelin Maden, Selin Ernam, Begüm Yılmaz and Öznur Kavak for being with me during my research.

Last but not the least, I would like to thank to my beloved family, my mother Songül Özdemir, my father Hüseyin Özdemir, and my sister Gözde Ertem, who encouraged me to take the first step towards my master's education and supported me both financially and morally throughout my research.

TABLE OF CONTENTS

LIST OF TABLES

TABLES

LIST OF FIGURES

FIGURES

LIST OF ABBREVIATIONS

ABBREVIATIONS

RT: Rushton Turbine

o/w: oil-in-water

w/o: water-in-oil

Re: Reynolds number

PWM: Pulse Width Modulation

RO: Reverse osmosis

UP: Ultra-pure

e/T: eccentricity ratio

sf: surface feeding

izf: impeller zone feeding

LIST OF SYMBOLS

Roman Letters

a_v: interfacial area per unit volume

A: impeller blade width (m)

c: volume concentration of the solid particles

C: impeller off-bottom clerance (m)

d: impeller disc diameter (m)

d_i: diameter of drops in size class i

d_n: number mean diameter (μm)

d_{32}: Sauter mean diameter (μm)

d_{43}: De Brouckere mean diameter (μm)

d_{v50}: average particle diameter (μm)

d_{v90} - d_{v10}: width of distribution (μm)

D: impeller diameter (m)

e: eccentricity (m)

H: liquid height (m)

m: number of size classes

m_p: mass of the solid particles (kg)

m_w: mass of the water (kg)

n_i: number of drops

N: impeller speed (rps)

N_p: power number of the impeller

P: power consumption (W)

r: particle radius (m)

R: tank radius (m)

S: sampling points

t_{circ}: circulation time

t_m: mixing time

T: tank diameter (m)

V_{tip}: impeller tip speed (m/s)

V_L: volume of the liquid (m^3)

W: impeller blade height (m)

W_c: current weight of silicone oil (g)

$W_{desorption}$: work required to remove a spherical solid particles from oil-water interface

W_i: initial weight of oil (g)

W_p: pumped weight of silicone oil (g)

W_{ref}: instantenous weight of oil (g)

W_t: target weight of oil (g)

Greek Letters

γ_{ow}: interfacial tension between oil phase and water phase (N/m)

γ_{ws}: interfacial tension between water phase and solid particles (N/m)

γ_{os}: interfacial tension between oil phase and solid particles (N/m)

θ_{ow}: contact angle between oil and water phases

Φ: volume fraction of the dispersed phase

ρ: density of the emulsion (kg/m^3)

ρ_c: density of the continuous phase (kg/m^3)

ρ_w: density of the water (kg/m^3)

ρ_p: density of the solid particle (kg/m^3)

μ_r: relative viscosity of the emulsion (cSt)

μ_s: viscosity of the emulsion (cSt)

μ_c: viscosity of the continuous phase (cSt)

CHAPTER 1

INTRODUCTION

Mixing is one of the most used unit operations in process production industries such as food, cosmetic, pharmaceutical, petroleum, defense, and paper. Mixing is the interaction of two or more components with each other by an energy given into the system. It aims to provide a certain degree of uniformity throughout non-reactive systems and to optimize the process conditions to reach the desired product yield in reactive systems. The main mixing design topics are homogeneous blending in tanks and in in-line mixers, dispersion of gases in liquids with subsequent mass transfer, suspension and distribution of solids in liquids, immiscible or miscible liquid-liquid mixing, heat transfer, and reactions: both homogeneous and heterogeneous (Paul et al., 2004). This thesis focuses on immiscible liquid-liquid mixing, or more specifically on the production of emulsions.

Emulsions are heterogeneous systems with a homogeneous appearance. They consist of two immiscible liquids in separate phases. These two immiscible liquids are generally oil and water phases. The oil phase is called the dispersed or drop phase, and the water phase is called the continuous phase. When the oil phase is dispersed in the water phase, oil-in-water (o/w) emulsions form. On the contrary, when the water phase is dispersed in the oil phase, water-in-oil (w/o) emulsions form. Emulsions may also contain other solids and liquids. When the two immiscible liquids are stirred in a beaker over a certain time, drop formation can be observed. After the stirring process is stopped, the drops come together, forming larger volumes. The liquids, then, return to their initial separate phases. This indicates that the emulsion drops are not stable. To prevent these phases separating from each other and to produce stable emulsion drops, a stabilizing agent is required. Most

commonly, chemical surfactants are used as the stabilizing agents. These emulsions are known as surfactant-based emulsions. Solid particles can also be used as the stabilizing agents. These types of emulsions are called Pickering emulsions. Briefly, stabilization process takes place with the adsorption of stabilizing agents onto the formed oil-water interfaces. The solid particles are adsorbed at the oil-water interface irreversibly. This irreversible adsorption makes Pickering emulsions more stable than surfactant-based emulsions. Pickering emulsions pose some other advantages over the surfactant-based emulsions. Their preparation is easy, and they give less damage to the environment due to the possibility of using environmentally friendly particles. Due to these factors, Pickering emulsions are promising for more general use in production of emulsion-based products.

There are two key points that should be considered for producing Pickering emulsions: first one is the selection of the dispersed and continuous phases and solid particles to be used, second one is the selection of the tank geometry and impeller to be used. The physicochemical properties of dispersed and continuous phases, and solid particles and the hydrodynamics of the tank and the flow pattern of the impeller used directly affect the emulsion drop size and drop size distribution and therefore, emulsion stability.

To stabilize Pickering emulsions various solid particles can be used such as chitosan, zinc-oxide, silica, glass beads, etc. The affinity of solid particles, which determines how well the solid particles are adsorbed at the formed oil-water interfaces, is an important parameter since the higher the affinity of the solid particle used to produce the Pickering emulsion, the easier to obtain Pickering emulsion drops. As a dispersed phase, toluene, corn oil, paraffin oil, shea nut oil, silicone oil are some of the commonly used oils for producing emulsion drops. Distilled water is often preferred as continuous phase.

Emulsion production is usually accomplished in stirred tanks equipped with baffles. In unbaffled stirred tanks, as the impeller speed increases, a swirling motion around the impeller shaft occurs at the center which is called vortex formation. Vortex

formation in stirred tanks is a sign of poor mixing since it affects the flow pattern of the impeller unfavorably and weakens the radial circulations in the tank. Vortex formation creates a dominant flow in the center of the tank, preventing dispersion of the particles throughout the tank, resulting in agglomeration of the particles. The axial circulations also weaken due to the dominant flow in the center of the tank. Moreover, by increasing the impeller speed, the central vortex reaches the bottom of the impeller and air bubbles begin to enter the tank from the contact of the impeller blades with the air-liquid interface. As a result of all these problems, the efficiency of mixing decreases and thus, mixing results are affected. These negative impacts cause the baffled stirred tanks to be preferred over the unbaffled stirred tanks. There are, however, some applications for emulsion production where the presence of baffles is undesired, and the use of unbaffled stirred tanks is required. For example, in biological processes, cells can be damaged by hitting the baffles or they can stay in dead zones formed behind the baffles. For some other applications related to pharmaceutical fields, presence of baffles present difficulty in cleaning. For these cases, a common application to break the primary vortex in the center of an unbaffled tank is to position the impeller shaft away from the center of the tank.

Another key point in emulsion production is the selection of the impeller. Process requirements should be well known for selecting the impeller type. Impellers can be classified with regard to their shear levels, flow patterns and applications. Radial flow impellers are preferred for emulsion production. They are also known as high shear impellers. They perform very well in creating high shear and turbulence around the impeller. The dispersed phase can be broken down into smaller drops when it comes near the impeller. The more shear provided to the dispersed phase, the smaller the emulsion drops and thus, the higher the stability of the emulsion. In the production of Pickering emulsions, one other concern is the suspension of solid particles in the tank. The solid particles to be used in the production of Pickering emulsions should be suspended in the tank, considering that the stabilization process takes place every region of the tank. For the purpose of solids suspension, an axial or mixed flow impeller is often preferred. These types of impellers generate both

axial and radial circulations in the tank to provide the solid particles that settle on the bottom of the tank can be suspended. These impellers do not provide high shear; therefore, are not preferred for emulsion production. As the impeller speed is increased, the shear that is provided to the system increases; however, there are concerns related to power consumption and air entrainment. The impeller selection for Pickering emulsions production should be carefully made to accomplish both solids suspension and drop size reduction successfully and simultaneously.

In emulsion research, drop size and drop size distribution analysis is essential for product quality. The smaller the drop size and the narrower the drop size distribution, the more stable the emulsion. The smallest drop size and narrowest drop size distribution also mean increasing the shelf life of the product; in other words, the product quality increases. For this reason, decreasing the drop size and narrowing the drop size distribution are among the ultimate goals of emulsion production research. Until now, many studies have been carried out on the effects of the physicochemical properties of the materials used in Pickering emulsion production on drop size and emulsion stability. However, studies in terms of design perspective such as the effect of different processing parameters and tank hydrodynamics on drop size and emulsion stability are very few. In this thesis, the effect of feeding conditions in terms of feeding positions and feeding times of the dispersed phase on the production of Pickering emulsions in unbaffled stirred tanks was investigated. The physicochemical properties of the emulsion components were kept constant. In order to eliminate or minimize the vortex formation on the process results, the position of the impeller shaft was varied from center to two different eccentricity ratios.

The thesis is presented in five chapters. In Chapter 2, the literature related to Pickering emulsions and an immiscible liquid-liquid mixing are reviewed and the objective of the thesis is given. The work is done experimentally. The experimental setup, experimental procedure and the materials used are described in Chapter 3. In Chapter 4, the results of the experiments are given in detail and discussed. The results are laid out in four sub-sections. In the first sub-section, the effect of feeding

conditions on drop size of Pickering emulsions is investigated. The data in this sub-section is for all three positions of the impeller shaft. The results showed that varying the feeding condition of the dispersed phase can result in a decrease in drop size. The configuration for which a significant reduction in drop size is obtained is designated as the optimum configuration. This optimum configuration is selected for further analysis of the effect of feeding condition of the dispersed phase on drop size. In the second sub-section, the effect of increasing the feeding time of the dispersed phase is investigated. In the third sub-section, the effect of varying impeller speeds during the production process on drop size is investigated. In the last sub-section, different production processes and their effect on the final drop size are given in combination with power consumption analysis. Finally in Chapter 5, the conclusions are listed and possible future work in this area is expressed.

CHAPTER 2

LITERATURE REVIEW

2.1 Immiscible Liquid-Liquid Mixing

Immiscible liquid-liquid mixing aims to disperse one immiscible liquid into another, and thus, to increase the interfacial area between the two phases. This process results in an emulsion where drops of one immiscible liquid is dispersed in the other one. Immiscible liquid-liquid mixing finds applications in many industries. Some examples are petroleum, chemical, cosmetics, food, and mining industries. The most important parameters that affect the production process and the end result are mixing time, circulation time, power consumption and drop size distribution (DSD). These parameters are reviewed in the next sections.

2.1.1 Parameters that Affect Immiscible Liquid-Liquid Mixing

2.1.1.1 Mixing Time

Mixing time, t_m, is the time required to reach a certain level of uniformity throughout the tank. Mixing time is commonly measured by following the concentration of a tracer at fixed positions of the tank. Sodium chloride solution, rhodamine, acids, and bases can be shown as examples of tracers. The mixing time can also be found by measuring the temperature response of the system after a heated liquid is added to the system. Mixing time can be used as a tool for evaluating impeller efficiency (Montante et al., 2005, Doran, 1995). Mixing time is strongly affected by the following factors in stirred tanks: impeller and tank diameter, impeller eccentricity,

baffles, and liquid properties. An equation has been developed for predicting the mixing time in stirred tanks under turbulent flow regime by Nienow (1997):

$$t_m = 5.9\, T^{\frac{2}{3}} \left(\frac{\rho\, V_L}{P}\right)^{\frac{1}{3}} \left(\frac{T}{D}\right)^{\frac{1}{3}} \tag{2.1}$$

Here T and D are the tank and impeller diameter (m), respectively, ρ is the density of the liquid (kg/m^3), P is the power consumption of the impeller (W) and V_L is the volume of the liquid (m^3). Equation 2.1 is only valid for baffled stirred tanks with a single impeller and liquid height equals to tank diameter (Doran, 1995). According to Doran (1995), the volume of the liquid, V_L, can be expressed for a cylindrical tank as follows:

$$V_L = \frac{\pi}{4} T^3 \tag{2.2}$$

Power consumption, P, can be calculated using the following equation:

$$P = N_p\, \rho\, N^3 D^5 \tag{2.3}$$

Here N_p is the dimensionless power number of the impeller and N is the impeller speed. When Equations 2.2 and 2.3 are substituted into Equation 2.1, mixing time can be expressed as the following:

$$t_m = \frac{5.4}{N} \left(\frac{1}{N_p}\right)^{\frac{1}{3}} \left(\frac{T}{D}\right)^2 \tag{2.4}$$

According to Equation 2.4, when impeller speed, N, is increased, mixing time decreases. When the power number of the impeller is increased, mixing time again decreases. As the impeller speed, N, and tank diameter, T, were kept constant, increasing the impeller diameter, D, reduces the mixing time.

There are no terms related to the eccentricity of the impeller shaft in Equation 2.4 since it was originally developed for baffled tanks. Szopolik and Karcz (2008) studied the effect of eccentricity of the impeller shaft on mixing time. They obtained the lowest value of mixing time at the highest eccentricity ratio of the impeller shaft. This means that when the impeller shaft is positioned away from the center of the tank, mixing time decreases.

2.1.1.2 Circulation Time

Circulation time is the time that passes when the fluid leaving the impeller zone returns back to the impeller after travelling through the tank. It provides information about how quickly fluid moves all over the tank. In stirred tanks, the possibility of obtaining an efficient mixing result near the impeller is quite high since near the impeller turbulence, which is created by the movement of the impeller, has the maximum value and thus, the fluid is exposed to high shear. Turbulence, however, gradually decreases when the fluid moves away from the impeller toward the tank walls and top and bottom parts of the tank. This means that the turbulence, and thus shear distribution, is not uniform throughout the tank. The mixture reaches the desired degree of uniformity when the entire fluid passes through the impeller zone. This takes more time than one round of impeller discharge coming back to the impeller zone. For this reason, mixing time is greater than the circulation time. According to Nienow (1997), the mixing time is four times greater than the circulation time for single-phase liquid mixing in stirred tanks. This means that the mixture becomes uniform after four circulations.

2.1.1.3 Power Consumption

An impeller generates kinetic energy due to its rotational motion which is provided by the power of the motor. This kinetic energy is then distributed throughout the tank. Power consumption is an important parameter in the design of stirred tanks and it can be calculated by Equation 2.3 which is given in Section 2.1.1.1.

The power number of impellers, N_p, depends on the type of the impeller. Once the impeller power number is known, the impeller power consumption can be calculated. For example, impeller power numbers of Rushton turbine (RT) and Pitched blade turbine (PBT) are 5.0 and 1.3, respectively (Doran, 1995). Based on these impeller power numbers, RT gives more energy, and therefore gives more shear, to the system than PBT at the same impeller speed. Kumaresan et al. (2005) observed in their study that, in the presence of baffle clearance which is the distance between the bottom of the tank and bottom of the baffle, the increase in the number of baffles in the tank increased the power number. As can be seen in Equation 2.3, increasing the power number of the impeller, impeller speed and impeller diameter increases power consumption of the process.

2.1.1.4 Drop Size Distribution (DSD)

In liquid-liquid mixing, the control parameter representing the drop size distribution is called the Sauter mean diameter, d_{32}, (Zhou & Kresta, 1998, Lemenand et al., 2003). The Sauter mean diameter, d_{32}, is given as follows:

$$d_{32} = \frac{\sum_{i=1}^{i=m} n_i d_i^3}{\sum_{i=1}^{i=m} n_i d_i^2} \tag{2.5}$$

Here m is the number of size classes characterizing the DSD, n_i is the number of drops, and d_i is the diameter of drops in size class i. d_{32} is also known as surface area

moment mean diameter and commonly preferred representing the drop size and drop size distribution since it is directly related to the ϕ and a_v (Paul et al., 2004):

$$d_{32} = \frac{6\phi}{a_v} \tag{2.6}$$

Here ϕ is the volume fraction of the dispersed phase, a_v is the total interfacial area per unit volume of mixed phases.

The De Brouckere mean diameter, d_{43}, is the ratio of the fourth to third moments of the DSD which is another commonly used mean drop diameter. It is also known as volume moment mean diameter. The reason it reflects the volume-weighted average is that the drop mass is proportional to the cube of the diameter (Paul et al., 2004).

$$d_{43} = \frac{\sum_{i=1}^{i=m} n_i d_i^4}{\sum_{i=1}^{i=m} n_i d_i^3} \tag{2.7}$$

Generally, the number mean diameter is presented by (Paul et al., 2004);

$$d_n = \frac{\sum_{i=1}^{i=m} n_i d_i}{\sum_{i=1}^{i=m} n_i} \tag{2.8}$$

d_{10} is 10% by volume of all drops smaller than d_{10}, d_{50} is 50% by volume of all drops smaller than d_{50}, and d_{90} is 90% by volume of all drops smaller than d_{90} (Paul et al., 2004).

2.2 Pickering Emulsions

Emulsions consist of two immiscible liquids. When two immiscible liquids are mixed, one is dispersed in the other one in the form of drops, and it is called the dispersed phase. The other one is called the continuous phase. As one of the liquid phases is dispersed in the other one, the interfacial area between the two phases becomes larger. When mixing is stopped, the drops coalesce after some time. Eventually, dispersed and continuous phases are separated, indicating thermodynamic unstability of emulsions.

McClements (1999) discussed the emulsion formation by considering free energy analysis. The expression based on second law of thermodynamics is given below:

$$\Delta G_{emul} = \gamma_{ow} \Delta A - T\Delta S \tag{2.9}$$

Here ΔG_{emul}, ΔA, and ΔS indicate the change in free energy, interfacial area, and entropy of a system before and after the emulsification process, respectively, γ_{ow} indicates the interfacial tension between oil and water phases, and T indicates the temperature. If ΔG_{emul} is positive, then the emulsification process is unfavorable; therefore, phases tend to exist as two separate phases, whereas if ΔG_{emul} is negative, then the emulsification process is favorable; therefore, the phases tend to mix with each other (McClements, 1999). If $\Delta G_{emul} \approx 0$, then the phases are partly miscible and partly immiscible. When the dispersed and continuous phases are mixed with each other, the changes in both the interfacial area, ΔA, between the phases and the entropy of the system, ΔS, are positive. The change in the entropy of the system, ΔS, is always positive, indicating that $T\Delta S$, the term on the right side of Equation 2.9, continuously increases and thus, the free energy of emulsification process decreases (McClements, 1999). The schematic representation of analysis of the change in free energy and entropy during the emulsification process is given in Figure 2.1. According to Lopetinsky et al. (2006), in the absence of a stabilizing agent, which

may be solid particles or surfactants adsorbed at the oil-water interface, the increase in free energy change in the emulsification process is much greater than the increase in entropy change; therefore, the entropy change term can be neglected. Then, the change in free energy in the emulsification process becomes:

$$\Delta G_{emul} = \gamma_{ow} \Delta A \tag{2.10}$$

Considering the above information, ΔG_{emul} takes a positive value, indicating that the emulsions are thermodynamically unstable.

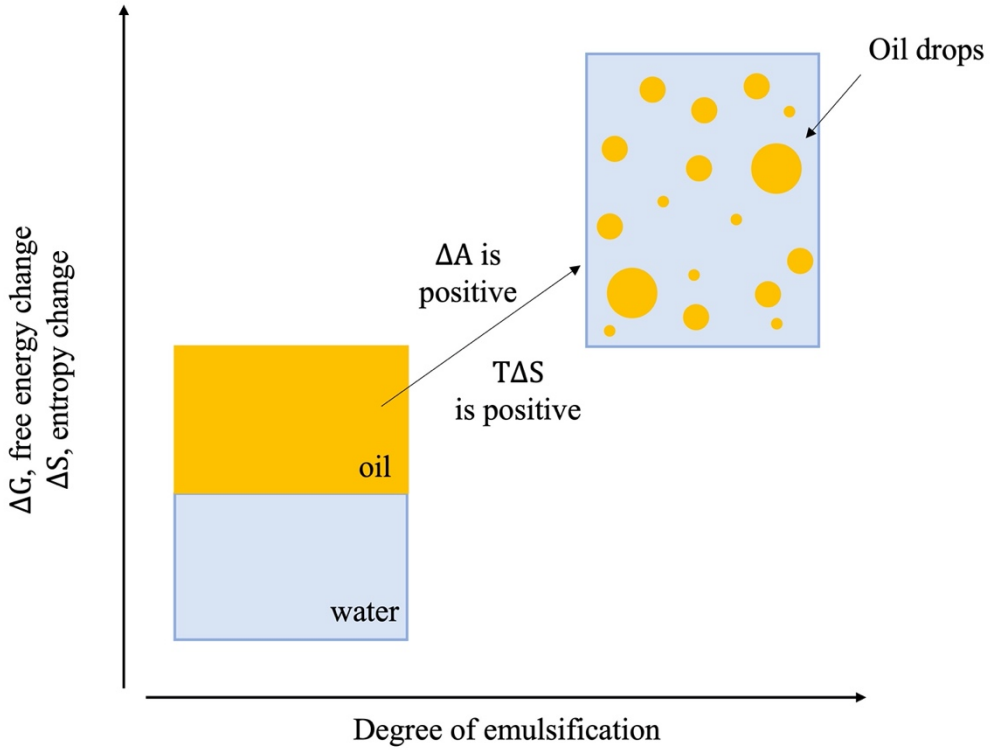

Figure 2.1. Schematic representation of analysis of change in free energy and entropy during the emulsification process

A stabilizing agent is needed to obtain a stable emulsion. Stabilizing agents can be chemical surfactants, or solid particles. While a large part of the research and current production methods employ chemical surfactants, solid particles pose great advantages for emulsion production. The first researcher in the literature to claim that solid particles could stabilize a water-in-oil emulsion was Ramsden in 1903. He, however, did not present any experimental studies on this topic. Later, Pickering reported that a stable emulsion was formed by the adsorption of solid particles on the surface of paraffin oil drops in 1907. Emulsions stabilized by solid particles are called as Pickering emulsions along with this research. The schematic representation of oil-in-water (o/w) and water-in-oil (w/o) Pickering emulsions are given in Figure 2.2. Performing the stabilization process with solid particles offers some advantages compared to surfactant-based emulsions (Yang et al., 2017). Solid particles keep the probability of drop coalescence minimum, ensuring higher stability of the emulsion. Food industry requires the use of no or low toxicity materials. For stabilization process in food industries, solid particles that have low toxicity can be used. Such particles are suitable to be used in in vivo studies which is a process performed in a living organism or they are suitable for applications of food packaging.

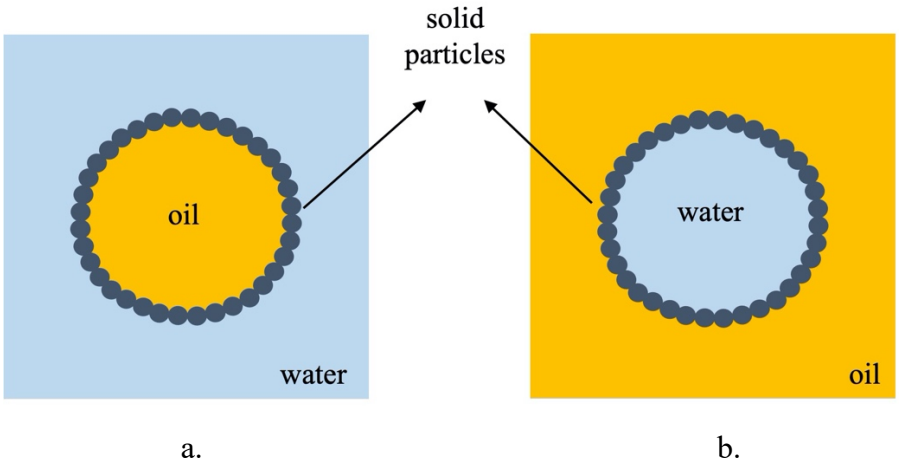

Figure 2.2. Schematic representation of Pickering emulsions: a. o/w and b. w/o

Pickering emulsions are well known in industry and in academic research, and there is an increasing interest in this type of emulsion due to its advantages. Food, petroleum, cosmetic and pharmaceutical industries can be shown among the common usage industrial areas of Pickering emulsions. Lopetinsky et al. (2006) stated that emulsions are divided into two groups according to their use in industry: desirable and undesirable. Food, skin moisturizers, and sun protector oils can be shown as examples of the desired emulsions. For this group of emulsions, long-term stabilization should be required. To provide the long-term stabilization, in emulsion production process, the chemical properties of the dispersed and continuous phases, the geometries of the tank and impeller and the tank hydrodynamics should be considered. On the other hand, emulsion stability is undesirable in the petroleum industry and often harms the oil recovery process, according to Menon & Wasan (1988). The aim for undesirable emulsions is not to enhance the conditions of emulsion production process to increase emulsion stabilization but to find out a way to separate the continuous and dispersed phases from each other. In this thesis, the produced emulsions belong to the desirable emulsion group. The production of stable Pickering emulsions in stirred tanks is targeted. For this reason, in the following sub-sections, first, emulsification mechanisms in a stirred tank, and then the factors affecting emulsion stability are reviewed.

2.3 Emulsification Mechanism in Stirred Tanks

In this section, the mechanisms that take place during emulsification and stabilization in a stirred tank are reviewed. To better understand the emulsification mechanism in stirred tanks, first stirred tank hydrodynamics is considered. In stirred tanks, the fluid movement inside the tank is provided by the movement of the impeller. There are three zones in the stirred tank in terms of emulsion production which are high shear zone, stabilization zone and coalescence zones. High shear zone and coalescence zones are directly associated with the energy dissipation rate. Energy dissipation rate is related to the amount of energy given into the tank, and it is not uniform throughout

the tank. It reaches the maximum value at the vicinity of the impeller. This region is called high shear zone. High shear zone covers the impeller blades and its discharge streams. The value of energy dissipation rate continuously decreases moving away from the high shear zone toward the tank walls and top and bottom parts of the tank. These regions are called coalescence zones. In stabilization zone, the solid particles are adsorbed at the oil-water interfaces generated. Stabilization process can take place every part of the tank.

The schematic representation of the emulsification mechanism is given in Figure 2.3. According to Tsabet & Fradette (2015a), the drops are first broken into smaller ones in the high shear zone since the desired high shear takes place in this zone. Then, the generated oil-water interfaces are stabilized by solid particles in the stabilization zone. But some of the oil-water interfaces may not be covered or they may be partially covered by solid particles. These uncovered and partially covered drops then go to the coalescence zone with the flow and coalesce there. These coalesced drops then come back to the high shear zone due to the flow cycle and are again broken into smaller drops. This flow cycle continues until all the oil-water interface generated is covered by solid particles, and thus drop sizes reach their equilibrium size.

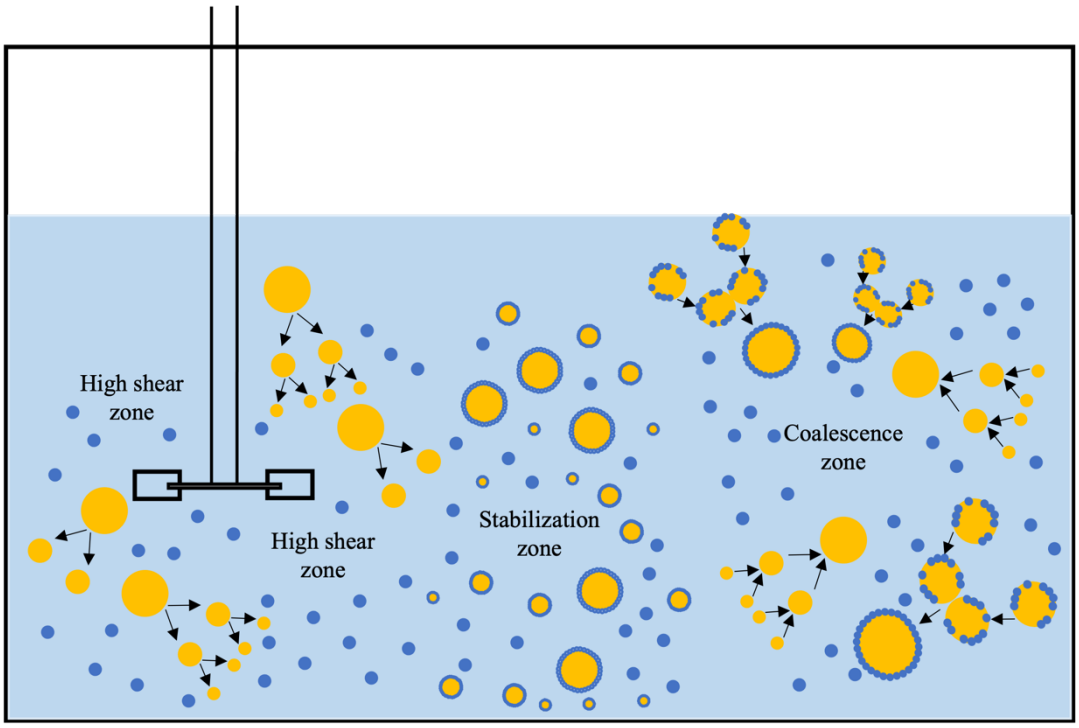

Figure 2.3. Schematic representation of emulsification mechanism for off-center Rushton Turbine (adapted from Tsabet & Fradette (2015c))

According to Tsabet & Fradette (2015c), equilibrium drop sizes are evaluated in two ways. The schematic representation of the controlling mechanisms of equilibrium drop size and drop size distribution is given in Figure 2.4. First, suppose there are enough solid particles to cover all the oil-water interfaces generated. In that case, the drop size depends on the capacity of the system to generate an oil-water interface. In other words, the drop size and drop size distribution are controlled by the oil-water interface generation capacity. In the second case, suppose there are not enough solid particles to cover all the oil-water interfaces generated, the drops which are uncovered and partially covered by solid particles coalesce until the coverage capacity of the system is maintained. The drop size and drop size distribution are controlled by the coverage potential of the system.

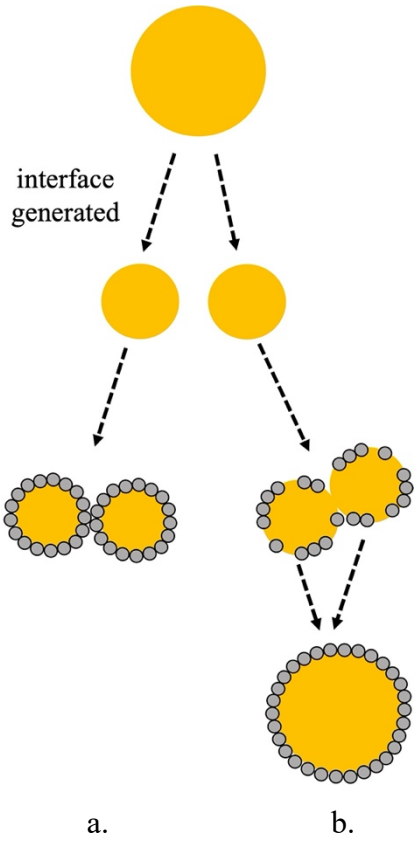

Figure 2.4. Schematic representation of controlling mechanisms of equilibrium drop size and drop size distribution: a. interface generation capacity and b. coverage potential (adopted from Tsabet & Fradette (2015c))

Determination of amount of solid particle to be used in emulsion production is one of the core parameters. Tsabet & Fradette (2015b) investigated the effect of the properties of solid particle on the production of Pickering emulsion. Their results showed that the coverage capacity of the system decreased along with increasing the amount of solid particle in the tank. Because adding more solid particles to the system means that some of the energy given into the system is used to increase the kinetic energy of these excess solid particles. The solid particle-drop collision force decreases, and thus the adsorption of solid particles at the generated oil-water interfaces decrease; therefore, both stabilization process and efficiency reduce.

2.4 Factors Affecting the Emulsion Stability

There are three different zones in the emulsification mechanism as seen in Figure 2.3: high shear zone, stabilization zone, and coalescence zones. The stabilization efficiency of the emulsion can be assessed by the balance between these zones, which depends on the particle attachment process. According to Menon & Wasan (1988), the stabilization of Pickering emulsions by solid particles takes place in three steps:

i. solid particles approaching the oil-water interface,
ii. adsorption of solid particles at the oil-water interface, and
iii. stabilization of the oil-water interface by forming particle networks.

Each of the steps of the solid stabilization process depends on the properties of the material used in the emulsion formation (Menon & Wasan, 1988). The first step requires information about the size and concentration of the solid particles and energy given into the system. The second step depends on the three-phase contact angle, size and concentration of the solid particles. The formation of particle networks at the interface depends on the magnitude of particle interactions, and this is related to the parameters in the first two steps. All significant parameters affecting the emulsion stabilization are explained in detail below. It is worth noting that the smaller the drop size and the narrowest the drop size distribution of the emulsion, the more stable the emulsion.

2.4.1 Particle Wettability

Wettability refers to the contact angle of solid particles, θ_{ow}, measured throughout the water phase. According to Chevalier & Bolzinger (2013), for the solid particles to adsorb strongly at the oil-water interface, the surface of the solid particles must be partially wetted by continuous or dispersed phases. Solid particles with a contact angle greater than 90° are called hydrophobic particles. Hydrophobic particles tend

to stay on the oil side of the generated oil-water interface; therefore, hydrophobic solid particles are used to stabilize w/o emulsions. On the other hand, particles with a contact angle less than 90° are called hydrophilic particles. Hydrophilic particles tend to stay on the water side of the generated oil-water interface; therefore, hydrophilic solid particles are used to stabilize o/w emulsions. In Figure 2.5, the schematic representation of the three-phase contact angle, the attachment of the spherical solid particles to the oil-water interface and the positioning of spherical solid particles in the oil-water interface are given. Three-phase contact angle indicates the region between the disperse phase, continuous phase and the solid particles. In Figure 2.5, γ_{ws}, γ_{os}, and γ_{ow} indicates that the interfacial tension between continuous phase and solid particle, dispersed phase and solid particle, and dispersed phase and continuous phase, respectively, and θ_{ow} indicates the contact angle between dispersed and continuous phases.

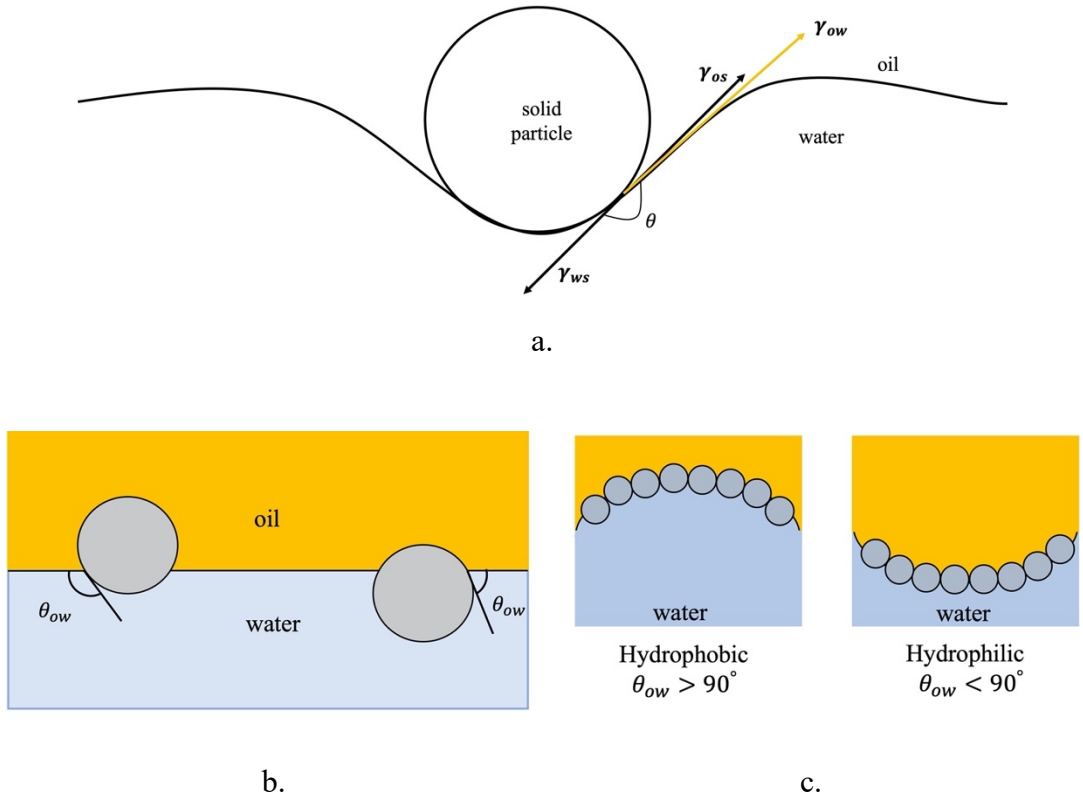

Figure 2.5. a. schematic representation of the three-phase contact angle, b. the attachment of the spherical solid particles to the oil-water interface and c. the positioning of spherical solid particles in the oil-water interface

Finkle et al. (1923) proposed that the type of emulsions obtained with a solid powder is determined by the contact angle of the oil-water interface with the solid particle. Schulman & Leja (1954) conducted a study on this theory of Finkle et al. (1923), and their results showed that good, stable, and self-forming emulsions were obtained when the contact angle of the solid particle is close to 90°.

Particle wettability also affects the energy required to desorb the solid particle that is adsorbed at the oil-water interface. The work required to remove a spherical solid particle from oil-water interface ($W_{desorption}$) is given in Equation 2.11 (Lopetinsky et al., 2006, Binks, 2002):

$$W_{desorption} = \pi r^2 \gamma_{ow} (1 + \cos\theta)^2 \quad (2.11)$$

Here r is the radius of the spherical particle. As seen in Equation 2.11 above, solid particles with a contact angle close to 90° have the highest adsorption energy to the oil-water interface, which minimizes the possibility of the solid particle desorption from the oil-water interface. In other words, a considerable amount of energy is required to desorb solid particles from the oil-water interface.

2.4.2 Particle Concentration

Solid particle concentration is another strong parameter affecting the emulsion stability. Arditty et al. (2003) stated that drop coalescence frequency is dependent on time and solid particle concentration in solids-stabilized systems. They observed that the drop size decreased as the amount of solid particles is increased in the system. This decrease, however, has a limit depending on the solid particle concentration. As the solid particle concentration increases, the system becomes saturated by the solid particles, all the oil-water interface that can be generated is covered by the solid particles and further decrease in the drop size cannot be observed.

Gelot et al. (1984) stated that the system should have enough solid particles to cover the generated oil-water interfaces. Suppose there are not enough solid particles in the system; an emulsion may be formed but not be stable due to the uncovered or partially covered drops. They also stated that if the system has more solid particles than the required amount for the stabilization process, emulsion stability is closely related to the concentration of solid particles adsorbed at the oil-water interface.

2.4.3 Oil type, Viscosity and Volume Fraction

The type and viscosity of the oil used in emulsion production and the ratio of dispersed phase to continuous phase are among the crucial factors affecting emulsion

stability. According to Aveyard et al. (2003), Binks & Lumsdon (2000), and Tsabet & Fradette (2015b), interfacial tension, the contact angle of solid particles, interactions between the surface of solid particles and the liquids, and the solid particle attachment to an oil-water interface are all affected by the type and viscosity of the oil used.

In the literature, there are many studies that investigated the effect of properties of the dispersed phase on the Pickering emulsion stabilization and emulsification processes. Tsabet & Fradette (2015b) studied the effect of the properties of oil on the production of Pickering emulsions. Their results showed that the smallest drop sizes and the narrowest drop size distribution were obtained with low oil viscosities. They also indicated that particle adsorption at the oil-water interfaces generated is slower at high oil viscosities, affecting the stabilization process. In addition to this study, A. El Hamouz et al. (2009) found that low oil viscosity reached equilibrium drop size faster than that of high oil viscosity. Chesters (1991) reported that increasing the oil viscosity prohibits the contact between oil drops and solid particles, and thus preventing the solid particle adsorbed at the oil-water interface.

2.4.4 Particle Size

According to Tambe & Sharma (1994), the size of the solid particles used in emulsion production controls the ability of the solid particles to stay at the oil-water interface and may be one of the most critical parameters influencing the effectivity of the solid particles for the stabilization of the emulsion. Binks & Lumsdon (2001) investigated the effect of particle size on emulsion stability, and their results showed that when the particle size is increased, the drop size of the emulsion increases. Thus, the emulsion stability reduces as the drop sizes increase.

2.4.5 Particle Shape

The particle shape to be used in emulsion production affects the emulsion drop size and stability. Li et al. (2018) produced the o/w Pickering emulsions using cellulose nanocrystals (CNCs) solid particles as stabilizing agent. They tested two different shapes of CNCs which are needle-like and ellipsoid shape. They stated that the emulsion drop sizes obtained using needle-like shape CNCs are about two times smaller than the emulsion drop sizes obtained using ellipsoid shape CNCs. Thus, more stable emulsions were obtained with needle-like CNCs.

Apart from this, the effect of particle shape on emulsion stability can also be interpreted through particle roughness. According to Lopetinsky et al. (2006), particle roughness can affect the contact angles of solid particles, and its effect on emulsion stability may occur in the same way as particle contact angle. Vignati et al. (2003) studied o/w emulsions stabilized using silica colloids with smooth or rough surfaces. They found that surface roughness significantly reduces the efficiency of particles in stabilizing the emulsion drops. Increasing the surface roughness of the solid particle reduces the contact between the particle and the oil-water interface. Therefore, the solid particles have difficulty adsorption to the oil-water interface, and thus less stable emulsions are obtained.

2.4.6 Destabilization Mechanisms

An emulsion is stable if it is resistant to physical changes for a specific time; that is, there is no significant change in the size distribution of drops. Emulsions can become unstable by four mechanisms occurring simultaneously or sequentially: creaming or sedimentation, flocculation, coalescence, and Ostwald ripening. These mechanisms showing the instability of an emulsion and their relations with each other are given in Figure 2.6.

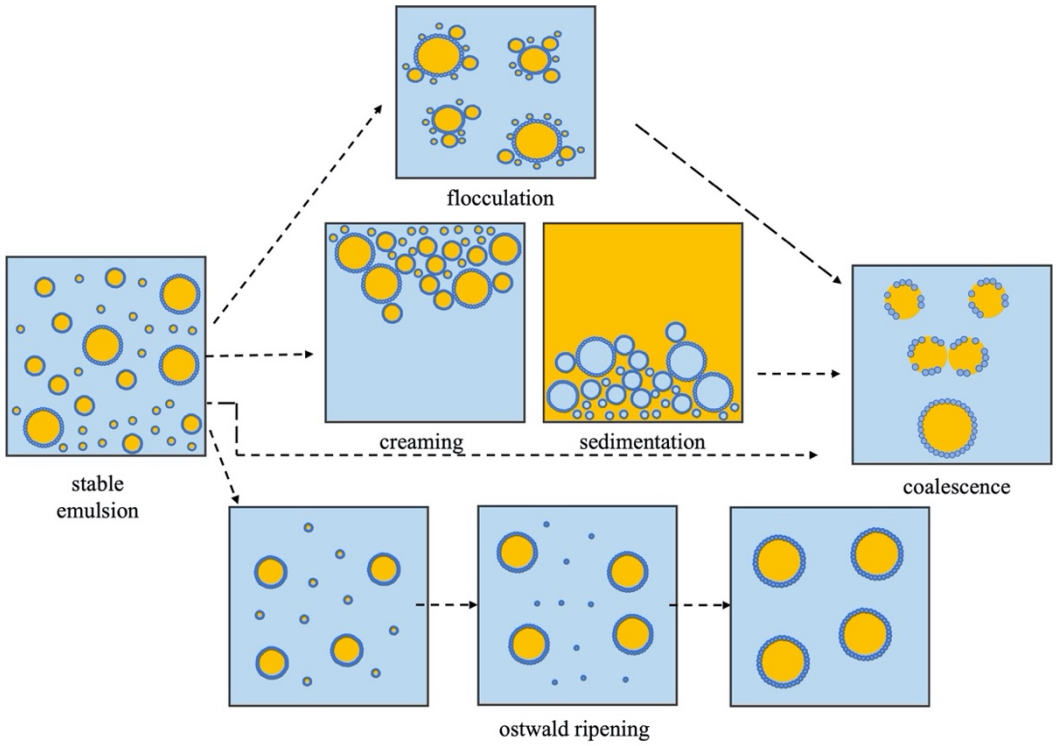

Figure 2.6. Schematic representation of the emulsion destabilization mechanisms and their relations with each other (adapted from Lopetinsky et al., 2006)

Creaming is the mechanism that indicates the instability of o/w emulsions. The movement of oil drops under gravity causes creaming. The oil drops form a layer on the top of the sample due to its lower density than the continuous phase. On the other hand, sedimentation is the equivalent destabilization mechanism for w/o emulsions. Creaming and sedimentation mechanisms do not result in a change in drop size and drop size distribution (Lopetinsky et al. (2006), Binks (1998)). The creaming and sedimentation mechanisms are reversible since an original homogeneous drop distribution can be achieved by gentle mixing (Binks, 1998).

Flocculation is a process that occurs when emulsion drops come together and form aggregates. The drop size and drop size distribution do not change during flocculation, as in creaming and sedimentation mechanisms. The flocculation

mechanism usually results in enhanced creaming since the aggregated drops are larger than the single drops, making them rise faster (Binks, 1998).

Coalescence is an irreversible process by which two or more drops form one or more larger drops. It occurs when the drops suspended in a moving liquid collide (Leng & Calabrese, 2004). According to Leng & Calabrese (2004), the collision of two drops does not always result in drop coalescence. An important parameter to observe drop coalescence is the critical film drainage time. The critical film drainage time is the time it takes for the continuous phase film to be thin enough to rupture. This continuous phase film forms between the dispersed phases, keeping the two drops apart when they come close to each other. This film must be ruptured for drop coalescence. Drop coalescence only occurs when the contact time of the drops with each other exceeds the critical film drainage time.

According to Binks (1998), Ostwald ripening mechanism occurs due to the solubility differences of dispersed phase contained within the drops of different sizes. Solubility means the dissolution of a certain amount of solute in a specific solvent. The mechanism is as the following: the soluble liquid contained in the small drops recondenses on the larger drops and diffuses into the dispersed phase through continuous phase. Thus, the size of the large drops increases as the size of the smaller drops decrease, and the interfacial area between dispersed and continuous phases decrease.

2.5 Production of Emulsions in Stirred Tanks

In this section, the studies related to emulsion production in stirred tanks in terms of a design perspective are reviewed.

Emulsion production is usually carried out in baffled stirred tanks. In unbaffled stirred tanks when the impeller speed increases, vortex formation takes place at the center of the tank. This vortex formation negatively affects the mixing results. Vortex formation is not observed in baffled stirred tanks due to the presence of baffles at the

tank walls, and thus good top-to-bottom mixing occurs. In baffled stirred tanks, however, dead zones may form behind the baffles and baffles cause difficulties in the cleaning of the tank in between batches. Due to these difficulties, in some cases the use of an unbaffled stirred tank is required. In unbaffled stirred tanks, Karcz & Szoplik (2004) and Hall et al. (2004) showed that in turbulent flow, impeller shaft eccentricity has the same effect as baffling. The distance between the center of the impeller shaft and the center of the tank is called eccentricity (e). Vortex formation can be prevented by positioning the impeller shaft eccentrically in unbaffled stirred tanks.

Demirdogan (2019) studied the effect of different hydrodynamic conditions on the production of o/w Pickering emulsions in an unbaffled stirred tank. She tested four hydrodynamic parameters: impeller tip speed ($V_{tip} = \pi ND$), impeller Reynolds number ($Re = \frac{\rho N D^2}{\mu}$), Weber number ($We = \frac{\rho_c N^2 D^3}{\sigma}$), and power per mass ratio ($\varepsilon = \frac{N^3 D^5 N_p}{V_{imp}}$). Impeller tip speed is the maximum speed in the tank that is obtained at the tip of the impeller blades. Impeller Reynolds number (Re) is the ratio of inertial forces to viscous forces. Weber number (We) is the ratio of inertial forces to surface forces. Power per mass ratio gives an information about the drop breakage when the energy is given in the system, and it is related to the energy dissipation rate. Demirdogan (2019) used three different types of impellers which are Rushton turbine (RT), down-pumping pitched blade turbine (PBTD), and up-pumping pitched blade turbine (PBTU) with two different sizes: T/2 and T/3. The impeller shaft was positioned at three locations: at the center, e/T=0, and at two eccentricity ratios, e/T=0.1 and e/T=0.2. She obtained the smallest drop size and the narrowest drop size distribution with the RT - T/3 at the eccentricity ratio of e/T=0.2.

Abdulrasaq & Ayranci (2019) investigated the effect of hydrodynamic parameters on the production of Pickering emulsions in baffled stirred tanks. For this purpose, they tested the same types and sizes of the impellers and hydrodynamic parameters as Demirdogan (2019). They found that RT - T/2 is the most effective impeller since

RT - T/2 produced smaller drop sizes in three of the four hydrodynamic parameters tested. Moreover, they also found that the energy dissipation at the impeller zone and the size of drop breakage zone are the controlling mechanisms of final emulsion drop size.

Controlling the feeding rate and feeding positions of the dispersed phase can affect the Pickering emulsion production in terms of drop size and drop size distribution. A. El Hamouz et al. (2009) produced o/w emulsions using chemical surfactants as the stabilizing agent. They tested the effect of adding the dispersed phase in the different zones of tank, which are from the liquid surface or into the impeller zone, on the drop size and drop size distribution. They obtained the smallest drop size and the narrowest drop size distribution when the dispersed phase is fed into the impeller zone. They also found that the drop breakage process was slow when the dispersed phase was fed from the liquid surface compared to into the impeller zone. In addition, they found that the tip speed is more effective in predicting the drop size than the mean energy dissipation rate.

Donmez & Ayranci (2020) investigated the effect of feeding time of the dispersed phase on drop size of Pickering emulsions produced in a baffled stirred tank. They tested three hydrodynamics parameters which are impeller tip speed, power per mass ratio and impeller Reynolds number. They tested three different types of impellers: RT, PBTU, and PBTD, with two different sizes, T/2 and T/3. The dispersed phase was fed into the tank in two ways: all at once from the liquid surface within 5 seconds using a graduated cylinder and into the impeller zone over 900 seconds using a pump. They stated that when the feeding conditions of the dispersed phase is changed from surface feeding to impeller zone feeding, initial breakage rate of the dispersed phase, and thus drop sizes can be controlled. They obtained a significant reduction in drop size by 24% using RT - T/3 at longer feed time of the dispersed phase, which is 3600 seconds and at lower impeller tip speed. They stated that impeller tip speed gave more predictable results in terms of drop size compared to other two hydrodynamic parameters tested. Their result also showed that the selection of the most effective

impeller in terms of drop size and power consumption is not straightforward for Pickering emulsion production.

2.6 Motivation of Thesis

Pickering emulsions and their applications have attracted significant attention due to their easy production, less environmental damage, and their capability of stabilization which is more effective than emulsions stabilized with chemical surfactants. In the literature, many studies investigated the effects of properties of dispersed and continuous phases and solid particle on the production of Pickering emulsions in terms of emulsion drop size and stability. However, there are not many studies investigating the effect of the tank and impeller geometries used for Pickering emulsion production and hydrodynamics on the drop size. The available studies show that the feeding conditions of the dispersed phase and the eccentricity ratio of the impeller shaft in an unbaffled tank can be critical in controlling the drop size and drop size distribution of the emulsion. In this thesis, the effect of varying feeding conditions of the dispersed phase on the drop size and drop size distribution of Pickering emulsions produced in unbaffled stirred tanks was studied. The physicochemical properties related to emulsion formulation such as the viscosity of the dispersed phase, solid particle-to-dispersed phase ratio, and dispersed phase volume-to-continuous phase volume ratio were kept constant. The effect of only hydrodynamics on drop size and drop size distribution was studied. The feeding of the dispersed phase was done either from the liquid surface within 5 seconds or into the impeller zone over 900 seconds. Based on the previous studies given in Section 2.5, RT - T/3 was selected as the impeller, and impeller tip speed (V_{tip}) was selected as the hydrodynamic parameter. Three impeller speeds, all corresponding to turbulent regime, were tested. The impeller shaft was positioned at the center of e/T=0 and at two eccentricity ratios, e/T=0.1 and e/T=0.2. The results not only showed an optimum configuration – eccentricity ratio of the impeller shaft, impeller tip speed and feeding position of the dispersed phase – to reach the smallest drop

sizes and the narrowest drop size distribution, but also showed how the shape and size of the vortex formed in unbaffled stirred tanks and eccentricity ratios of the impeller shaft affect the drop size, flow hydrodynamics in the tank and processes of drop breakage, coalescence, and stabilization during the emulsion production.

CHAPTER 3

EXPERIMENTAL PROCEDURE

3.1 Materials and Emulsion Formulation

3.1.1 Materials

The solid particle to be used in Pickering emulsion production is very important in terms of its effect on both emulsion formation and emulsion stabilization. According to Tsabet & Fradette (2015b), the smallest drop sizes and narrowest drop size distribution were obtained using small solid particles, low oil viscosity and good oil/particle affinity. Kołodziejczak-Radzimska & Jesionowski (2014) stated that zinc-oxide (ZnO) solid particles have numerous physical and chemical properties, such as very high chemical stability; in other words, ZnO solid particles have high affinity. Emulsion production is made easier by the high affinity of the solid particles. Therefore, to produce o/w Pickering emulsions, hydrophilic ZnO solid particles were used. The particle size analysis of the ZnO solid particles was done using Malvern Mastersizer 3000. The volumetric size distribution of ZnO solid particles is given in Figure 3.1. According to the volumetric size distribution, $d_{v50,}$ which is an average particle diameter, of ZnO particles, is 2.80 μm.

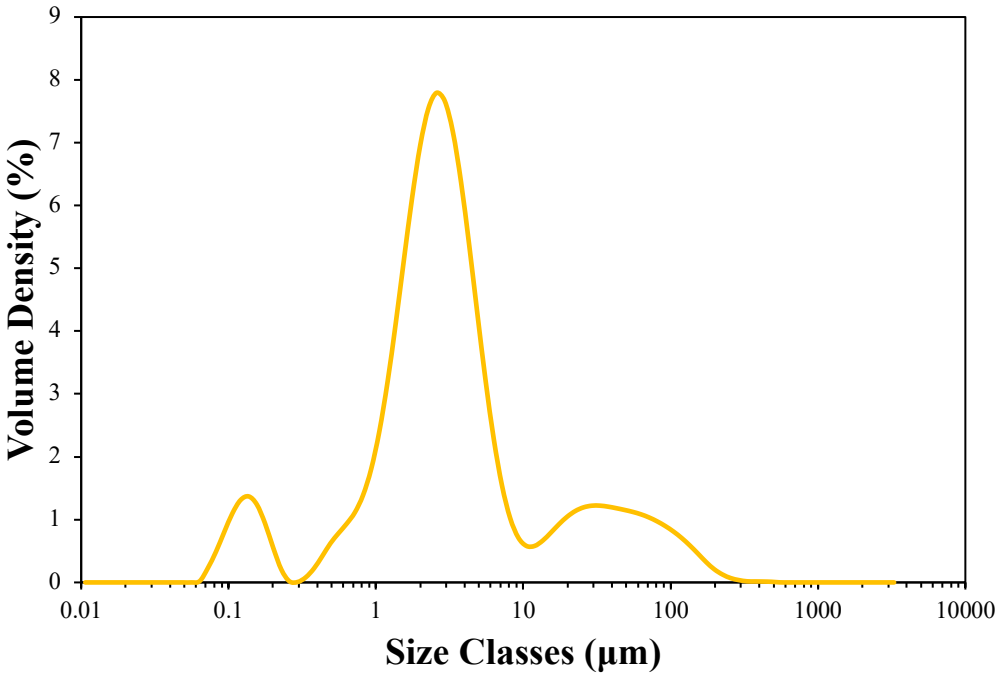

Figure 3.1. Volumetric size distribution of ZnO solid particles

100 cSt silicone oil (XIAMETER® PMX-200, Dow Corning) was used as the dispersed phase. The physical properties of the silicone oil are given in Table 3.1. The silicone oil-to-distilled water ratio was set as 43% (vol/vol) to investigate concentrated emulsions. In all experiments, 230 ml of silicone oil and 532 ml of distilled water were used.

Table 3.1 The physical properties of silicone oil

Appearance	Off – white solid
Density at 25℃	964 kg/m^3
Surface Tension at 25℃	0.0209 N/m

The solid particle-to-silicone oil ratio and the type of distilled water (reverse osmosis (RO) or ultra-pure (UP)) were determined based on some preliminary experiments.

Details of these preliminary experiments and the determined conditions for emulsion formulation are given in the following sub-sections.

3.1.2 Amount of Solid Particles

Varying solid particle-to-silicone oil ratios, 1, 3, 5, 7, 8 and 10%, were tested to find out how much solid particles should be used to stabilize the generated oil-water interfaces. Experiments were performed by 20 ml vials. First, ZnO solid particles and distilled water were shaken by hand for 1 minute to wet the surfaces of ZnO solid particles and prevent them from sticking to each other. Silicone oil was then added to the water-solid particle mixture, and the vial was shaken by hand for 4 minutes. Finally, the drop size analysis was done with Malvern Matersizer 3000. For the experiments performed here, the effect of solid particle concentration on the drop size is given in Figure 3.2.

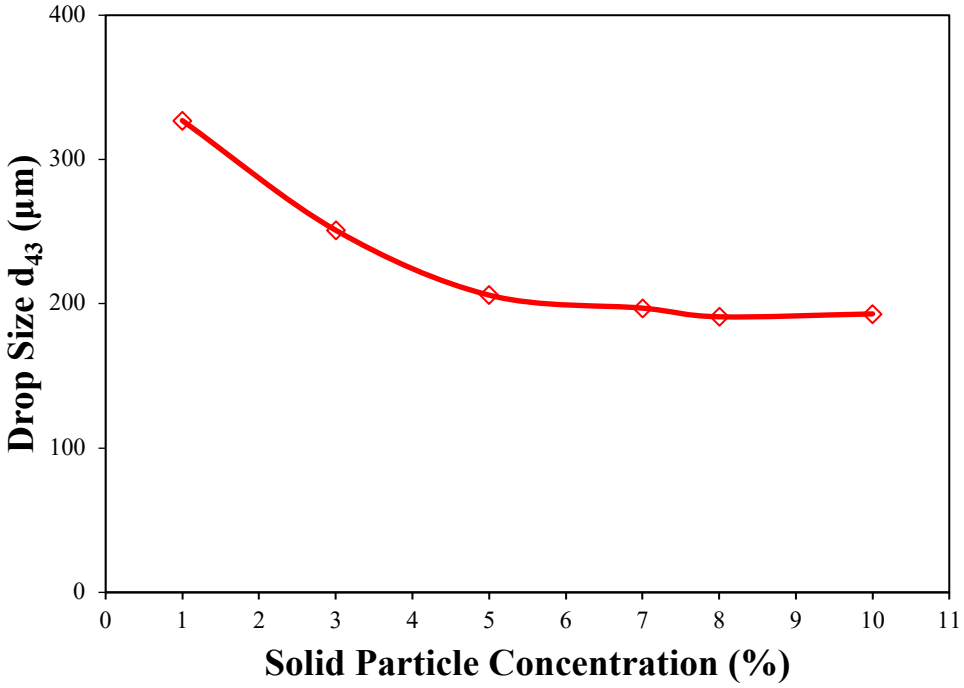

Figure 3.2. The effect of solid particle concentration on drop size

In Figure 3.2, the emulsion drop size decreased when solid particle concentration is increased. At 1 and 3% solid particle-to-silicone oil ratios, the silicone oil that is not covered by solid particles was visible in the vial after a certain period. The presence of silicone oil in the vial means that the amount of solid particles used was insufficient to cover the generated oil-water interfaces. There is, however, no drop size change was observed at 7, 8, and 10% solid particle-to-silicone oil ratios. This means that all the oil-water interface that is generated is covered by the solid particles starting from 7%. For the rest of the experiments conducted in this study, solid particle-to-silicone oil ratio was set as 7%, which corresponds to 15.5 g of ZnO solid particles.

3.1.3 Type of Water

The presence of ions in the water that is used to produce the Pickering emulsions may have an effect on the drop size. To determine the suitable water type for the production of emulsion drops, experiments were conducted using two types of distilled water: reverse osmosis (RO) and ultra-pure (UP). One set of experiments were conducted at one of the eccentricity ratios of the impeller shaft, e/T=0.2, where e, the distance between the center of the tank and the boundary of the impeller shaft closer to the tank center, is called eccentricity, and T is the tank diameter. Emulsification process was conducted during 1 hour and a sample was taken every 15 minutes. Drop size analysis was done with Malvern Mastersizer 3000. The effect of distilled water type on the drop size is given in Figure 3.3.

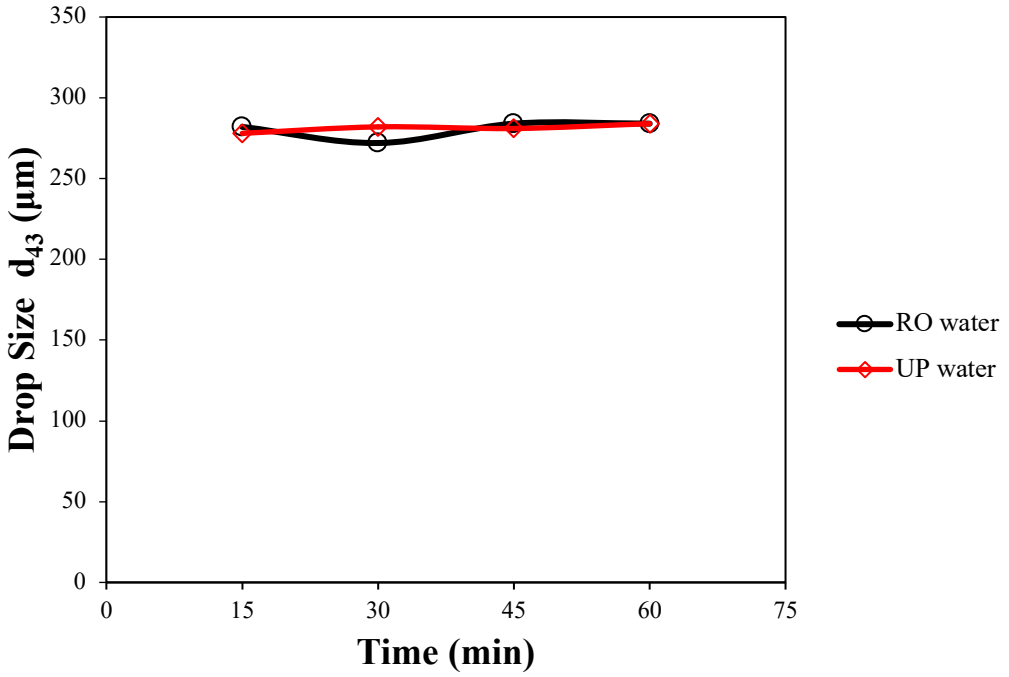

Figure 3.3. The effect of water type on drop size

As seen in Figure 3.3 the type of distilled water does not have a significant effect on drop size. UP water (resistivity = 18.2 MΩ.cm, @25℃) was selected as the continuous phase.

3.2 Stirred Tank Configuration

ZnO stabilized Pickering emulsions were produced using an unbaffled stirred tank (1 L glass beaker) with an inner diameter of T=9.9 cm. The schematic representation of an unbaffled stirred tank is given in Figure 3.4. The dimensions of the impeller and tank geometries are given in Table 3.2. In all the experiments, the tank was filled with the oil-water-solid particle mixture up to a level, H, that is equal to the tank diameter, T. A standard six-bladed Rushton turbine (RT) with a diameter of D=T/3 was used as the impeller. The impeller was located at an off-bottom clearance of C=T/3. Off-bottom clearance (C) is the distance between the middle of the impeller blades to the bottom of the tank.

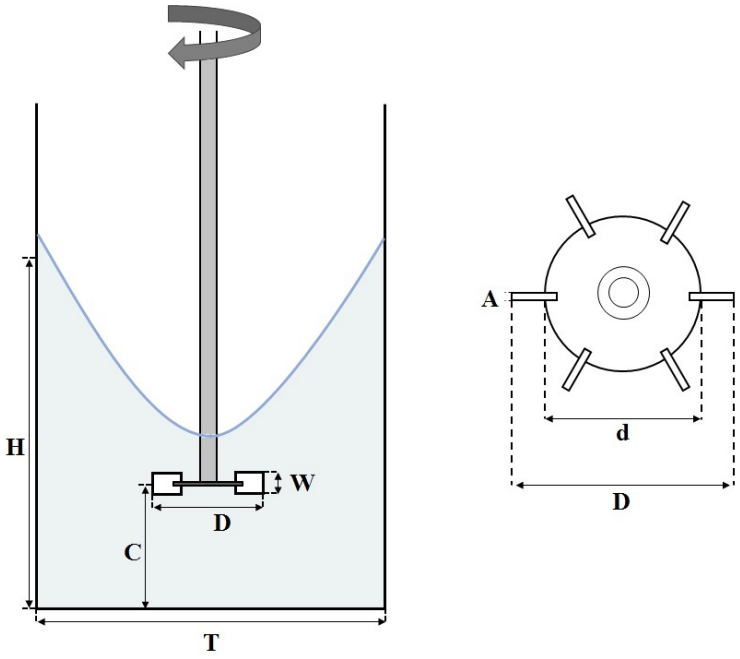

a. b.

Figure 3.4. Schematic representation of a. unbaffled stirred tank with centrally located RT and b. top view of the RT

Table 3.2 Tank and impeller dimensions

Tank diameter (T)	**Impeller diameter (D)**	**Liquid height (H)**	**Off-bottom clearance (C)**	**Impeller disc diameter (d)**	**Impeller blade height (W)**	**Impeller blade width (A)**
-	T/3	T	T/3	0.64 D	0.18 D	0.03 D
9.9 cm	3.3 cm	9.9 cm	3.3 cm	2.1 cm	0.6 cm	0.1 cm

In unbaffled stirred tanks, increasing the impeller speed results in the central vortex at the liquid surface. The vortex formation on the liquid surface has negative impacts on the emulsification process as it reduces the mixing intensity, prevents the

spreading of turbulence created by the movement of the impeller throughout the tank, and causes air to enter the tank. These negative impacts directly affect the drop sizes and drop size distribution. Therefore, in some of the experiments, the impeller shaft was positioned at an eccentric position to break the central vortex on the liquid surface. Three positions were used for the impeller shaft: at the center, e/T=0, and at two eccentric positions, e/T=0.1 and e/T=0.2. The schematic representation of the position of the impeller shaft is given in Figure 3.5. A lid was also used to prevent air from entering the tank due to the vortex formation.

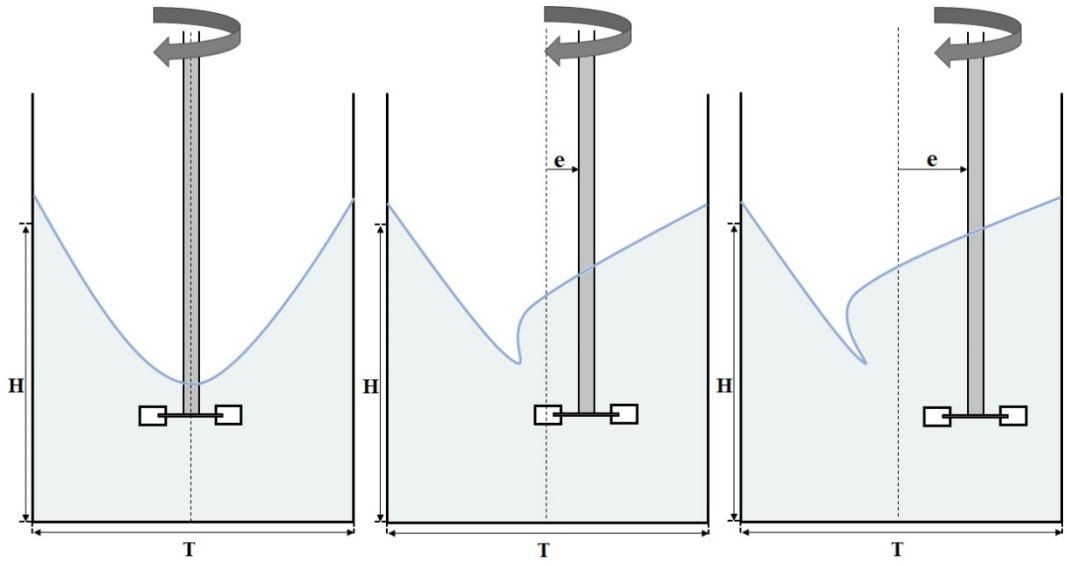

a. b. c.

Figure 3.5. Positions of the impeller shaft a. e/T=0, b. e/T=0.1 and c. e/T=0.2

In the emulsification process, high fluid shear rates and recirculation are required to achieve more stable drops by decreasing drop size (Norwood and Metzner, 1960). These features are necessary for the dispersed phase to be dispersed effectively in the continuous phase. To provide this fact, the flow regime was set at turbulent flow. In turbulent flow regime, eddies form and it causes more effective fluid movement in the stirred tank. A fully turbulent regime is maintained at an impeller Reynolds

number higher than 20,000. The impeller Reynolds number can be calculated using Equation 3.1 given below:

$$\mathrm{Re} = \frac{\rho\, N\, D^2}{\mu} \tag{3.1}$$

Here ρ is the density of the emulsion (kg/m^3), N is impeller speed (rps), D is impeller diameter (m), and μ is viscosity of emulsion (kg/m s).

Minimum mixing speed is the minimum speed that is required for the flow to be in turbulent regime. It should be calculated to find out working impeller speeds (N), thus impeller tip speeds (V_{tip}). The first step to find minimum mixing speed is to calculate the emulsion density. The density of the dispersed phase was given as 964 kg/m^3 in section 3.1.1 at Table 3.1. The density of the continuous phase, ρ_c was calculated by considering the fact that the water and solid particles form the continuous phase using Equation 3.2 given below:

$$\rho_c = \frac{m_p + m_w}{\frac{m_p}{\rho_p} + \frac{m_w}{\rho_w}} \tag{3.2}$$

Here m_p and m_w are the mass of the solid particles and the distilled water (kg), respectively. ρ_p and ρ_w are the density of the solid particles and the distilled water (kg/m^3), respectively. The density of continuous phase was found as 996.03 kg/m^3. The emulsion density was then calculated as 986.421 kg/m^3 by taking into consideration of the volume concentrations of dispersed and continuous phases in the tank.

The second step is to calculate the viscosity of the emulsion. Emulsion viscosity was calculated by using Equation 3.3 with the assumption of rigid spheres of very diverse sizes for solid particles (Roscoe, 1952):

$$\mu_r = \frac{\mu_s}{\mu_c} = (1 - c)^{-2.5} \tag{3.3}$$

Here μ_r is the relative viscosity of emulsion (kg/m s), μ_s is the viscosity of emulsion (kg/m s), μ_c is the viscosity of continuous phase (kg/m s), and c is the volume concentration of rigid spheres. The emulsion viscosity was calculated as 0.8998 cSt. The calculated values of emulsion density and viscosity and the value of impeller diameter, which is given in section 3.2 at Table 3.2, were put in Equation 3.1. As a result, the minimum impeller speed that is required for the flow to be in turbulent regime was found as 1069 rpm for RT, D=T/3. Then the working impeller speeds (N) were set at 1105, 1195, and 1385 rpm. Thus, the impeller tip speeds ($V_{tip} = \pi ND$) that is corresponding to these working impeller speeds are 1.85, 2, and 2.32 m/s, respectively.

3.3 Analysis of Size and Size Distribution

3.3.1 Method

The size and size distribution of produced emulsion drops and solid particles were analyzed using Malvern Mastersizer 3000. The Mastersizer comprises three parts: the main optical unit, one or more sample dispersion units, and a measurement cell. The Mastersizer uses the dynamic light scattering while performing size analysis. In this technique, a laser beam passes through a dispersed sample, and the angular change in intensity of the scattered light is measured. Large particles scatter the light at small angles, while small particles scatter the light at large angles. The size and

size distribution of sample are reported using the intensity of the scattered light. This entire process occurs in the main optical unit. Sample dispersion units are divided into two groups: wet and dry. In this study, wet dispersion unit was used. In the wet dispersion unit, the sample is dispersed in a liquid dispersant. The measurement cell ensures the connection between the sample dispersion and the main optical units. It directs the sample which is present in the wet dispersion unit to the measurement windows so that sample can be exposed to laser light. Finally, the optical unit and sample dispersion unit are controlled by a computer using Mastersizer application software.

There are two types of scattering models applied for the measurements in Mastersizer: Mie theory and Fraunhofer theory. Mie theory assumes that the shape of the sample to be analyzed is spherical, and Fraunhofer theory assumes that it is non-spherical. Since the shape of the obtained emulsion drops is spherical based on the visual observation, Mie theory is used as a scattering model. Mie theory also forms the basis of Mastersizer 3000 and provides accurate results in a wide range of sizes (Mastersizer 3000 User Manual, 2013). To apply Mie theory in measuring size and size distributions, refractive indices of the ZnO solid particles and dispersant, which is water in this study, and absorption index of ZnO solid particles must be known. The refractive index gives information about the degree of refraction of light as it passes from one medium to another. The absorption index measures the amount of light absorbed by particles. Transparent particles have low or no absorption value; in contrast, colored or black particles have a higher value (Mastersizer 3000 User Manual, 2013). The refractive indices of ZnO solid particles and water, were taken as 2 and 1.33, respectively, and the absorption index of ZnO solid particles was set at 0.

To obtain an accurate drop size measurement, attention should be paid to two points: one is the elimination of solid particles from the measurement after the drop size analysis, and the other is the stirrer speed of the wet dispersion unit during the drop size analysis. These two critical points in drop size analysis are explained in detail below.

3.3.2 Critical Points in Drop Size Analysis

3.3.2.1 Elimination of Solid Particles

The samples collected into the vials from the stirred tank often contain free solid particles. These are the particles that are not adsorbed at the oil-water interfaces. For the emulsion drop sizes to be analyzed correctly, these free solid particles in the sample must be eliminated after the analysis. In Figure 3.6, a representative volumetric size distribution data for drop size analysis with free solid particles (red curve) and where free solid particles are eliminated (black curve) is given.

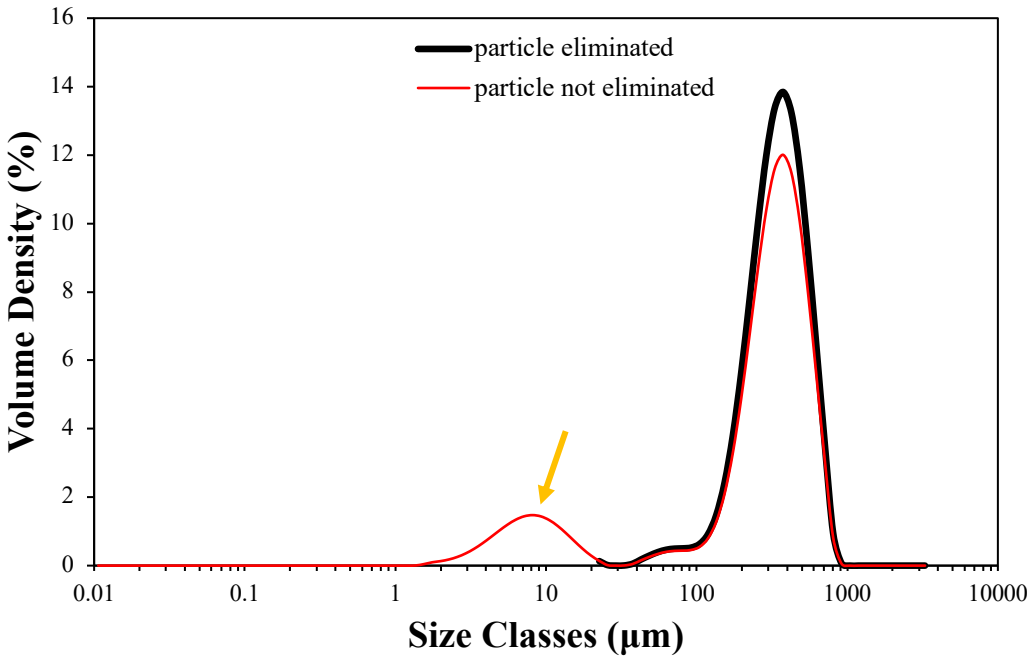

Figure 3.6. The effect of solid particle elimination on the volumetric size distribution: emulsion drops with free solid particles (red curve) and emulsion drops only (black curve)

The small peak below 20 µm, marked with a yellow arrow on Figure 3.6 indicates the presence of free solid particles in the sample. When these free solid particles are eliminated, the volumetric size distribution of only the emulsion drops was obtained as shown with the black curve. Elimination of free solid particles directly affects the emulsion drop size. The effect of free solid particle elimination on the emulsion drop size is shown in Table 3.3.

Table 3.3 The effect of solid particle elimination on emulsion drop size

	d_{32} (µm)	**d_{43} (µm)**
Solid particle not eliminated	41.5	317
Solid particle eliminated	283	364

As seen in Table 3.3, Sauter mean diameter, d_{32}, was more affected than that of De Brouckere mean diameter, d_{43}, in eliminating free solid particles from the drop size measurement. Using d_{43} is more appropriate for Pickering emulsions considering the possibility of a small amount of free solid particles still being present in the sample, even though free solid particles have been eliminated from the measurement.

3.3.2.2 Stirrer Speed of the Wet Dispersion Unit

In the wet dispersion unit, the emulsion drops are suspended in distilled water. The dispersion of emulsion drops in the distilled water lowers their surface energies and reduces the attractive forces between them. Therefore, emulsion drops separate and remain suspended in the water. If the stirrer speed of the wet dispersion unit is too high, the emulsion drops are more likely to break before reaching the measurement unit. In order to receive the drop size correctly and interpret it clearly, the possibility of drop breakage should be minimized by taking the lowest stirrer speed at which small and large emulsion drops can circulate and a representative sample enters the measurement unit. A reasonable stirrer speed of the wet dispersion unit that provides this condition was selected based on a preliminary experiment. An emulsion sample

was poured into the wet dispersion unit. Measurements were then taken by increasing the stirrer speed of the wet dispersion unit by 150 rpm. 5 measurements were taken for each stirrer speed. The effect of stirrer speed of the wet dispersion unit on the drop size is given in Figure 3.7.

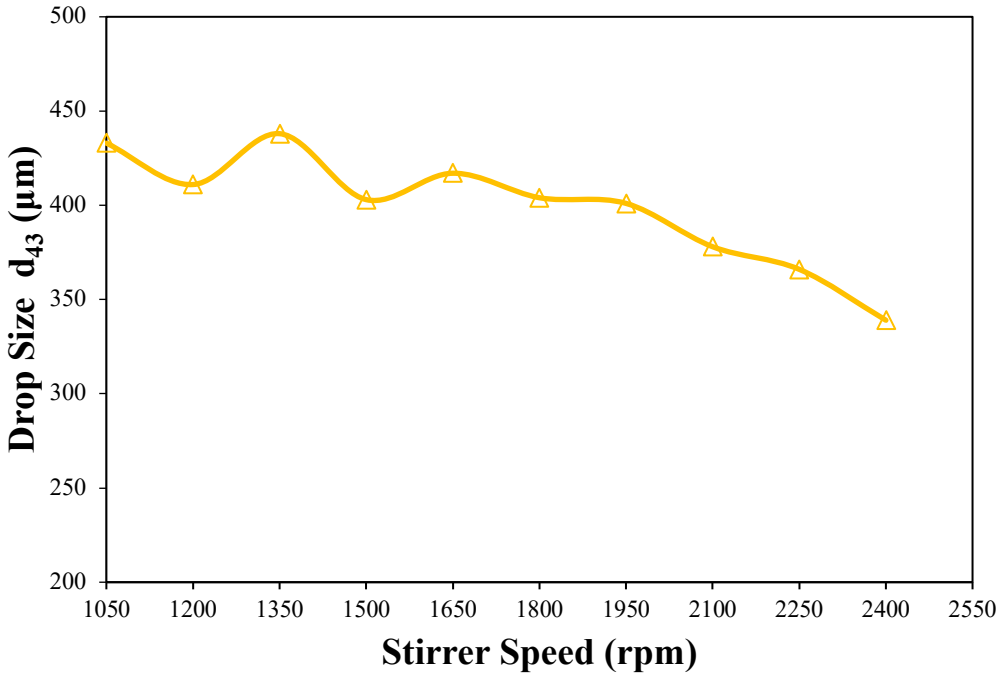

Figure 3.7. The effect of different stirrer speeds of wet dispersion unit on drop size, d_{43} (µm)

According to the Figure 3.7, a considerable reduction in emulsion drop size occurs when the stirrer speed of the wet dispersion unit is increased beyond 1500 rpm. Between 1050 and 1500 rpm, however, the drop sizes fluctuate between an upper and lower limit, indicating that the measured drop size is not significantly affected by the stirrer speed. Therefore, the stirrer speed of the wet dispersion unit was set as 1050 rpm for the rest of the experiments. It should be also noted that 1050 rpm is less than the selected impeller speeds and thus impeller tip speeds (V_{tip}) which means

that the intensity of mixing applied to the sample in the wet dispersion unit was certainly below the one applied in the actual stirred tank.

3.4 Emulsification Time and Sampling Points

In order to determine the emulsification time, two experiments were conducted where the impeller shaft is positioned at the center, e/T=0, and at an eccentricity ratio of e/T=0.2. The impeller speed was set as 1105 rpm, which is one of the selected working impeller speeds, for all runs. When the impeller shaft is positioned at the center, e/T=0, the sample was taken from the right side of the impeller shaft since the distance of the impeller shaft to the right and left tank walls is equal. But, when the impeller shaft is positioned eccentrically in the tank, the distance of the impeller shaft to the right and left tank walls is not equal. To determine whether this distance affects the drop size and drop size distribution, samples were taken from both the right and left sides of the impeller shaft for the eccentricity ratio of e/T=0.2. Another reason for taking samples from both the right and left sides of the impeller shaft for the eccentric position is to test whether the drop size represents the whole tank. If the samples taken from different locations in the tank return the same drop size, this can be interpreted as the samples represent the entire tank. The sampling points regarding the position of the impeller shaft are given in Figure 3.8. In Figure 3.8, S_1 and S_2 are the sampling points of the emulsion drops taken from right and left side of the impeller shaft, respectively. These points correspond to the midpoint between the impeller and the liquid surface in the axial direction and the midpoint of the impeller shaft and the tank wall in the radial direction.

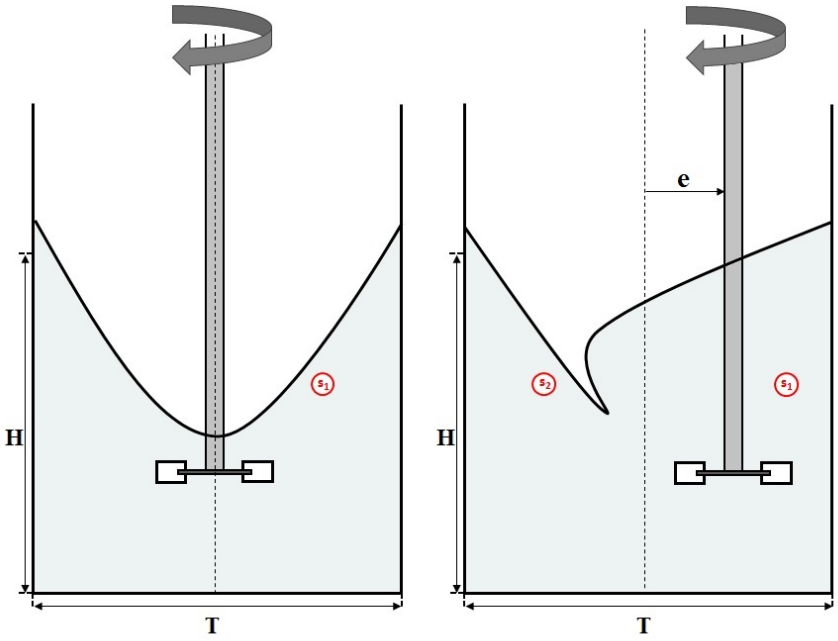

Figure 3.8. Schematic representation of sampling points: a.e/T=0 and b.e/T=0.2

The experiments were conducted for 1 hour, and samples were taken every 15 minutes from the determined points while stirring is continued. The drop size analysis of the collected samples was done by Malvern Mastersizer 3000. The effect of emulsification time on the drop size is given in Figure 3.9.

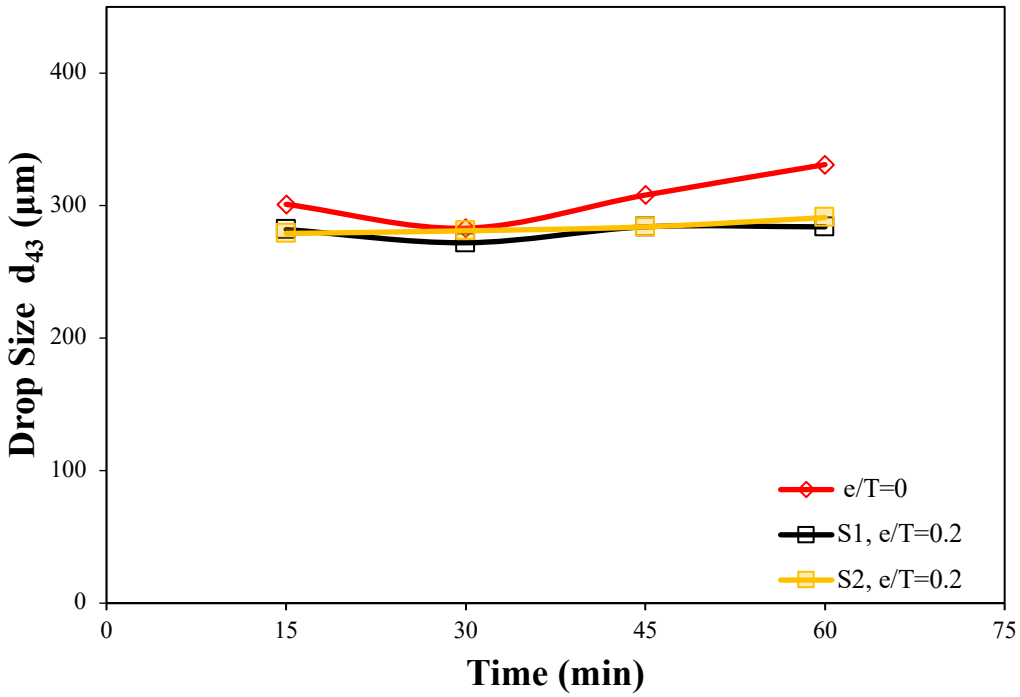

Figure 3.9. The effect of emulsification time on drop size

As seen in Figure 3.9, the drop sizes slightly increase toward 1 hour of mixing when the impeller shaft is positioned at the centre, e/T=0, but the trend indicates that the drop sizes reach a plateau. This plateau indicates that possibly no more increase in drop size will be seen in the data. In the case of impeller shaft is positioned eccentrically, the drop size is almost not affected by the emulsification time. Thus, at the end of 1 hour of mixing, all the oil-water interface generated is covered by the solid particles and the emulsion drops reached their equilibrium sizes. When the sampling points at the right and the left sides of the impeller shaft are compared in terms of eccentricity, almost the same drop sizes were obtained. Based on these, the emulsification time was selected as 1 hour for the rest of the experiments, and for the eccentrically positioned impeller shaft positions, the samples were collected from the right side of the impeller shaft which corresponds to S_1 in Figure 3.8.

3.5 Feeding Conditions of the Dispersed Phase

To test the effect of feeding conditions of the dispersed phase on the drop size of Pickering emulsions, two feeding conditions of the dispersed phase were tested: from the liquid surface within 5 seconds using a graduated cylinder which is referred to as surface feeding in the rest of the thesis and into the impeller zone over 900 seconds using a peristaltic pump whose flow rate is controlled by a computer program which is referred to as impeller zone feeding in the rest of the thesis. These two processes are shown below in Figures 3.10 and 3.11.

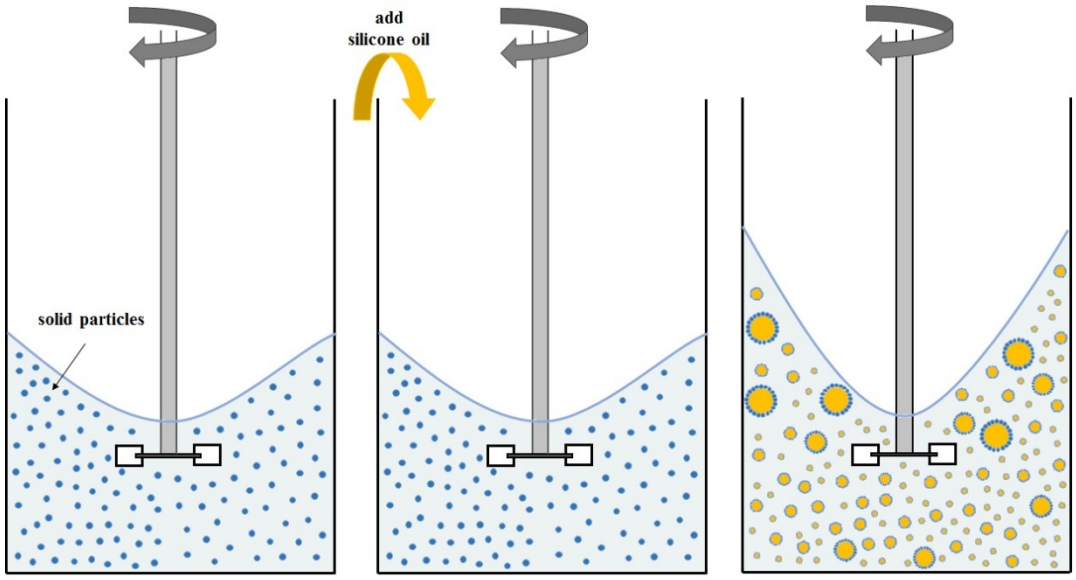

Figure 3.10. Schematic representation of surface feeding of the dispersed phase

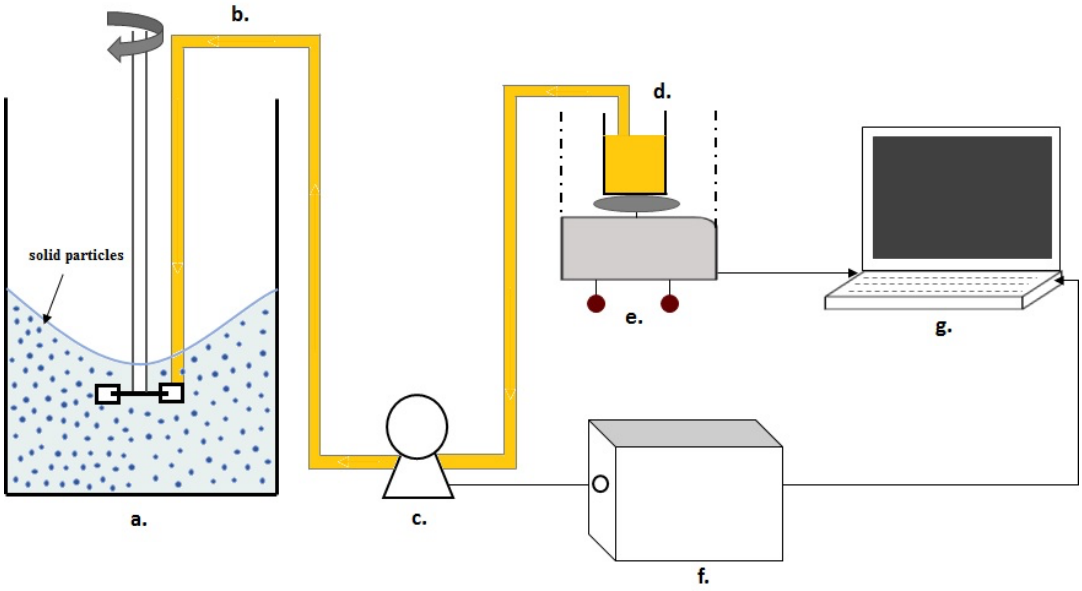

Figure 3.11. Schematic representation of impeller zone feeding of the dispersed phase: a. an unbaffled stirred tank with centrally positioned impeller shaft, b. feed tube, c. SEKO peristaltic pump, d. silicone oil, e. OHAUS analytical balance, f. pump flow rate control unit (Arduino UNO and motor driver), and g. computer

A peristaltic pump was used in the impeller zone feeding. In order to keep the flow rate, also called output voltage, of the pump under control, a microprocessor Arduino UNO with a motor driver was used. The Pulse Width Modulation (PWM) signals coming to the motor driver shows whether the pump flow rate is under control. The PWM technique is the switching method used to produce an analog signal. To produce the analog signal, it takes help from a digital source. Arduino code is given in Appendix A.

The interface of the pump flow rate control unit associated with the impeller zone feeding is given in Figure 3.12. The aim of the pump flow rate control unit is to minimize the instantaneous error and thus, to feed the desired amount of dispersed phase into the tank at the specified time. Suppose the instantaneous error is above

zero and continues to increase as time passes. In that case, the PWM signal that is sent to the motor driver also increases over time, increasing the flow rate of pump and trying to balance the instantaneous error to zero. On the other hand, suppose the instantaneous error is below zero and continues to decrease as time passes. The PWM signal that is sent to the motor driver also decreases over time, reducing the flow rate of pump and trying to balance the instantaneous error to zero. For example, Figure 3.12 is a snapshot of an ongoing experiment. Using the information given above, since the instantaneous error is below zero, the PWM signal must decrease to less than its current value so that the instantaneous error can approach zero. Thus, the desired amount of silicone oil is fed into the tank at the specified time.

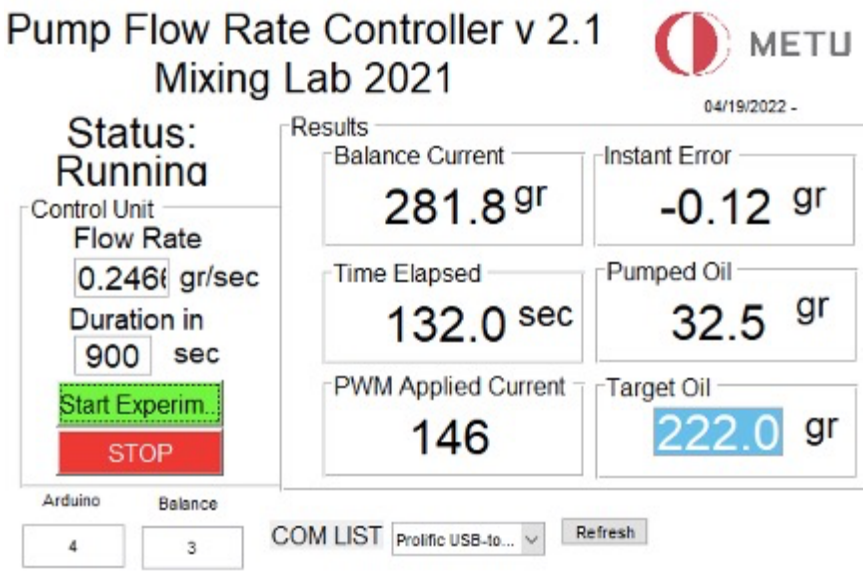

Figure 3.12. The software interface of the pump flow rate control unit

The flow rate of pump can also be controlled with the information received from the analytical balance. The MATLAB code which is used for the impeller zone feeding of the dispersed phase is given in Appendix A, and Equations 3.4, 3.5, and 3.6 used in the code are given below:

$$W_t(t) = \dot{m} \, . \, t \tag{3.4}$$

$$W_{ref}(t) = W_i(t) - \dot{m} \, . \, t \tag{3.5}$$

$$W_p(t) = W_i(t) - W_c(t) \tag{3.6}$$

Here W_t is the target silicone oil that should be fed into the tank; in other words, how much silicone oil needs to be fed into the tank for the specified time. $\dot{m}$ is the mass flow rate of the silicone oil. W_i is how much silicone oil being initially present on the analytical balance. W_{ref} is how much silicone oil is left on the analytical balance at any time t. W_p and W_c are the weight of pumped oil and current oil, respectively.

The most crucial point for the impeller zone feeding is to know where the turbulent energy dissipation rate reaches maximum value in the tank since the increase in energy dissipation rate directly affects the drop size and the drop size distribution. According to Zhou and Kresta (1996), the turbulent energy dissipation rate reaches maximum value at the tip of the impeller blades for the radial impeller in the baffled tanks. Costes and Couderc (1988) also found that the turbulence created by Rushton Turbine (RT) was measured by using laser Doppler anemometry and is greatest near the impeller. It is desired to feed the dispersed phase into the region with the highest turbulent kinetic energy since this also means that this is the region for the production of the smallest drops. Therefore, the region with the maximum energy dissipation rate, the tip of the impeller blades, was selected for each position of the impeller shaft to examine better how different feeding conditions of the dispersed phase affect the drop size and drop size distribution of emulsion drops produced. Selected dispersed phase feeding points based on these studies are given in Figure 3.13 for different positions of the impeller shaft.

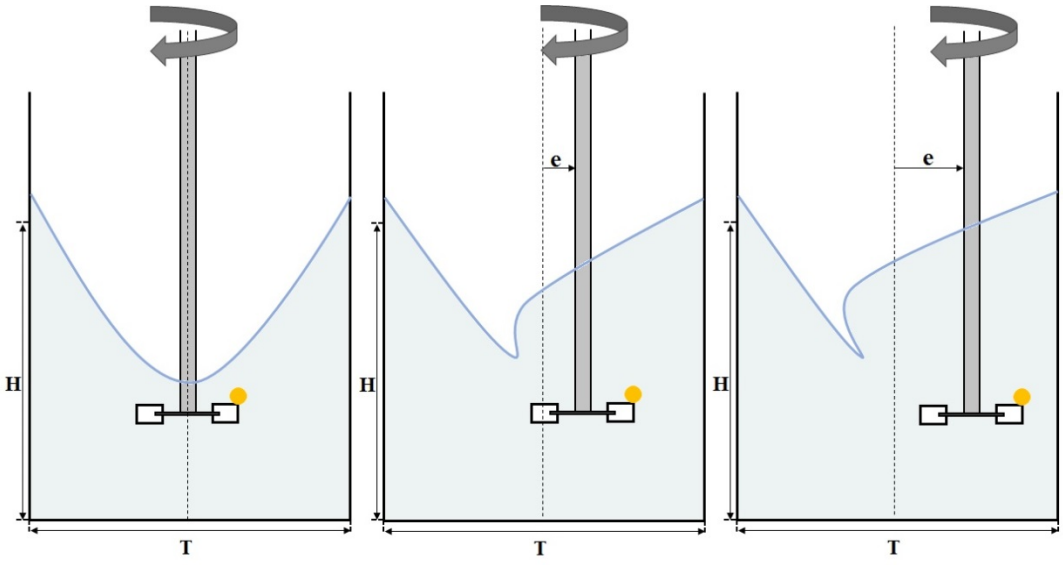

a. b. c.

Figure 3.13. Dispersed phase feeding points corresponding to different positions of the impeller shaft (yellow dot indicates the feeding point of the dispersed phase): a. e/T=0, b. e/T=0.1, and c. e/T=0.2.

3.6 Emulsification Procedure

First, 15.5 g of ZnO solid particles was put into the tank. According to Arditty et al. (2003), an increase in particle concentration above the necessary limit will no longer decrease the drop size. Thus, the required amount of ZnO solid particles was used for emulsion production, not an excess amount. The position of the impeller shaft was set in terms of the axial position (off-bottom clearance) and radial position (eccentrically or at the center). Then, a 532 ml of UP water was put into the tank, and the solid particle-water mixture was stirred for 10 minutes to prevent solid particles from sticking to each other and to wet the surface of solid particles at an impeller speed of 650 rpm. The decision to pre-mix solid particles and water for 10 minutes was chosen according to the study by Demirdogan (2019). After that, 230 ml of silicone oil was fed into the tank either by surface feeding or by impeller zone

feeding. The oil-water-solid particle mixture was then stirred for 1 hour at a determined impeller speed. At the end of 1 hour, a sample was taken from the designated point for each tank configurations while stirring the mixture at the desired impeller speed. If there are solid particles in the sample that are not adsorbed to the oil-water interface, it was waited for 20 minutes for them to settle to the bottom of the vial. Finally, the drop size and the drop size distribution analysis of produced emulsion drops were done using Malvern Mastersizer 3000. The microscopic image of obtained emulsion drops is given in Figure 3.14. Every experiment was conducted at least two times for all conditions. Ten measurements of emulsion drop size were taken from every sample. In other words, the average of at least 20 drop size measurements for each condition was presented as the drop size of the emulsion. The difference from the emulsion drop size presented as the mean of the experiments for each condition was calculated with the standard deviation and the standard deviation is given as the error bar.

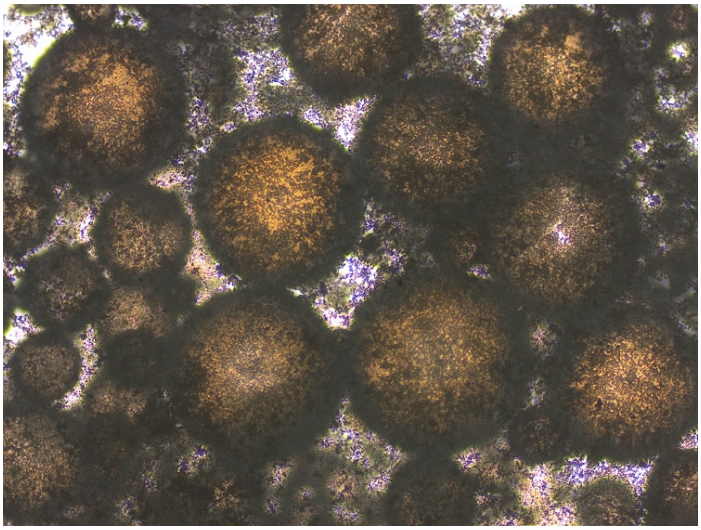

Figure 3.14. Microscopic image of produced emulsion drops

CHAPTER 4

RESULTS AND DISCUSSION

The effect of feeding conditions of the dispersed phase on the drop size of Pickering emulsions was investigated for the cases where the impeller shaft is positioned at the center, e/T=0 and at two eccentricity ratios, e/T=0.1 and e/T=0.2, at three impeller tip speeds. Based on the results, the optimum configuration in terms of eccentricity ratio of the impeller shaft and impeller tip speed that yields a significant change in drop size and drop size distribution was determined. This optimum configuration was used to investigate the effect of increased feeding times of the dispersed phase on drop size and varying the impeller tip speeds during the production process on drop size and power consumption. This chapter is laid out to give the findings of these investigations in the aforementioned order.

4.1 Effect of Feeding Conditions on Drop Size

In this section, results of the effect of feeding conditions of the dispersed phase on drop size are presented. The feeding of the dispersed phase was done either from the liquid surface at once or into the impeller zone over a certain time. The results were summarized and compared in the last sub-section.

4.1.1 Surface Feeding

All the drop size data in this section were obtained by feeding 230 ml of silicone oil into the tank from the liquid surface within 5 seconds using a graduated cylinder. The effect of the position of the impeller shaft and impeller tip speed (V_{tip}) on drop size is given in Figure 4.1. When the impeller tip speed is increased, the drop size decreases for all positions of the impeller shaft. This is expected since increasing the

impeller tip speed introduces more shear to the system, which helps breaking the drops into smaller ones. For all impeller tip speeds, the drop sizes obtained at an eccentricity ratio of e/T=0.1 are smaller than the drop sizes obtained when the impeller shaft is positioned at the center, e/T=0 and at an eccentricity ratio of e/T=0.2. The smallest drop size was obtained at the eccentricity ratio of e/T=0.1, at the highest impeller tip speed, 2.32 m/s.

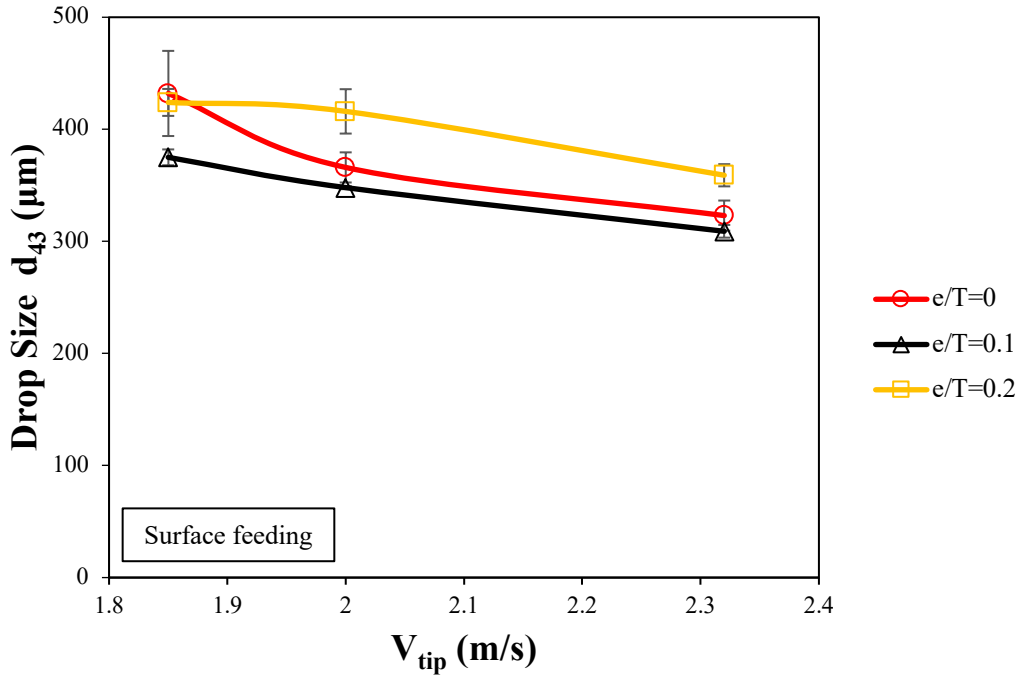

Figure 4.1. The effect of position of the impeller shaft and impeller tip speed on drop size for surface feeding

There is only one study available in the literature that investigated the effect of hydrodynamics and position of the impeller shaft on drop size of Pickering emulsions in unbaffled stirred tanks: Demirdogan (2019). The geometries of the impeller and tank, and the dispersed and continuous phases are the same as this study. Demirdogan (2019) used glass beads as solid particles and excess amount of solid

particles to stabilize generated oil-water interfaces. The smallest drop size and the narrowest drop size distribution were obtained at the eccentricity ratio of e/T=0.2. This result is different than the findings of this thesis. There are two main differences between these two studies: the type, therefore the affinity, of the particles and the amount of particles. The affinity of the particles determines how well the particles are adsorbed at the oil-water interface. An excess amount of solid particles directly affects the flow hydrodynamics in the tank. The particles used in this thesis have high affinity, so they form drops easily. This allowed for use of much smaller amount of particles with almost no excess particles. It is well known that the affinity and amount of the particles, impeller and tank geometry, mixing conditions and hydrodynamics are all strong parameters for the production of Pickering emulsion drops; hence, it is expected to observe different results between these two studies even though the impeller and tank geometries are the same. To better understand the results of this thesis, single-phase unbaffled stirred tank hydrodynamics, in terms of the effect of position of the impeller shaft on vortex formation is considered next.

Vortex formation is one of the most critical parameters affecting fluid movement in an unbaffled stirred tank. It has many adverse effects on mixing efficiency. When impeller tip speed is increased, the depth of vortex increases toward the impeller blades and air bubbles may enter the tank from the contact of the air-liquid interface with the impeller blades, and it is doubtful that they could be later removed from the tank. The region in the tank that is covered by vortex also increases along with the increasing impeller tip speed and thus, axial and radial circulations weaken. In other words, vortex formation is an indication of poor mixing, and it should be avoided or minimized in unbaffled stirred tanks to maintain good mixing between top and bottom parts of the tank.

Positioning the impeller shaft eccentrically reduces the adverse effect of the vortex formation on mixing efficiency and fluid movement and increases the axial and radial circulations in the tank. In Figure 4.2, snapshots of single-phase flow in an unbaffled stirred tank with varying positions of the impeller shaft are given. Figure 4.2a shows the impeller shaft is positioned at the center, e/T=0. At this position, the

central vortex occupies almost one-third of the tank. The central vortex extends toward the tank bottom when the impeller speed is increased. In this case, the region dominated by central vortex gets larger in the tank and even the entire impeller can remain within the central vortex. Thus, the contact between the impeller blades and the liquid reduces, changing the flow completely throughout the tank.

In order to keep the impeller blades in contact with liquid, the impeller shaft can be positioned eccentrically. In Figures 4.2b and 4.2c the snapshots of the flow in the tank at two eccentricity ratios of e/T=0.1 and e/T=0.2 are given, respectively. As the eccentricity ratio of the impeller shaft is increased, the shape and length of the vortex change. In Figure 4.2b, the vortex shows a radial inclination which is from liquid surface toward the tip of the impeller blades, and it begins to narrow compared to the case where the impeller shaft is positioned at the center, e/T=0. In Figure 4.2c, the radial inclination of the vortex increases more than that of an eccentricity ratio of e/T=0.1. Vortex becomes narrower compared to other two positions of the impeller shaft but still present in the tank, and it is almost disconnected from the impeller blades. Eccentrically positioned impeller shaft may be interpreted as reduced impact of vortex formation on the fluid movement and increased contact between the impeller blades and the liquid. To complete this discussion, the effect of eccentricity ratios of the impeller shaft on velocity profile is considered.

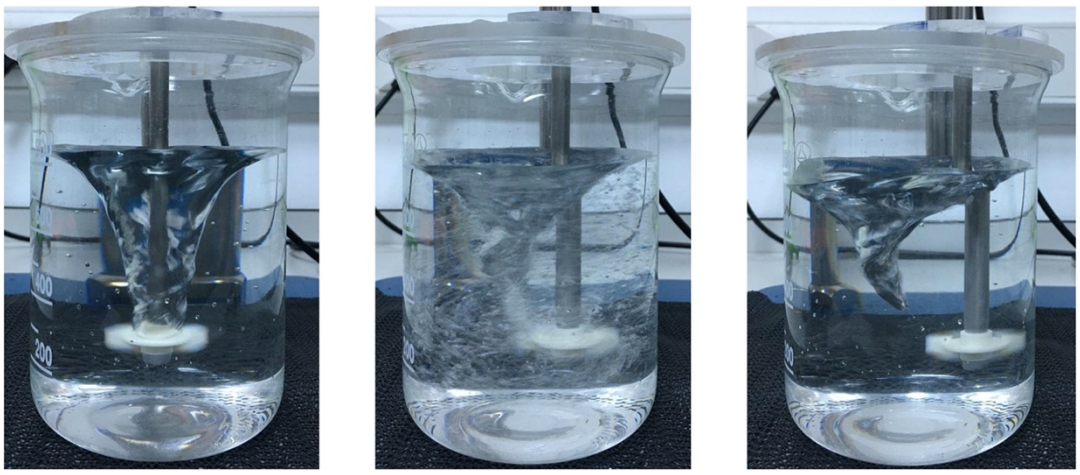

a. b. c.

Figure 4.2. The effect of position of the impeller shaft on vortex formation: a. e/T=0, b. e/T=0.1, and c. e/T=0.2 (The photos were taken at an impeller speed of 850 rpm.)

Musik & Talaga (2016) measured the radial and axial components of the mean flow velocity using Laser Doppler Anemometry (LDA) for an unbaffled stirred tank equipped with RT. Their results showed that for the eccentricity ratio of e/R=0.25, the largest values of the radial mean velocity are recorded in two zones of the tank: in the vortex zone which is from impeller blades toward the top of the tank, and the region under the RT which is from bottom of the RT to the bottom of the tank. They also measured the mean velocities when the impeller shaft is positioned at an eccentricity ratio of e/R=0.5. At this higher eccentricity ratio of impeller shaft, the radial and axial mean velocities were much lower throughout the tank compared to the eccentricity ratio of e/R=0.25, indicating that increasing the eccentricity ratio of the impeller shaft results in a decrease in the magnitude of the mean velocities. This finding supports the findings of this thesis. The smallest drop sizes were obtained at the eccentricity ratio of e/T=0.1 for all impeller tip speeds tested. The drop sizes increased as the eccentricity ratio of the impeller shaft is increased, possibly because

the mean velocities decreased in the tank as the impeller shaft is moved closer to the tank walls.

Musik & Talaga (2016) also stated that the radial velocity component values increase in the vortex zone as the impeller shaft is moved closer to the tank wall. This increase in velocity has an effect on the fluid movement on both sides of the impeller: the region closer to the tank wall (similar to the right side of the impeller in Figure 4.2c) and the region away from the tank wall (similar to the left side of the impeller in Figure 4.2c). In the region where the impeller blades are away from the tank wall, the vortex radially inclines toward the impeller blades. The tip of the vortex gets in contact with the tip of the impeller blades. The impeller discharge stream, which should be directly radial when the impeller shaft is positioned at the center, is directed towards the bottom of the tank with an angle, giving both radial and axial components of velocity. In the region where the impeller blades are closer to the tank wall, the velocity profile is negatively affected by the impeller discharge stream-wall interactions. The impeller discharges fluid radially out; however, the tank wall is very close to the tip of the impeller blades. The very strong impeller discharge hits the tank wall, and as a result it cannot develop the radial flow and loses momentum. Due to this impeller discharge stream-wall interactions, the impeller flow pattern changes and thus, impeller efficiency decreases.

In stirred tanks, the force that cause drop breakage is not uniform since the local energy dissipation rate is not equal all over the tank. This force reaches its maximum value close to the impeller, which is the high shear zone. High shear zone covers the entire impeller and its discharge streams. The effect of this force gradually decreases, moving away from the high shear zone toward the tank walls, the bottom of the tank and the liquid surface, which are coalescence zones for emulsion production. In this study, the highest eccentricity ratio of the impeller shaft is e/T=0.2. As seen in Figure 4.2c, at this eccentricity, the distance between the tank wall and impeller blades is relatively small on the right side of the image. This means that the impeller discharge stream hits the tank wall directly. The higher the impeller tip speed, the stronger the interaction between the impeller discharge stream and the tank wall. Based on these,

with the increased impeller discharge stream-wall interactions and the connection between the tip of the vortex and the tip of the impeller blades, the possibility of movement of partially covered or uncovered drops that are formed in the breakage zone toward the coalescence zones may increase. These drops then coalesce and possibly form larger drops. This increased discharge stream-wall interaction, the decrease in the mean velocities and the presence of vortex and its connection with impeller blades at the highest eccentricity ratio of the impeller shaft are possibly the reasons for observing the largest drop sizes at this eccentricity ratio, e/T=0.2.

The effect of position of the impeller shaft and impeller tip speed on the width of distribution is given in Figure 4.3. The width of distribution was calculated using d_{v90} and d_{v10} where d_{v90} and d_{v10} represent the maximum drop size of the sample volume below 90% and 10%, respectively. How d_{v10}, d_{v50} and d_{v90} values are obtained from Malvern Mastersizer is given in Appendix B. Figure 4.3 shows that when the impeller tip speed is increased, the width of distribution decreases for all positions of the impeller shaft. The change in the width of distribution with increasing impeller tip speed is the most pronounced when the impeller shaft is positioned at the center, e/T=0. In this position, the change in the width of distribution is 41% when the impeller tip speed is increased from 1.85 m/s to 2.32 m/s. The changes in the widths of distribution are 19% and 16% when the impeller shaft is positioned at two eccentricity ratios, e/T=0.1 and e/T=0.2, respectively. At the highest impeller tip speed, 2.32 m/s, the width of distribution for all positions of the impeller shaft is quite similar. This data suggests that the advantage that come with the eccentrically positioned impeller shaft over the centrally positioned impeller shaft on the width of distribution is neutralized when the dispersed phase is fed from the liquid surface.

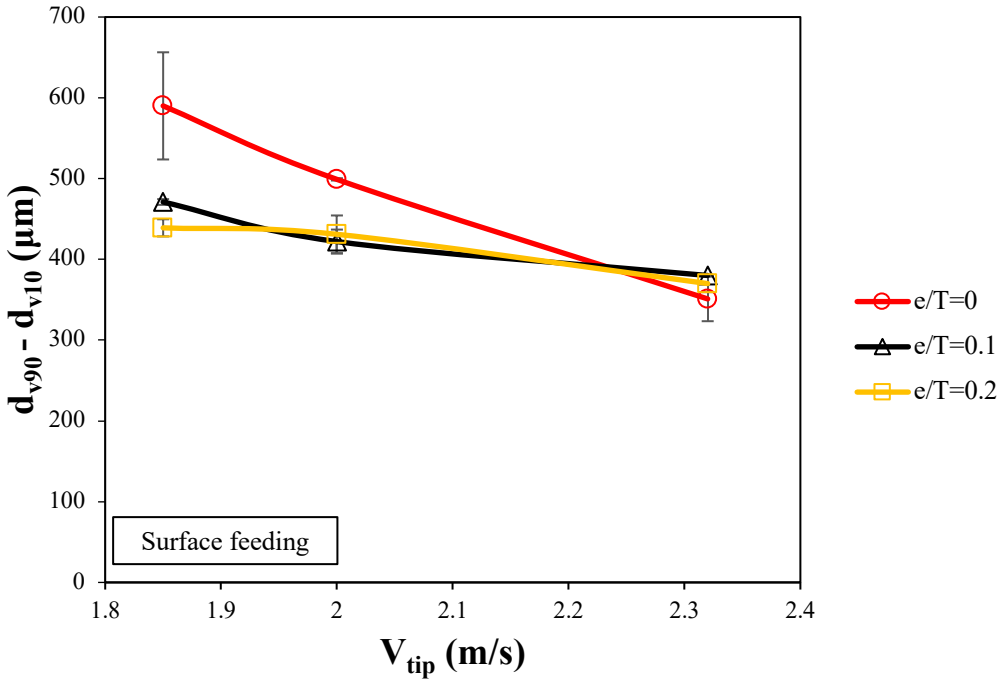

Figure 4.3. The effect of position of the impeller shaft and impeller tip speed on the width of distribution for surface feeding

4.1.2 Impeller Zone Feeding

All the drop size data in this section were obtained by feeding 230 ml of silicone oil into the impeller zone over 900 seconds using a peristaltic pump. The effect of position of the impeller shaft and impeller tip speed on drop size is given in Figure 4.4. Figure 4.4 shows that when the impeller tip speed is increased, the drop sizes show a decreasing trend. For all impeller tip speeds, the drop sizes obtained at the eccentricity ratio of e/T=0.1 are smaller than the drop sizes obtained when the impeller shaft is positioned at the center, e/T=0 and at an eccentricity ratio of e/T=0.2. The smallest drop size was obtained at the eccentricity ratio of e/T=0.1, at the highest impeller tip speed, 2.32 m/s.

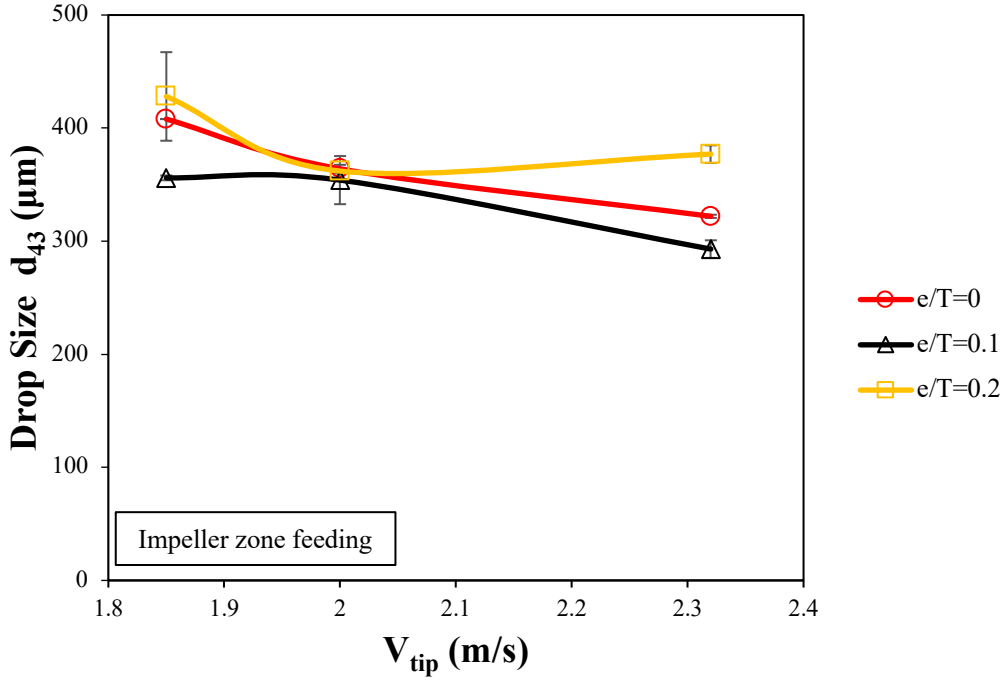

Figure 4.4. The effect of position of the impeller shaft and impeller tip speed on drop size for impeller zone feeding

The smallest drop sizes were also obtained at an eccentricity ratio of e/T=0.1 for all impeller tip speeds tested when the dispersed phase was fed from the liquid surface. There is, however, one small difference. The drop sizes are slightly smaller when the dispersed phase is fed into the impeller zone. This drop size difference can be related to the local energy dissipation rate. The local energy dissipation rate is not uniform throughout the tank. For the impeller zone feeding, the feeding of the dispersed phase was done at the tip of the RT over 900 seconds. This is the high shear zone where the local energy dissipation rate reaches the maximum value. Since the drop breakage occurs near the impeller, feeding the dispersed phase to the impeller zone causes the dispersed phase to be exposed to the desired high shear as soon as it is fed into the tank; thus, producing small drops from the beginning of the emulsion production process. In surface feeding, however, the dispersed phase was fed to the tank all at once from the liquid surface within 5 seconds, which is a region where the

local energy dissipation rate is low. This region is also known as the coalescence zone. Feeding the dispersed phase into the coalescence zone means that the dispersed phase is initially exposed to low shear; therefore, the initial drops that are generated tend to be larger. They can get smaller only when they reach the high shear zone, through circulation. These drops are potentially covered or partially covered with particles, which may have an effect on the breakage of the drops.

The effect of the position of the impeller shaft and impeller tip speed on the width of distribution is given in Figure 4.5. The width of distribution decreases for all positions of the impeller shaft when the impeller tip speed is increased. The change in the width of distribution with increasing the impeller tip speed is the most pronounced when the impeller shaft is positioned at the center, e/T=0. In this position, the change in the width of distribution is 37% when the impeller tip speed is increased from 1.85 m/s to 2.32 m/s. The changes in the width of distribution are 18% and 15% when the impeller shaft is positioned at two eccentricity ratios, e/T=0.1 and e/T=0.2, respectively. It is worth noting that at the highest impeller tip speed, 2.32 m/s, the width of distribution for all positions of the impeller shaft is quite similar. This data suggests that when the dispersed phase is fed into the impeller zone at the highest impeller tip speed, 2.32 m/s, the same width of distribution is obtained regardless of the position of the impeller shaft.

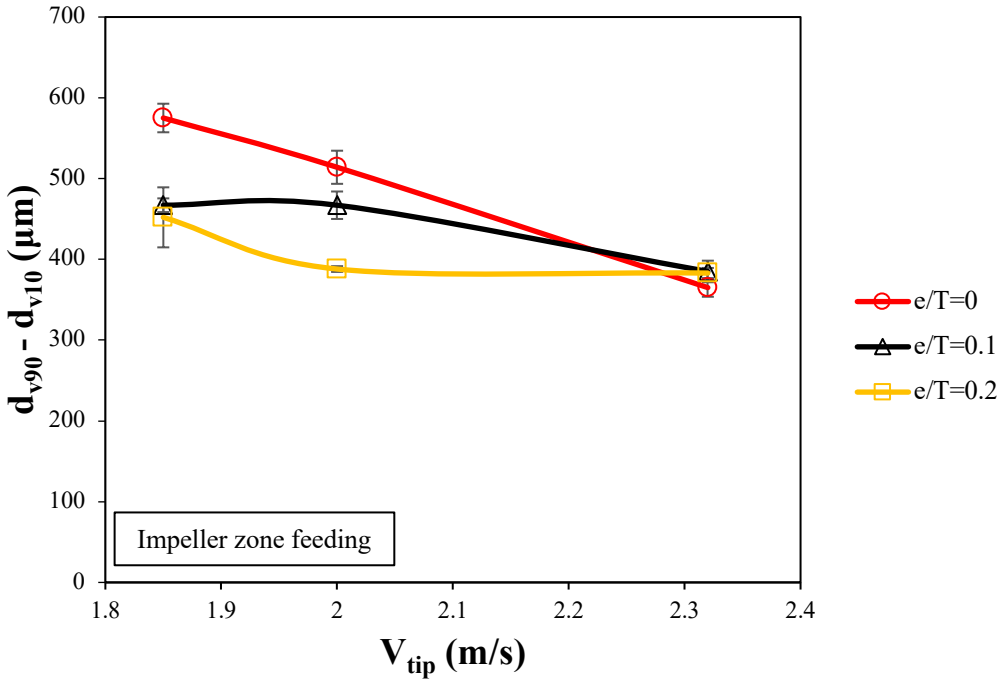

Figure 4.5. The effect of position of the impeller shaft and impeller tip speed on the width of distribution for impeller zone feeding

4.1.3 Effect of Dispersed Phase Feeding Conditions on Drop Size

The effect of feeding position and feeding time of the dispersed phase on drop size at varying impeller tip speeds is given in Figures 4.6, 4.7, and 4.8 for e/T=0, e/T=0.1, and e/T=0.2, respectively.

Figure 4.6 shows the data when the impeller shaft is positioned at the center, e/T=0. The change in drop sizes when the feeding of the dispersed phase is changed from surface feeding to impeller zone feeding for impeller tip speeds of 1.85, 2, and 2.32 m/s were recorded as -5.56%, -0.55%, and -0.31%, respectively. Here, '-' indicates a decrease in drop size. The change in drop size is negligible at two impeller tip speeds, 2 m/s and 2.32 m/s. This result suggests that the drop sizes are not affected by the feeding conditions of the dispersed phase at these two impeller tip speeds. At an impeller tip speed of 1.85 m/s, however, the energy dissipation possibly shows

larger variation throughout the tank and therefore, feeding the dispersed phase to the impeller zone, the high shear zone, results in a slight decrease in drop size.

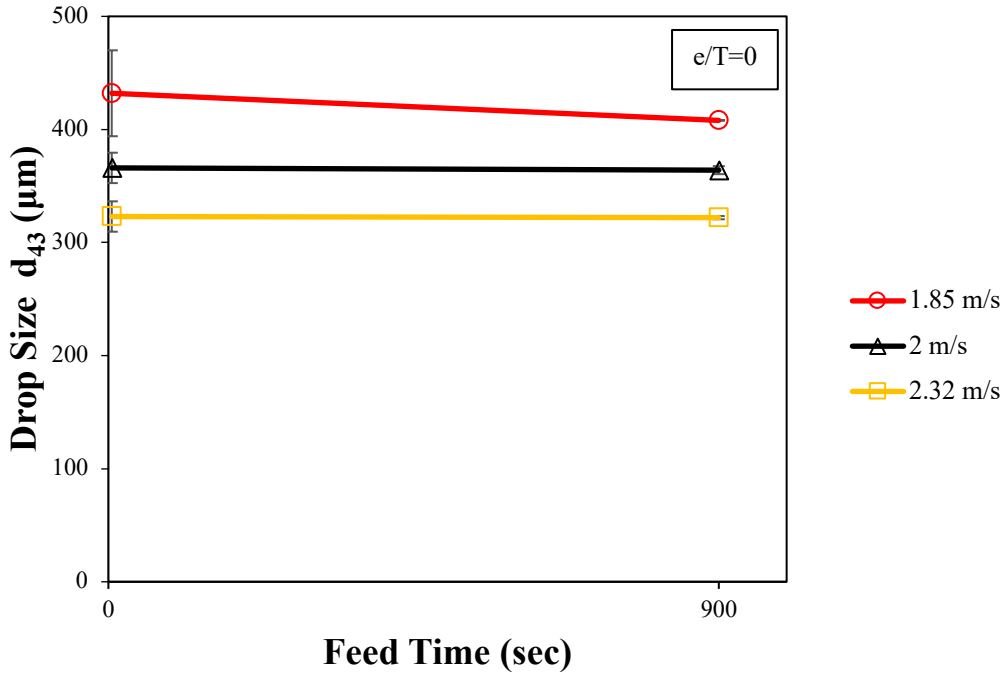

Figure 4.6. The effect of dispersed phase feeding conditions on drop size at e/T=0 for varying impeller tip speeds

Donmez & Ayranci (2020) investigated the effect of dispersed phase feeding conditions on drop size of Pickering emulsions produced in a baffled stirred tank. In their study, the impeller shaft is positioned at the center, e/T=0. The feeding times and feeding positions, which are surface and impeller zone, of the dispersed phase are the same as this study. Their results showed that when the feeding time and feeding position of the dispersed phase are changed from surface feeding to impeller zone feeding, the drop size that is produced with RT, D=T/3, did not change. In this study, using an unbaffled tank, 5.56% of change in drop size was obtained at the impeller tip speed of 1.85 m/s when the dispersed phase feed time and feed position

were changed from surface feeding to impeller zone feeding. While the baffled stirred tanks are more commonly used due to the absence of vortex formation and the adverse effects that come with vortex formation, this result shows an advantage over baffled stirred tanks. A reduction in the drop size was obtained when the feeding conditions of the dispersed phase was changed in spite of the very complex flow field of unbaffled stirred tanks.

Figure 4.7 shows the data when the impeller shaft is positioned at an eccentricity ratio of e/T=0.1. The change in drop sizes when the feeding of the dispersed phase is changed from surface feeding to impeller zone feeding for impeller tip speeds of 1.85, 2, and 2.32 m/s were recorded as -5.07%, +1.72%, and -5.18%, respectively. Here, '-' indicates a decrease and '+' indicates an increase in drop size. The changes in drop size at the impeller tip speeds of 1.85 m/s and 2.32 m/s are almost identical. There is almost no change in drop size at an impeller tip speed of 2 m/s, similar to the data in Figure 4.6 where the impeller shaft was positioned at the center, e/T=0. The smallest drop sizes were obtained at the eccentricity ratio of e/T=0.1 with both feeding conditions of the dispersed phase – surface feeding and impeller zone feeding – and this data shows that impeller zone feeding is more advantageous as it yields smaller; therefore, possibly more stable drops.

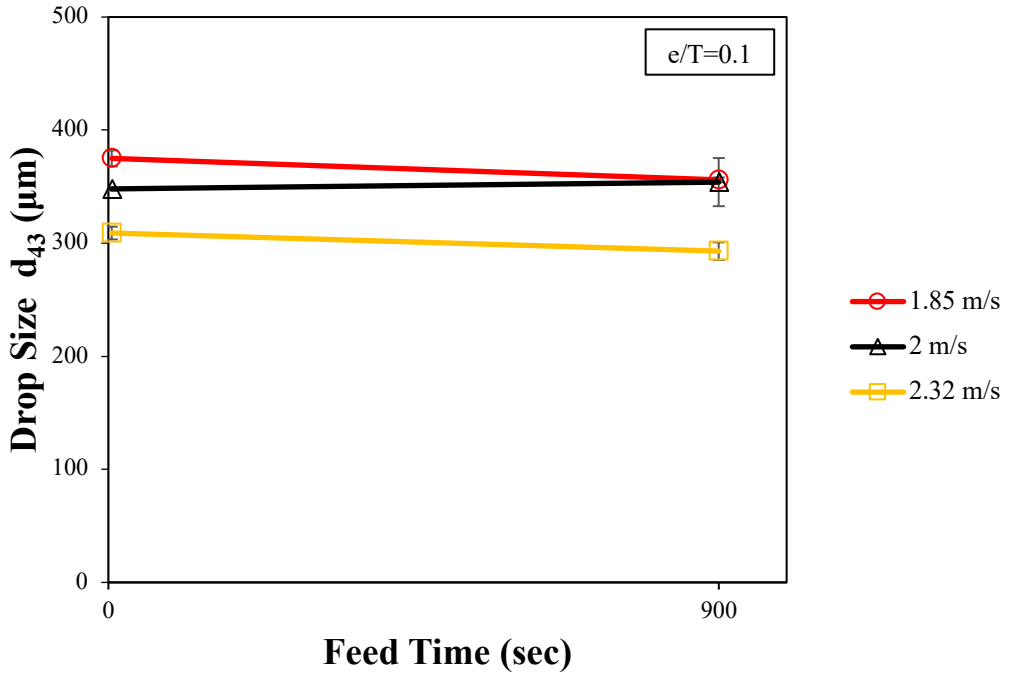

Figure 4.7. The effect of dispersed phase feeding conditions on drop size at e/T=0.1 for varying impeller tip speeds

Figure 4.8 shows the data when the impeller shaft is positioned at an eccentricity ratio of e/T=0.2. The change in drop sizes when the feeding of the dispersed phase is changed from surface feeding to impeller zone feeding for impeller tip speeds of 1.85, 2, and 2.32 m/s were recorded as +0.94%, -12.98%, and +5.01%, respectively. Here, '-' indicates a decrease and '+' indicates an increase in drop size. Almost no change in drop size was found at an impeller tip speed of 1.85 m/s, contrary to what was observed at the center, e/T=0, and eccentricity ratio of e/T=0.1. A slight increase in drop size was found at the highest impeller tip speed, 2.32 m/s. At the intermediate impeller tip speed, 2 m/s, drop size decreased by ~13% when the feeding condition of the dispersed phase was changed from surface feeding to impeller zone feeding.

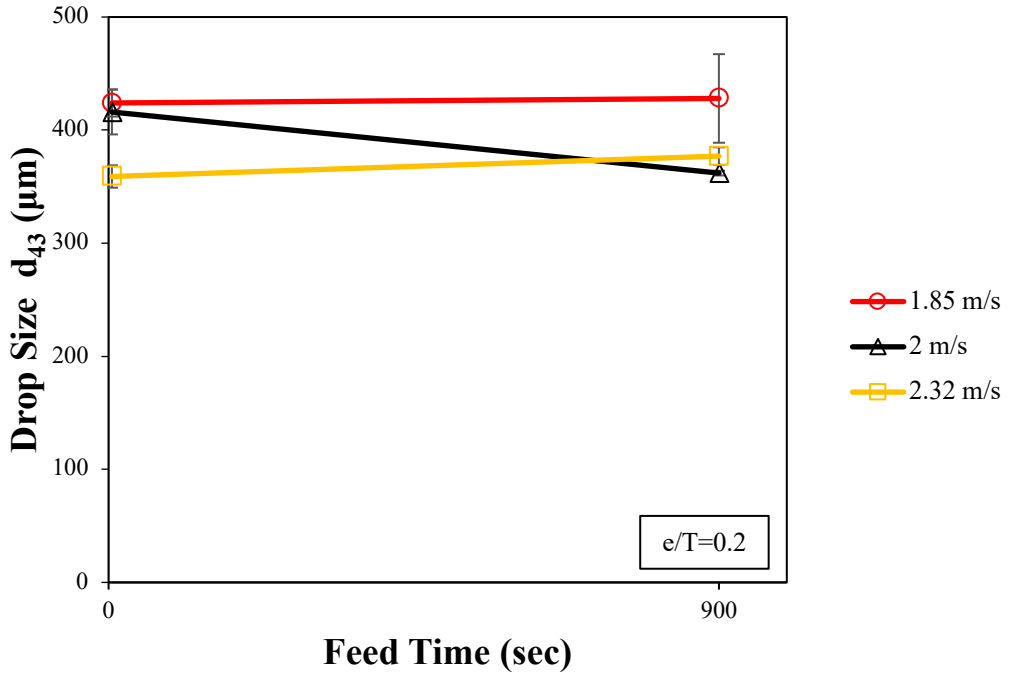

Figure 4.8. The effect of dispersed phase feeding conditions on drop size at e/T=0.2 for varying impeller tip speeds

As mentioned in section 4.1.1, moving the impeller shaft closer to tank walls, resulted in a decrease in the mean velocities throughout the tank. As a consequence of these decreased velocities, larger drops were obtained at almost all impeller tip speeds tested when the dispersed phase is fed from the liquid surface within 5 seconds for an eccentricity ratio of e/T=0.2. Musik & Talaga (2016) showed that at high eccentricity ratios of the impeller shaft, the tip of the vortex interacts with the discharge of the impeller, yielding increased velocities at the tip of the impeller. The data in Figure 4.8 shows that when the dispersed phase is fed into the impeller zone at an impeller tip speed of 2 m/s, the increased velocities at the tip of the impeller work toward decreasing the drop sizes. This discussion, however, is not valid for the highest impeller tip speed of 2.32 m/s.

A slight increase in drop size is found at the highest impeller tip speed, 2.32 m/s. When the impeller shaft is positioned at an eccentricity ratio of e/T=0.2, the distance

between the impeller blades and tank wall decreases significantly on one side of the impeller (right side on Figure 4.2c) and increases significantly on the other side of the impeller (left side on Figure 4.2c). Impeller flow pattern is affected by the decrease in the distance between the impeller blades and the tank wall since it does not have sufficient space to be properly developed. This was referred to as impeller discharge stream-wall interactions. In the impeller zone feeding, the dispersed phase is fed into the tip of the impeller blades where the distance between the impeller blades and the tank wall is smallest and therefore, the impeller discharge stream-wall interactions is the largest. As a result, the drops are quickly directed toward the coalescence zone, and they get slightly larger. The impeller discharge stream-wall interactions must have shown a major effect on the impeller flow pattern at the highest impeller tip speed of 2.32 m/s compared to other impeller tip speeds tested when the feeding conditions of the dispersed phase is changed from surface feeding to impeller zone feeding. This results in decreased impeller efficiency, yielding larger drop sizes.

This slight increase in drop size at the highest impeller tip speed, 2.32 m/s, can also be interpreted using the mean circulation time, t_{circ}. According to Leng & Calabrese (2004), circulation time refers to the time elapsed between the drops leaving the high shear zone, going to other zones of the tank and returning to the high shear zone with the help of impeller pumping rate. The circulation time for a RT can be calculated using the equation given below (Bujalski et al., 1987):

$$N\, t_{circ} = 4\left(\frac{T}{D}\right)^2 \tag{4.1}$$

In Equation 4.1, when the $\frac{T}{D}$ ratio is constant, N and t_{circ} vary inversely. The higher the impeller speed, the lower the circulation time. Tsabet & Fradette (2015a) investigated the effect of processing parameters on the production of Pickering emulsions. Their findings showed that the circulation time decreased as the impeller

speed is increased. They also stated that the adsorption rate of solid particles to the oil-water interface decreases along with the decrease in circulation time. As the particles do not have enough time to adsorb to the oil-water interface, stabilization efficiency decreases. The drops get larger, and the drop size distribution also broadens.

The purpose of feeding the dispersed phase into the impeller zone is to expose the dispersed phase to the desired high shear. If the solid particles are not adsorbed or do not have enough time to be adsorbed at the oil-water interfaces generated, the drops can be broken, but stable emulsions cannot be obtained. Broken drops coalesce and form larger drops. When the dispersed phase is fed into the impeller zone, the solid particles may not have enough time to adsorb to the oil-water interfaces at the highest impeller tip speed of 2.32 m/s due to the small circulation time and the impeller discharge stream-wall interactions; however, the data suggests that there is no such concern at an impeller tip speed of 2 m/s.

The effect of position of the impeller shaft on the width of distribution for varying dispersed phase feeding conditions is given in Figure 4.9. The smallest widths of distribution for surface feeding and impeller zone feeding were obtained when the impeller shaft is positioned at the center, e/T=0, and at the highest impeller tip speed, 2.32 m/s. When the impeller tip speed is 1.85 m/s and 2.32 m/s, the width of distribution is almost the same for surface feeding and impeller zone feeding for all positions of the impeller shaft. At an impeller tip speed of 2 m/s, however, at an eccentricity ratio of e/T=0.1 surface feeding yields ~10% smaller, and at an eccentricity ratio of e/T=0.2 surface feeding yields ~10% larger width of distribution compared to the impeller zone feeding. The presence of vortex may have an effect on fluid movement when the impeller shaft is positioned at an eccentricity ratio, e/T=0.1, and thus, large width of distribution is obtained when the feeding time of the dispersed phase is increased from 5 seconds to 900 seconds. On the other hand, the disadvantage of low velocities occurred when the impeller shaft is positioned at an eccentricity ratio, e/T=0.2, is eliminated by increasing the feeding time of the dispersed phase from 5 seconds to 900 seconds, and therefore the width of

distribution decreases. In Appendix C figures that show d_{v10}, d_{v50}, and d_{v90} data for surface and impeller zone feeding are given for all positions of the impeller shaft at varying impeller tip speeds.

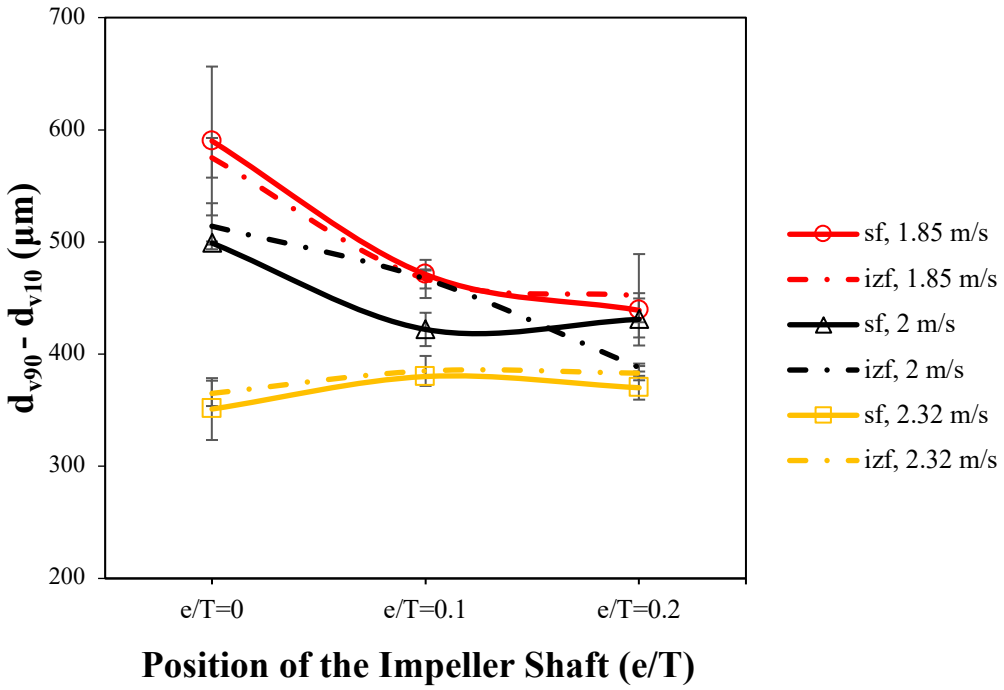

Figure 4.9. The effect of position of the impeller shaft on the width of distribution for varying feeding conditions of the dispersed phase (sf and izf are the first letters of surface feeding and impeller zone feeding, respectively)

To sum up, a significant effect of varying feeding conditions of dispersed phase on drop size and drop size distribution was seen at an impeller tip speed of 2 m/s and eccentricity ratio of e/T=0.2. According to Patterson et al. (2004), from the perspective of varying feeding conditions of the dispersed phase, the fastest dispersion of dispersed phase in the continuous phase occurs when the dispersed phase is fed into the region of the highest energy dissipation in stirred tanks.

Controlling the feed rate or feed time of the dispersed phase increases the possibility of contact between the dispersed and continuous phases in the high shear zone. Since, during surface feeding, the dispersed phase is fed into the coalescence zone, the oil tends to stay in chunks, or form large drops that tend to coalesce until they reach the high shear zone with the flow circulation. During impeller zone feeding, however, the dispersed phase is fed into the high shear zone, the drops were first exposed to the desired high shear, and smaller drops are obtained from the beginning, compared to the surface feeding.

Varying feeding conditions of the dispersed phase did not cause a reduction in drop size for all impeller tip speeds and positions of the impeller shaft tested. Leng & Calabrese (2004) stated that the dispersed phase concentration is one of the most critical parameters affecting drop coalescence. Dispersed phase concentration is usually stated as volume fraction. When the volume fraction of the dispersed phase is increased, the collision frequency between oil drops and the coalescence rate increases; therefore, drops coalesce. If the volume fraction of the dispersed phase is larger than 0.2, it is called a more concentrated system. In this study, the ratio of the dispersed phase volume to the whole tank volume was 0.3 which indicates that the oil drops are prone to coalesce. The energy given into the system may not dominate the drop breakage since it is already working in a system prone to drop coalescence, thus larger drops can be generated in some of the tested impeller tip speeds and positions of the impeller shaft.

4.2 Effect of Increasing Dispersed Phase Feed Time on Drop Size

This study aimed to investigate the effect of feeding conditions of the dispersed phase on drop size and drop size distribution in an unbaffled stirred tank. As a result of all the experiments, a significant effect of varying feeding conditions of the dispersed phase on drop size and drop size distribution was seen at an impeller tip speed of 2 m/s and eccentricity ratio of e/T=0.2. In this section, the effect of increasing dispersed phase feed time beyond the previously tested feed time on drop

size and drop size distribution is investigated using this optimum configuration. In addition to the previously tested feed time of 900 seconds, 1800 seconds and 3600 seconds were tested. The effect of increasing dispersed phase feed time on drop size and drop size distribution are given in Figures 4.10 and 4.11, respectively.

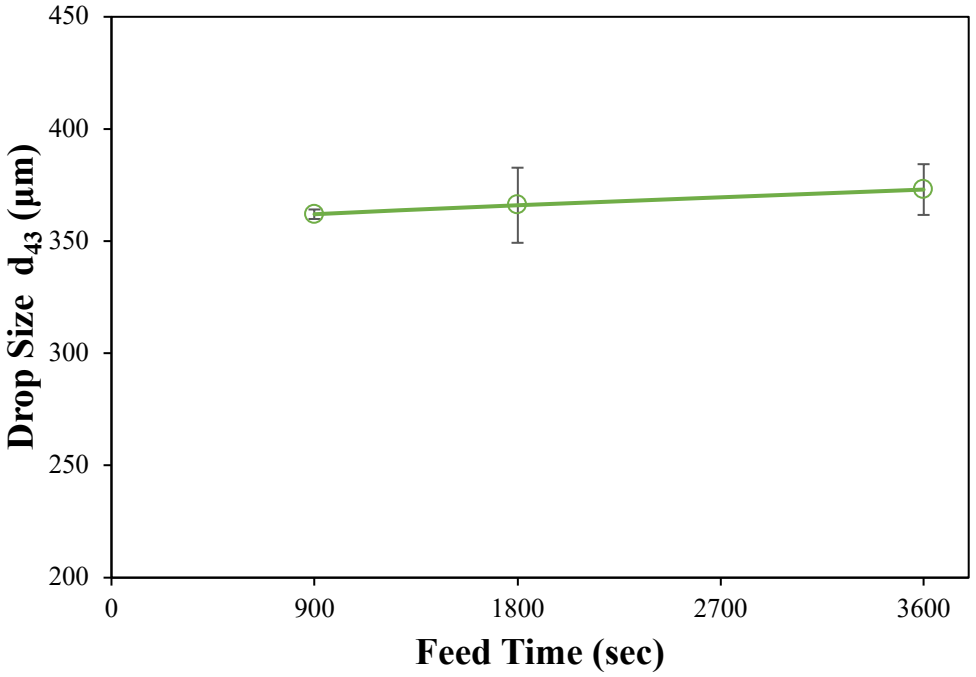

Figure 4.10. The effect of increasing dipersed phase feed time on drop size

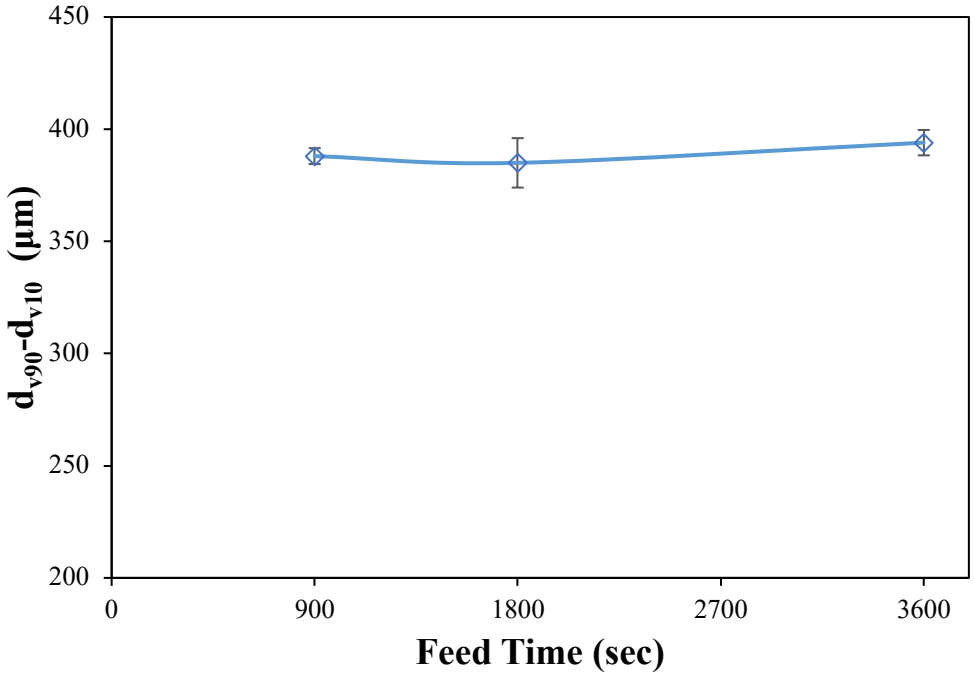

Figure 4.11. The effect of increasing dispersed phase feed time on the width of distribution

In Figures 4.10 and 4.11, no effect of feed time on drop size and drop size distribution is observed. According to Tsabet & Fradette (2015a), dispersed phase begins to break close to the impeller, in the high shear zone and thus, form oil-water interfaces. Solid particles are then adsorbed to these formed oil-water interfaces, and the emulsion drops stabilize. Some oil-water interfaces, however, are partially covered or not covered with solid particles. These partially covered or uncovered drops move to the different parts of the tank with circulation and may coalesce there, or they come back to the high shear zone and break. This flow cycle continues until all the oil-water interface that is generated is covered by solid particles and thus, the drops reach their equilibrium size and size distribution. The data suggests that feeding time of 900 seconds is sufficient to observe the advantages of feeding the dispersed phase to the high shear zone. All the oil-water interface generated is covered by solid particles and the drops reached their equilibrium size and size distributions. Further increases

in the feeding time of the dispersed phase allows for small, covered drops to circulate, but do not bring advantages toward decreasing the drop size.

Donmez & Ayranci (2020) investigated the effect of feeding conditions of the dispersed phase on drop size using a constant impeller tip speed. They used a baffled stirred tank to obtain oil-in-water Pickering emulsions. Their results showed that changing the feeding conditions of the dispersed phase from surface feeding to impeller zone feeding did not affect the drop sizes produced with RT, D=T/3. They, however, further increased the dispersed phase feed time along with decreasing the impeller tip speed and achieved a 24% reduction in drop size. This decreased impeller tip speed and increased feeding time of the dispersed phase possibly gives a good balance between sufficient breakage of drops and thus, forming oil-water interfaces and sufficient time for adsorption of solid particles at these oil-water interfaces. In our study, when the impeller shaft is positioned at an eccentricity ratio of e/T=0.2, the region that is occupied by vortex reduces; however, the vortex still present in the tank as seen in Figure 4.2c, in Section 4.1.1. The presence of vortex complicates the flow field in an unbaffled stirred tank. In the very complex flow field of unbaffled stirred tanks, no change in drop size was observed with increased feed times of the dispersed phase.

4.3 Effect of Varying Impeller Speeds During the Production Process on Drop Size

Up to this section, in all the experiments, the oil-water-solid particle mixture was continuously stirred during 1 hour at one of the pre-determined impeller tip speeds to obtain an emulsion. In this section, the effect of gradual increase of the impeller tip speed on drop size during emulsion production process is investigated. The impeller tip speed and the eccentricity ratio of the impeller shaft were fixed at 2 m/s and e/T=0.2, which is the optimum configuration where a significant effect of varying feeding conditions of the dispersed phase on drop size was seen. Increasing the impeller tip speed above 2 m/s caused the drop size to increase and the drop size

distribution to broaden at an eccentricity ratio of e/T=0.2. For this reason, 2 m/s was determined as the maximum impeller tip speed that could be reached. In order to stay in the turbulent flow regime, 1.85 m/s was determined as the minimum impeller tip speed. The total emulsification time remained the same at 1 hour. Thus, the mixture is initially stirred at an impeller tip speed of 1.85 m/s for the first 30 minutes. At the end of the first 30 minutes of mixing, a sample was taken from the tank for drop size analysis. Then, the impeller tip speed is increased to 2 m/s for the following 30 minutes of mixing without turning off the shaft motor. At the end of the second 30 minutes of mixing, a second sample was taken from the tank for drop size analysis.

The drop sizes obtained at the end of the first 30 minutes and the second 30 minutes of mixing were discussed among themselves in terms of both surface feeding and impeller zone feeding. The effect of the gradual increase of impeller tip speed on drop size for varying feeding conditions of the dispersed phase is given in Figure 4.12. The drop sizes indicated by the yellow and green arrows are the drop sizes of the emulsion for both feeding conditions when the mixture is stirred at an impeller tip speed of 1.85 m/s for the first 30 minutes, and at an impeller tip speed of 2 m/s for the second 30 minutes.

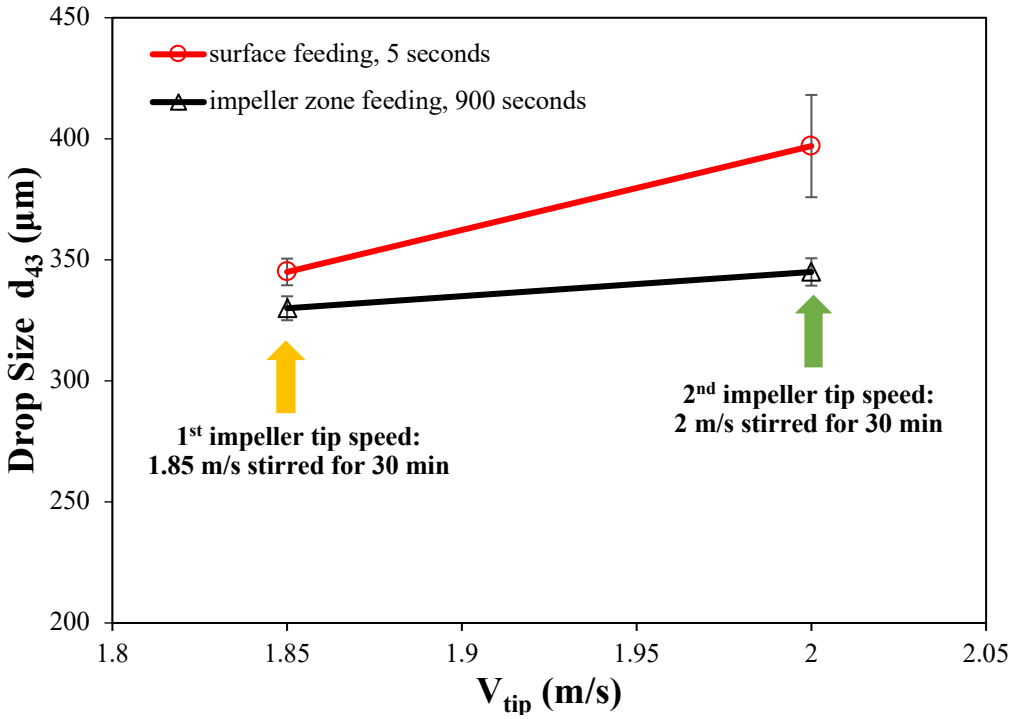

Figure 4.12. The effect of gradual increase of impeller tip speed on drop size for varying feeding conditions of the dispersed phase

Figure 4.12 shows that when the impeller tip speed is increased from 1.85 m/s to 2 m/s, the drop size increases in both feeding conditions of the dispersed phase. The increase in drop size is 13% and 4% for surface and impeller zone feeding, respectively. As can be seen both from Figure 4.12 and the percent change, the increase in drop size is more pronounced for the surface feeding of the dispersed phase.

In the first 30 minutes of this emulsion production process, with the energy given into the system, the drops break in the high shear zone and are stabilized by adsorption of solid particles at the formed oil-water interfaces. Then, when the impeller tip speed is increased to 2 m/s, the energy given into the system increases, and the drops obtained at the end of first 30 minutes of mixing begin to be broken.

Movement of the emulsion throughout the tank increases along with the increasing impeller tip speed. This increase results in a reduction in circulation time due to the fact that N and t_{circ} are inversely proportional to each other, as discussed in Section 4.1.3. As the circulation time increases, the frequency of the drops passing through the high shear zone also increases and causes the drop sizes to decrease. However, increasing the circulation time also decreases the adsorption rate of the solid particles to the oil-water interfaces. The inability of solid particles to be adsorbed on the oil-water interfaces formed may cause the drops to coalesce when the drops collide with each other. Thus, stabilization efficiency decreases, and possibly the drops obtained at the end of the first 30 minutes of mixing coalesce during the second 30 minutes of mixing, yielding larger drop sizes at the end of a total of 1 hour.

4.4 Effect of Production Process on Drop Size and Power Consumption

The effect of production process on drop size at varying feeding conditions of the dispersed phase is given in Figure 4.13. Here, Process 1 is the emulsion production process where the impeller tip speed is kept constant at 2 m/s during 1 hour of mixing and Process 2 is where the impeller tip speed is increased gradually from 1.85 m/s to 2 m/s after 30 minutes during a total of 1 hour mixing. The data shown in this figure for Process 2 constitutes part of the data shown in Figure 4.12.

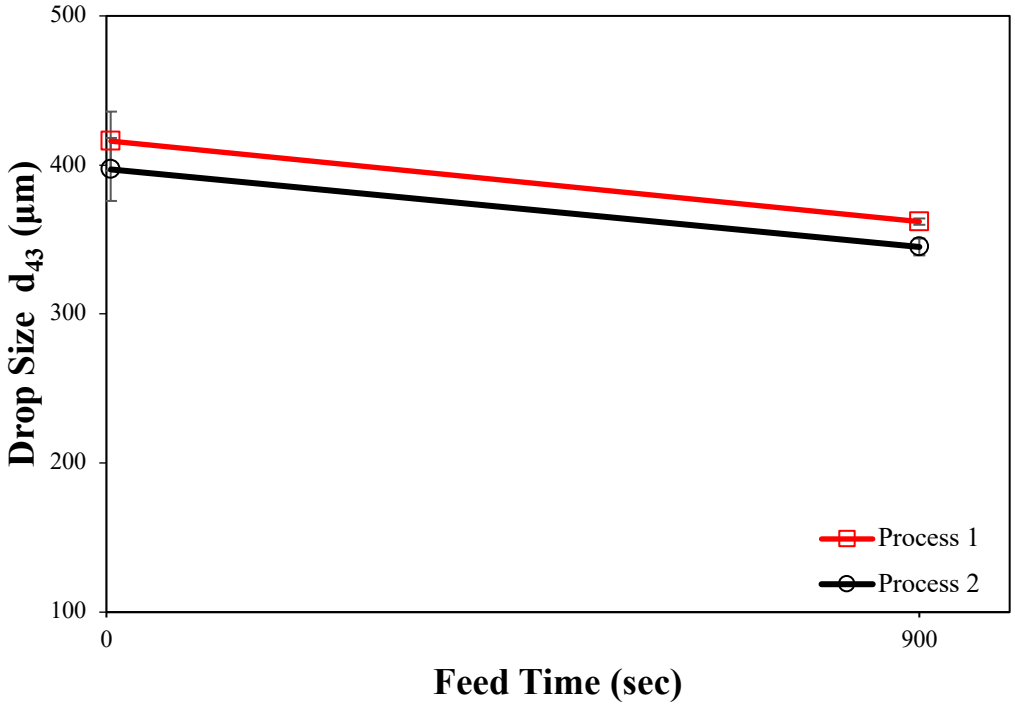

Figure 4.13. The effect of production process on drop size at varying feeding conditions of the dispersed phase

In Figure 4.13, a decrease in drop size is obtained when the feeding conditions of the dispersed phase is changed in both Process 1 and Process 2. The decrease in drop size was found as 13.10% for Process 2. The decrease in drop size had been found as 13% for Process 1, as mentioned in Section 4.1.3. This result shows that the varying production process for the ZnO stabilized Pickering emulsion did not further affect the change in drop size when the feeding conditions of the dispersed phase is changed from surface feeding to impeller zone feeding. This, however, is not completely valid in terms of drop size. In Figure 4.13, the drop sizes obtained by Process 2 are smaller than drop sizes obtained by Process 1 by 4.56% and 4.70% for surface feeding and impeller zone feeding, respectively.

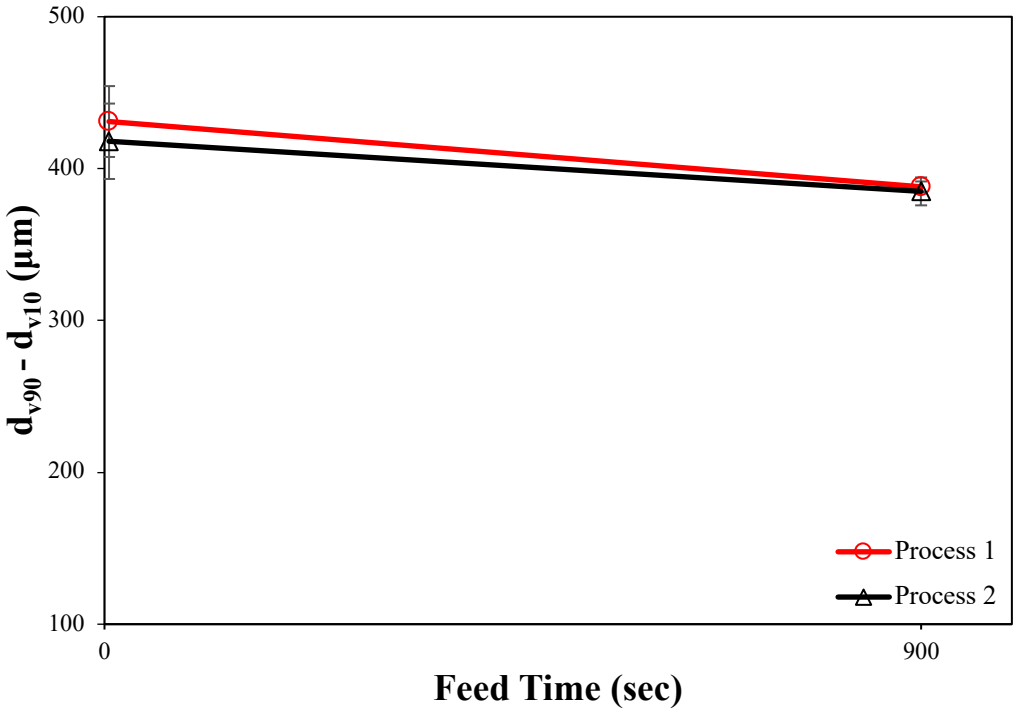

Figure 4.14. The effect of production process on the width of distribution at varying feeding conditions of the dispersed phase

The effect of production process on drop size distribution at varying feeding conditions of the dispersed phase is given in Figure 4.14. A decrease in the widths of distribution was observed in both Process 1 and Process 2 when the feeding time of the dispersed phase is changed from 5 seconds to 900 seconds. Both processes gave almost the same widths of distribution.

Based on these results, there is not much difference in the final emulsion drop sizes at the end of the two processes. In one of the processes, however, the emulsion production is at a much lower impeller tip speed. Next, these processes are compared in terms of power consumption since in industry, the ultimate goal is to produce the target product while keeping the cost of the process at a minimum value. Power consumption (P) can be calculated using Equation 2.3 which is given in Section 2.1.1.1. The power consumption increases or decreases in direct proportion to the

increase or decrease in the power number of an impeller, continuous phase density, impeller speed, and impeller diameter, as can be seen from Equation 2.3. The only parameter that varies between the two emulsion production processes is the impeller tip speed. The power consumption of Process 1 was calculated as 0.00153 kWh and the power consumption of Process 2 was calculated as 0.00137 kWh.

As a result, nearly identical changes in drop size are obtained when the emulsion production process is changed from Process 1 to Process 2, but in the case of Process 2, the power consumption is reduced by ~10.5%. Considering the fact that Process 2 gives better result in terms of power consumption than Process 1, producing Pickering emulsions by Process 2 which is gradually increasing the impeller tip speed was found to be more efficient than Process 1.

CHAPTER 5

SUMMARY, OUTCOMES AND FUTURE WORK

5.1 Summary and Outcomes

In this thesis, the effect of varying feeding conditions of the dispersed phase on drop size of Pickering emulsions was investigated. Silicone oil and UP water were selected as dispersed and continuous phases, respectively. Zinc-oxide solid particle stabilized oil-in-water Pickering emulsions were produced. Unbaffled stirred tank was used to produce o/w Pickering emulsions. A standard six bladed RT - T/3 was used as impeller. Three positions were used for the impeller shaft: at the center, e/T=0 and at two eccentric positions, e/T=0.1 and e/T=0.2. Three impeller tip speeds – 1.85, 2 and 2.32 m/s –, all corresponding to turbulent flow regime, were tested. The feeding of the dispersed phase was done in the tank either from the liquid surface within 5 seconds which is referred to as surface feeding, or into the impeller zone over 900 seconds which is referred to as impeller zone feeding. The drop size and drop size distribution analysis was done using Malvern Mastersizer 3000. The outcomes of this thesis are listed as follows:

- In general, the drop sizes decreased as the impeller tip speed is increased for all positions of the impeller shaft. For both feeding conditions of the dispersed phase (surface and impeller zone), the smallest drop size was obtained at an eccentricity ratio of e/T=0.1, at the highest impeller tip speed, 2.32 m/s. When the dispersed phase is fed into the impeller zone smaller drop sizes were obtained. Based on these results, feeding the dispersed phase into the impeller zone was found more effective in obtaining smaller drop sizes.

- The central vortex occupies a large region in the tank when the impeller shaft is positioned at the center, e/T=0. When the impeller tip speed is increased, the region occupied by the central vortex also increases. In this case, the impeller may remain within the central vortex as the depth of the vortex reaches impeller blades. When the eccentricity ratio of the impeller shaft is increased from e/T=0 to e/T=0.2, the shape and length of the vortex changed and its contact between impeller blades reduces. For both feeding conditions of the dispersed phase, however, the largest drop sizes were obtained at an eccentricity ratio of e/T=0.2 compared to the other positions of the impeller shaft even though the contact between the impeller blades and vortex is reduced.

- The increased discharge stream-wall interactions, the decrease in the mean velocities and the presence of vortex and its connection between the impeller blades were found as possible reasons for obtaining the larger drop sizes at an eccentricity ratio of e/T=0.2.

- In general, the width of distribution decreased as the impeller tip speed is increased for all positions of the impeller shaft. For both feeding conditions of the dispersed phase, the most pronounced reduction in the width of distribution was found when the impeller shaft is positioned at the center, e/T=0. This result neutralized the advantage of impeller shaft eccentricity on drop size distribution.

- When the feeding conditions of the dispersed phase was changed from surface feeding to impeller zone feeding, a significant change in drop size and drop size distribution was found at an eccentricity ratio, e/T=0.2, and at the impeller tip speed of 2 m/s. This configuration was designated as the optimum configuration.

- It was found that increasing the feeding time of the dispersed phase from 900 seconds to 1800 seconds and 3600 seconds had no effect on drop size and drop size distribution. This result indicates that 900 second of feeding time of the dispersed phase was sufficient to observe the constituted balance between the drop breakage and the adsorption of solid particles to the oil-water interface and the drops reached their equilibrium sizes and size distribution.

- In the process where the impeller tip speed was gradually increased at 30 minutes intervals during emulsion production, it was found that drop sizes increased for both feeding conditions of the dispersed phase when the impeller tip speed is increased from 1.85 m/s to 2 m/s. These results indicate that the energy given into the system should be chosen in a such a way that it provides the sufficient time for solid particles to be adsorbed at the oil-water interfaces generated.

- When the emulsion production process was changed from Process 1 which is impeller tip speed is kept constant at 2 m/s during 1 hour of mixing to Process 2 which is impeller tip speed is gradually increased at 30 minutes intervals from 1.85 m/s to 2 m/s, almost the same drop size and drop size distribution were obtained. But Process 2 was found to be more efficient than Process 1 in terms of power consumption.

5.2 Future Work

In this thesis, the effect of varying feeding conditions of the dispersed phase on drop size was investigated. The physicochemical properties of the emulsion components were kept constant. The focus was on the effect of different processing parameters and unbaffled stirred tank hydrodynamics on drop size. Some research topics that can be investigated based on the conclusions of this thesis can be listed as follows:

- The solid particle to be used in Pickering emulsion production is important for both emulsion formation and emulsion stabilization. Different type of solid particle can be used, and the results obtained can be compared with the conclusions of this thesis.

- Impeller off-bottom clearance (C) is one of the geometric parameters affecting the mixing performance. The flow pattern of the impeller may affect as the impeller off-bottom clearance is changed. The effect of different impeller off-bottom clearance on drop size can be tested.

- Pickering emulsions can be produced by increasing or decreasing the impeller speed at more than one-time intervals. The results obtained can be compared with the conclusions of this thesis.

- In unbaffled stirred tanks, the velocity profile of the oil-water mixture can be developed for all positions of the impeller shaft. The drop sizes obtained for all positions of the impeller shaft in this thesis can be interpreted with the obtained velocity profile.

- Multiple impellers can be used for emulsion production. Radial flow impellers generate high shear around the impeller, and they are commonly preferred for emulsion production. Axial or mixed flow impellers are used for solids suspension. More than one radial flow impeller can be used simultaneously to provide more shear on the system, or radial and axial flow impellers can be used simultaneously to ensure both the breaking the drops into smaller ones and suspension of the solid particles. Thus, the effect of multiple impellers on drop size can be tested.

REFERENCES

Aveyard, R., Binks, B. P., Clint, J.H., Emulsions stabilised solely by colloidal particles, Advances in Colloid and Interface Science 100–102 (2003) 503–546. https://doi.org/10.1016/S0001-8686(02)00069-6

Arditty, S., Whitby, C. P., Binks, B. P., Schmitt, V., and Leal-Calderon, F., Some general features of limited coalescence in solid-stabilized emulsions, Eur. Phys. J. E 11, (2003) 273–281.

Binks, B. P. Emulsions – Recent Advances in Understanding in Modern Aspects of Emulsion Science, ed. B. P. Binks, Royal Society of Chemistry, Cambridge, 1998, pp. 1-48.

Binks, B. P. Particles as surfactants- Similarities and differences. Current Opinion in Colloid and Interface Science, 7(1–2), 21–41 (2002). https://doi.org/10.1016/S1359-0294(02)00008-0

Binks, B. P. & Lumsdon, S. O., Influence of Particle Wettability on the Type and Stability of Surfactant-Free Emulsions, Langmuir, 16, 8622-8631 (2000). Doi:10.1021/la000189s

Chesters, A. K., The modelling of coalescence process in fluid-liquid dispersions: a review of current understanding. Chem. Eng. Res. Des. 69, 259-270 (1991).

Chevalier, Y. & Bolzinger, M.A., Emulsions stabilized with solid nanoparticles: Pickering emulsions. Colloids and Surfaces A: Physicochem. Eng. Aspects 439 23–34 (2013).

Costes, J., and J. P. Couderc. Influence of the size of the Units-II. Spectral Analysis and Scales of Turbulence. Chem. Eng. Sci., 43, 2765 (1988).

D.E. Leng, R.V. Calabrese, Immiscible liquid–liquid systems, in: E.L. Paul, V.A. Aiemo Obeng, S.M. Kresta (Eds.), Handbook of Industrial Mixing, Handbook of Industrial Mixing, John Wiley & Sons, 2004, pp. 639–754.

D.J. McClements, Food Emulsions: Principles, Practice and Techniques, CRC Press, Boca Raton, 1999.

Demirdogan, O. Effect of hydrodynamics on the production of Pickering emulsions in unbaffled stirred tanks. [Master's Thesis, METU]. METU Theses Collection, (2019). http://etd.lib.metu.edu.tr/upload/12624611/index.pdf

Donmez D, Ayranci I. Effect of dispersed phase feed time on the droplet size of Pickering emulsions produced in a stirred tank. AIChE J. 2020;66: e169142. https://doi.org/10.1002/aic.16942

Doran, P. M. In Bioprocess Engineering Principles, 300-303, Academic Press, London, (1995).

EL-Hamouz, A., Cooke, M., Kowalski, A., & Sharratt, P. Dispersion of silicone oil in water surfactant solution: Effect of impeller speed, oil viscosity and addition point on drop size distribution. Chemical Engineering and Processing: Process Intensification, 48(2), 633–642 (2009).

G.K. Patterson, E.L. Paul, S.M. Kresta, A.W. Etchells III. Mixing and Chemical Reactions, in: E.L. Paul, V.A. Aiemo Obeng, S.M. Kresta (Eds.), Handbook of Industrial Mixing, Handbook of Industrial Mixing, John Wiley & Sons, 2004, pp. 755-868.

Gelot, A., Friesen, W., Hamza, H. A. Emulsification of oil and water in the presence of finely divided solids and surface-active agents, Colloids and Surfaces, 12, 271-303 (1984).

Hall, J.F., Barigou, M., Simmons, M. J. H., Stitt, E. H. Mixing in Unbaffled High-Throughput Experimentation Reactors. Ind. Eng. Chem. Res., 43, 4149-4158, (2004).

J. H. Schulmann & J. Leja, Control of Contact Angles at the Oil-Water-Solid Interfaces, Trans. Far. Soc. 50, 598 (1954).

Karcz, J., Szoplik, J., An effect of the eccentric position of the propeller agitator on the mixing time. Chemical Papers 58 (1), 9–14 (2004).

Kołodziejczak-Radzimska, A. and Jesionowski, T. Zinc Oxide- From Synthesis to Application: A Review. Materials, 7, 2833-2881, (2014).

Kumaresan, T., Nere, N. K., and Joshi, J. B. Ind. Eng. Chem. Res., 44, 9951-9961 (2005).

Lemenand, T., Della Valle, D., Zellouf, Y., and Peerhossaini, H. Int. J. Multiph. Flow, 29, 813-840 (2003).

Li, X., Li, J., Gong, J., Kuang, Y., Mo, L., Song, T. Cellulose nanocrystals (CNCs) with different crystalline allomorph for oil in water Pickering emulsions. Carbohydrate Polymers 183, 303–310 (2018).

Lopetinsky, R.J.G., Masliyah, J.H., Xu, Z. Solids-Stabilized Emulsions: A Review. In, Binks, B. P. & Horozov, T. S. Colloidal Particles at Liquid Interfaces. Cambridge University Press, New York (2006). pp. 186-225.

Mastersizer 3000 User Manual. MAN0474 Issue 2.1, Malvern Instruments Ltd (2013).

Montante, G., Mostek, M., Jahode, M., and Magelli, F. Chem. Eng. Sci., 60, 2427-2437 (2005).

Musik, M. & Talaga, J. Investigation of Fluid Dynamics in an Unbaffled Stirred Vessel with an Eccentrically Located Rushton Turbine. Technical Transactions Mechanics, 2-M (2016).

Nienow, A. W. Chem. Eng. Sci., 52, 2557-2565 (1997).

Norwood, K. W., Metzner, A. B. Flow Patterns and Mixing Rates in Agitated Vessels. AIChE Journal, (1960).

P. Finkle, H.D. Draper & J. H. Hildebrand, The Theory of Emulsification, J. Am. Chem. Soc., 45, 2780 (1923).

Paul, E. L., & Victor A. Atiemo-Obeng, and S. M. K. Introduction. In: Paul EL, Atiemo-Obeng VA, Kresta. SM, eds. Handbook of Industrial Mixing: Science and Practice. John Wiley & Sons, Inc. (2004).

Roscoe, R. The viscosity of suspensions of rigid spheres. Br. J. Appl. Phys. 3 267, (1952).

S.U. Pickering, Emulsions, J. Chem. Soc. 91, 2001–2021 (1907).

Szoplik, J & Karcz, J. Mixing time of a non-newtonian liquid in an unbaffled agitated vessel with an eccentric propeller. Chemical Papers 62 (1) 70-77 (2008).

Tambe, D. E. & Sharma M. M., The Effect of Colloidal Particles on Fluid-Fluid Interfacial Properties and Emulsion Stability, Advances in Colloid and Interface Science, 52, l-63 (1994).

Tsabet, E. & Fradette, L., Effect of Processing Parameters on the Production of Pickering Emulsions, Ind. Eng. Chem. Res., 54, 2227−2236 (2015a). DOI: 10.1021/ie504338d

Tsabet, E. & Fradette, L., Effect of the properties of oil, particles, and wateron the production of Pickering emulsions, Chemical Engineering Research and Design 97, 9-17 (2015b). http://dx.doi.org/10.1016/j.cherd.2015.02.016

Tsabet, E. & Fradette, L., Semiempirical Approach for Predicting the Mean Size of Solid-Stabilized Emulsions, Ind. Eng. Chem. Res., 54, 11661−11677 (2015c). DOI: 10.1021/acs.iecr.5b02910

V. B. Menon & D. T. Wasan. A Review of the Factors Affecting the Stability of Solids-Stabilized Emulsions, Separation Science and Technology, 23:12-13, 2131-2142 (1988). DOI: 10.1080/01496398808075687

Vignati, E., Piazza, R. Lockhart, T. P. Pickering Emulsions: Interfacial Tension, Colloidal Layer Morphology, and Trapped-Particle Motion., Langmuir, 19, 6650-6656 (2003). Doi: 10.1021/la034264l

W. Bujalski, A.W. Nienow, S. Chatwin, M. Cooke, The dependency on scale of power numbers of Rushton disc turbines, Chem. Eng. Sci. 42, 317– 326 (1987).

W. Ramsden, Separation of solids in the surface-layers of solutions and 'suspensions', Proc. Royal Soc. London 72, 156–164 (1903).

Yang Y., Fang Z., Chen X., Zhang W., Xie Y., Chen Y., Liu Z. and Yuan W. An Overview of Pickering Emulsions: Solid-Particle Materials, Classification, Morphology, and Applications. Front. Pharmacol. 8:287 (2017). doi:10.3389/fphar.2017.00287

Zhou, G., Kresta, S. M. Correlation of mean drop size and minimum drop size with the turbulence energy dissipation and the flow in an agitated tank. Chemical Engineering Science, 53(11), 2063-2079 (1998).

Zhou, G., Kresta, S. M. Impact of Tank Geometry on the Maximum Turbulence Energy Dissipation Rate for Impellers. AIChE Journal, 42, 2476-2490 (1996).

APPENDICES

A. MATLAB and Arduino Codes

MATLAB code

Gui.m

```
function varargout = GUI(varargin)
% GUI MATLAB code for GUI.fig
%      GUI, by itself, creates a new GUI or raises the existing
%      singleton*.
%
%      H = GUI returns the handle to a new GUI or the handle to
%      the existing singleton*.
%
%      GUI('CALLBACK',hObject,eventData,handles,...) calls the
local
%      function named CALLBACK in GUI.M with the given input
arguments.
%
%      GUI('Property','Value',...) creates a new GUI or raises the
%      existing singleton*.  Starting from the left, property value
pairs are
%      applied to the GUI before GUI_OpeningFcn gets called.  An
%      unrecognized property name or invalid value makes property
application
%      stop.  All inputs are passed to GUI_OpeningFcn via varargin.
%
%      *See GUI Options on GUIDE's Tools menu.  Choose "GUI allows
only one
%      instance to run (singleton)".
%
% See also: GUIDE, GUIDATA, GUIHANDLES
```

```
% Edit the above text to modify the response to help GUI

% Last Modified by GUIDE v2.5 23-Dec-2020 20:47:00

% Begin initialization code - DO NOT EDIT
gui_Singleton = 1;
gui_State = struct('gui_Name',       mfilename, ...
    'gui_Singleton',  gui_Singleton, ...
    'gui_OpeningFcn', @GUI_OpeningFcn, ...
    'gui_OutputFcn',  @GUI_OutputFcn, ...
    'gui_LayoutFcn',  [] , ...
    'gui_Callback',   []);
if nargin && ischar(varargin{1})
    gui_State.gui_Callback = str2func(varargin{1});
end

if nargout
    [varargout{1:nargout}] = gui_mainfcn(gui_State, varargin{:});
else
    gui_mainfcn(gui_State, varargin{:});
end
% End initialization code - DO NOT EDIT

% --- Executes just before GUI is made visible.
function GUI_OpeningFcn(hObject, eventdata, handles, varargin)
% This function has no output args, see OutputFcn.
% hObject    handle to figure
% eventdata  reserved - to be defined in a future version of MATLAB
% handles    structure with handles and user data (see GUIDATA)
% varargin   command line arguments to GUI (see VARARGIN)
```

```
t =
timer('TimerFcn',{@(~,~)datetimer(handles)},'Period',1,'ExecutionMo
de','fixedRate');

start(t);

handles.arduPortNum=get(handles.arduPort,'String');

handles.balancePortNum=get(handles.balancePort,'String');

handles.serialports=IDSerialComs;

set(handles.popupmenu2,'String',[]);

[m,n]=size(handles.serialports);

if m==0

    handles.names{1}=['No SERIALCOMM'];

else

    for i= 1: m

        handles.names{i}=[handles.serialports{i,1},'
COM',num2str(handles.serialports{i,2})];

    end

end

set(handles.popupmenu2,'String',handles.names);

instrreset;

try


handles.balance=serial(['COM',handles.balancePortNum],'BaudRate',96
00);


handles.ardu=serial(['COM',handles.arduPortNum],'BaudRate',9600);

    fopen(handles.ardu);

catch

    warndlg('Please Choose Correct Ports')

end

%fopen(handles.balance);


axes(handles.axes1);

imshow('odtu.jpg');


% Choose default command line output for GUI
```

```
handles.output = hObject;

% Update handles structure
guidata(hObject, handles);

% UIWAIT makes GUI wait for user response (see UIRESUME)
% uiwait(handles.figure1);

% --- Outputs from this function are returned to the command line.
function varargout = GUI_OutputFcn(hObject, eventdata, handles)
% varargout  cell array for returning output args (see VARARGOUT);
% hObject    handle to figure
% eventdata  reserved - to be defined in a future version of MATLAB
% handles    structure with handles and user data (see GUIDATA)

% Get default command line output from handles structure

varargout{1} = handles.output;

function curWeight=curWeightCalc(s1)
try
    fopen(s1);
end
fprintf(s1,'IP');
pause(0.01)
fscanf(s1);
fscanf(s1);
fscanf(s1);
fscanf(s1);
fscanf(s1);
fscanf(s1);
gr=fscanf(s1);
```

```
curWeight=str2double(gr(1:6));%in gr
fclose(s1);

% --- Executes on button press in pushbutton1.
function pushbutton1_Callback(hObject, eventdata, handles)
% hObject    handle to pushbutton1 (see GCBO)
% eventdata  reserved - to be defined in a future version of MATLAB
% handles    structure with handles and user data (see GUIDATA)
% timeSamp=1;
pwmEst=100;

estpwmPerkgs=(pwmEst/14.4)*2; %kg/s per pwm  14.4*2 Ã§alÄ±ÅŸÄ±yor.
errorInt=0;

flowRat=str2double(get(handles.flowRate,'String')); %in gr/s
dur=str2double(get(handles.expDur,'String'));

targetWeight=flowRat*dur;
set(handles.targetvalue,'String',num2str(targetWeight));
set(handles.curFlow,'String',num2str(0.00));
set(handles.pumpedOil,'String',num2str(0.00));
set(handles.timeElap,'String',num2str(0.00));
try
    initialWeight=curWeightCalc(handles.balance);
    set(handles.balanceCur,'String',num2str(initialWeight));
    flowRateCur=flowRat;
    count=0;
    pumpedOil=0;
    try
        fopen(handles.ardu);
    end
    fprintf(handles.ardu,'%u',pwmEst);
```

```
    tIni=tic;
    set(handles.statu,'String','Running')


    while targetWeight-pumpedOil>=0.01 || toc(tIni) <
str2double(handles.expDur.String)


        curWeight=curWeightCalc(handles.balance);
        tcur=toc(tIni);
        Wref=initialWeight-flowRat*tcur;
        errorFlow=(curWeight-Wref)*estpwmPerkgs;
        errorInt=errorInt+errorFlow;
        a=double(int16(pwmEst+errorFlow+errorInt*0.1));
        %estpwmPerkgs=(a/14.4)*2; %kg/s per pwm  14.4*2
Ã§alÄ±ÅŸÄ±yor.
        if a<100 && a~=0
            a=10;
        end
        if a>255
            a=255;
        end
        fprintf(handles.ardu,'%u',a);
        set(handles.balanceCur,'String',num2str(curWeight))


        set(handles.pwmShow,'String',num2str(a));


        set(handles.curFlow,'String',num2str(curWeight-Wref));
        set(handles.pumpedOil,'String',num2str(pumpedOil));
        set(handles.timeElap,'String',num2str(toc(tIni)));


        pumpedOil=initialWeight-curWeight;
    end


    fprintf(handles.ardu,'%u',0);
```

```
    set(handles.timeElap,'String',num2str(toc(tIni)));

    % pause(2);
    set(handles.statu,'String','Completed')

    curWeight=curWeightCalc(handles.balance);
    set(handles.balanceCur,'String',num2str(curWeight));

    pumpedOil=initialWeight-curWeight;
    set(handles.pumpedOil,'String',num2str(pumpedOil));
catch
    warndlg('Please Choose Correct Ports')
    set(handles.statu,'String','COM ERR')
end

function flowRate_Callback(hObject, eventdata, handles)
% hObject    handle to flowRate (see GCBO)
% eventdata  reserved - to be defined in a future version of MATLAB
% handles    structure with handles and user data (see GUIDATA)
% Hints: get(hObject,'String') returns contents of flowRate as text
%        str2double(get(hObject,'String')) returns contents of
flowRate as a double
flowRat=str2double(get(handles.flowRate,'String')); %in gr/sec
dur=str2double(get(handles.expDur,'String'));
set(handles.targetvalue,'String',num2str(flowRat*dur));

% --- Executes during object creation, after setting all
properties.
function flowRate_CreateFcn(hObject, eventdata, handles)
% hObject    handle to flowRate (see GCBO)
% eventdata  reserved - to be defined in a future version of MATLAB
% handles    empty - handles not created until after all CreateFcns
called
```

```
% Hint: edit controls usually have a white background on Windows.
%       See ISPC and COMPUTER.
if ispc && isequal(get(hObject,'BackgroundColor'),
get(0,'defaultUicontrolBackgroundColor'))
    set(hObject,'BackgroundColor','white');
end


function expDur_Callback(hObject, eventdata, handles)
% hObject    handle to expDur (see GCBO)
% eventdata  reserved - to be defined in a future version of MATLAB
% handles    structure with handles and user data (see GUIDATA)


% Hints: get(hObject,'String') returns contents of expDur as text
%        str2double(get(hObject,'String')) returns contents of
expDur as a double
flowRat=str2double(get(handles.flowRate,'String')); %in gr/s
dur=str2double(get(handles.expDur,'String'));
set(handles.targetvalue,'String',num2str(flowRat*dur));


% --- Executes during object creation, after setting all
properties.
function expDur_CreateFcn(hObject, eventdata, handles)
% hObject    handle to expDur (see GCBO)
% eventdata  reserved - to be defined in a future version of MATLAB
% handles    empty - handles not created until after all CreateFcns
called


% Hint: edit controls usually have a white background on Windows.
%       See ISPC and COMPUTER.
if ispc && isequal(get(hObject,'BackgroundColor'),
get(0,'defaultUicontrolBackgroundColor'))
    set(hObject,'BackgroundColor','white');
end
```

```
function arduPort_Callback(hObject, eventdata, handles)
% hObject    handle to arduPort (see GCBO)
% eventdata  reserved - to be defined in a future version of MATLAB
% handles    structure with handles and user data (see GUIDATA)

% Hints: get(hObject,'String') returns contents of arduPort as text
%        str2double(get(hObject,'String')) returns contents of
arduPort as a double
handles.arduPortNum=get(handles.arduPort,'String');
handles.balancePortNum=get(handles.balancePort,'String');
instrreset;
try

handles.balance=serial(['COM',handles.balancePortNum],'BaudRate',96
00);

handles.ardu=serial(['COM',handles.arduPortNum],'BaudRate',9600);
    fopen(handles.ardu);
catch
    warndlg('Please Choose Correct Ports')
end
handles.output = hObject;

% Update handles structure
guidata(hObject, handles);

% --- Executes during object creation, after setting all
properties.
function arduPort_CreateFcn(hObject, eventdata, handles)
% hObject    handle to arduPort (see GCBO)
% eventdata  reserved - to be defined in a future version of MATLAB
% handles    empty - handles not created until after all CreateFcns
called
```

```
% Hint: edit controls usually have a white background on Windows.
%       See ISPC and COMPUTER.
if ispc && isequal(get(hObject,'BackgroundColor'),
get(0,'defaultUicontrolBackgroundColor'))
    set(hObject,'BackgroundColor','white');
end


function balancePort_Callback(hObject, eventdata, handles)
% hObject    handle to balancePort (see GCBO)
% eventdata  reserved - to be defined in a future version of MATLAB
% handles    structure with handles and user data (see GUIDATA)


% Hints: get(hObject,'String') returns contents of balancePort as
text
%        str2double(get(hObject,'String')) returns contents of
balancePort as a double
handles.arduPortNum=get(handles.arduPort,'String');
handles.balancePortNum=get(handles.balancePort,'String');
instrreset;
try



handles.balance=serial(['COM',handles.balancePortNum],'BaudRate',96
00);

handles.ardu=serial(['COM',handles.arduPortNum],'BaudRate',9600);
    fopen(handles.balance);
catch
    warndlg('Please Choose Correct Ports')
end


handles.output = hObject;
% Update handles structure
```

```
guidata(hObject, handles);


% --- Executes during object creation, after setting all
properties.
function balancePort_CreateFcn(hObject, eventdata, handles)
% hObject    handle to balancePort (see GCBO)
% eventdata  reserved - to be defined in a future version of MATLAB
% handles    empty - handles not created until after all CreateFcns
called


% Hint: edit controls usually have a white background on Windows.
%       See ISPC and COMPUTER.
if ispc && isequal(get(hObject,'BackgroundColor'),
get(0,'defaultUicontrolBackgroundColor'))
    set(hObject,'BackgroundColor','white');
end


function targetvalue_Callback(hObject, eventdata, handles)
% hObject    handle to targetvalue (see GCBO)
% eventdata  reserved - to be defined in a future version of MATLAB
% handles    structure with handles and user data (see GUIDATA)


% Hints: get(hObject,'String') returns contents of targetvalue as
text
%        str2double(get(hObject,'String')) returns contents of
targetvalue as a double
flowRat=str2double(get(handles.flowRate,'String')); %in gr/s
dur=str2double(get(handles.expDur,'String'));
set(handles.flowRate,'String',num2str(str2double(handles.targetvalu
e.String)/dur));


% --- Executes during object creation, after setting all
properties.
function targetvalue_CreateFcn(hObject, eventdata, handles)
% hObject    handle to targetvalue (see GCBO)
```

```
% eventdata  reserved - to be defined in a future version of MATLAB
% handles    empty - handles not created until after all CreateFcns
called


% Hint: edit controls usually have a white background on Windows.
%       See ISPC and COMPUTER.
if ispc && isequal(get(hObject,'BackgroundColor'),
get(0,'defaultUicontrolBackgroundColor'))
    set(hObject,'BackgroundColor','white');
end


% --- Executes on button press in stopbutton.
function stopbutton_Callback(hObject, eventdata, handles)
% hObject    handle to stopbutton (see GCBO)
% eventdata  reserved - to be defined in a future version of MATLAB
% handles    structure with handles and user data (see GUIDATA)
try
    fprintf(handles.ardu,'%u',0);
    set(handles.statu,'String','STOP')
catch
    warndlg('Please Choose Correct Ports')
    set(handles.statu,'String','COM ERR')
end


% --- Executes during object creation, after setting all
properties.
function stopbutton_CreateFcn(hObject, eventdata, handles)
% hObject    handle to stopbutton (see GCBO)
% eventdata  reserved - to be defined in a future version of MATLAB
% handles    empty - handles not created until after all CreateFcns
called


function popupmenu2_Callback(hObject, eventdata, handles)
% hObject    handle to stopbutton (see GCBO)
```

```
% eventdata  reserved - to be defined in a future version of MATLAB
% handles    structure with handles and user data (see GUIDATA)


% --- Executes during object creation, after setting all
properties.
function popupmenu2_CreateFcn(hObject, eventdata, handles)
% hObject    handle to popupmenu2 (see GCBO)
% eventdata  reserved - to be defined in a future version of MATLAB
% handles    empty - handles not created until after all CreateFcns
called


% Hint: popupmenu controls usually have a white background on
Windows.
%       See ISPC and COMPUTER.
if ispc && isequal(get(hObject,'BackgroundColor'),
get(0,'defaultUicontrolBackgroundColor'))
    set(hObject,'BackgroundColor','white');
end


function devices = IDSerialComs()
% IDSerialComs identifies Serial COM devices on Windows systems by
friendly name
% Searches the Windows registry for serial hardware info and
returns devices,
% a cell array where the first column holds the name of the device
and the
% second column holds the COM number. Devices returns empty if
nothing is found.


try
    devices = [];
    Skey = 'HKEY_LOCAL_MACHINE\HARDWARE\DEVICEMAP\SERIALCOMM';
    [~, list] = dos(['REG QUERY ' Skey]);
    if ischar(list) && strcmp('ERROR',list(1:5))
%         disp('Error: IDSerialComs - No SERIALCOMM registry
entry')
```

```
        return;
    end
    list = strread(list,'%s','delimiter',' '); %#ok<FPARK> requires
strread()
    coms = 0;
    for i = 1:numel(list)
        if strcmp(list{i}(1:3),'COM')
            if ~iscell(coms)
                coms = list(i);
            else
                coms{end+1} = list{i}; %#ok<AGROW> Loop size is
always small
            end
        end
    end
    key = 'HKEY_LOCAL_MACHINE\SYSTEM\CurrentControlSet\Enum\USB\';
    [~, vals] = dos(['REG QUERY ' key ' /s /f "FriendlyName" /t
"REG_SZ"']);
    if ischar(vals) && strcmp('ERROR',vals(1:5))
        disp('Error: IDSerialComs - No Enumerated USB registry
entry')
        return;
    end
    vals = textscan(vals,'%s','delimiter','\t');
    vals = cat(1,vals{:});
    out = 0;
    for i = 1:numel(vals)
        if strcmp(vals{i}(1:min(12,end)),'FriendlyName')
            if ~iscell(out)
                out = vals(i);
            else
                out{end+1} = vals{i}; %#ok<AGROW> Loop size is
always small
            end
        end
```

```
    end
    for i = 1:numel(coms)
        match = strfind(out,[coms{i},')']);
        ind = 0;
        for j = 1:numel(match)
            if ~isempty(match{j})
                ind = j;
            end
        end
        if ind ~= 0
            com = str2double(coms{i}(4:end));
            if com > 9
                length = 8;
            else
                length = 7;
            end
            devices{i,1} = out{ind}(27:end-length); %#ok<AGROW>
            devices{i,2} = com; %#ok<AGROW> Loop size is always
small
        end

    end
catch
    devices{1,1}=['No Connection'];
    devices{1,2}=[' '];
end

% --- Executes on button press in pushbutton3.
function pushbutton3_Callback(hObject, eventdata, handles)
% hObject    handle to pushbutton3 (see GCBO)
% eventdata  reserved - to be defined in a future version of MATLAB
% handles    structure with handles and user data (see GUIDATA)
handles.serialports=IDSerialComs;
```

```
set(handles.popupmenu2,'String',[]);
[m,n]=size(handles.serialports);
if m==0
    handles.names{1}=['No SERIALCOMM'];
else
    for i= 1: m
        handles.names{i}=[handles.serialports{i,1},'
COM',num2str(handles.serialports{i,2})];
    end
end
set(handles.popupmenu2,'String',handles.names);


function datetimer(handles)
    text=datestr(now,'mm/dd/yyyy - HH:MM:ss');
    set(handles.datetime,'String',text);
```

Gui_mainfcn.m

```
function varargout = gui_mainfcn(gui_State, varargin)
% GUI_MAINFCN Support function for creation and callback dispatch
of GUIDE GUIs.
%   GUI_MAINFCN is called from inside MATLAB code files generated
by GUIDE to handle
%   GUI creation, layout, and callback dispatch.
%
%   See also: GUIDE.


%   GUI_MAINFCN provides these command line APIs for dealing with
GUIs
%
%      UNTITLED, by itself, creates a new UNTITLED or raises the
existing
%      singleton*.
%
```

```
%      H = UNTITLED returns the handle to a new UNTITLED or the
handle to
%      the existing singleton*.
%
%      UNTITLED('CALLBACK',hObject,eventData,handles,...) calls the
local
%      function named CALLBACK in UNTITLED.M with the given input
arguments.
%
%      UNTITLED('Property','Value',...) creates a new UNTITLED or
raises the
%      existing singleton*.  Starting from the left, property value
pairs
%      are
%      applied to the GUI before untitled_OpeningFunction gets
called.  An
%      unrecognized property name or invalid value makes property
application
%      stop.  All inputs are passed to untitled_OpeningFcn via
varargin.
%
%      *See GUI Options on GUIDE's Tools menu.  Choose "GUI allows
only one
%      instance to run (singleton)".


%   Copyright 1984-2015 The MathWorks, Inc.


gui_StateFields =  {'gui_Name'
    'gui_Singleton'
    'gui_OpeningFcn'
    'gui_OutputFcn'
    'gui_LayoutFcn'
    'gui_Callback'};
gui_Mfile = '';
for i=1:length(gui_StateFields)
    if ~isfield(gui_State, gui_StateFields{i})
```

```
        error(message('MATLAB:guide:StateFieldNotFound',
gui_StateFields{ i }, gui_Mfile));
    elseif isequal(gui_StateFields{i}, 'gui_Name')
        gui_Mfile = [gui_State.(gui_StateFields{i}), '.m'];
    end
end


numargin = length(varargin);


if numargin == 0
    % UNTITLED
    % create the GUI only if we are not in the process of loading
it
    % already
    gui_Create = true;
elseif local_isInvokeActiveXCallback(gui_State, varargin{:})
    % UNTITLED(ACTIVEX,...)
    vin{1} = gui_State.gui_Name;
    vin{2} = [get(varargin{1}.Peer, 'Tag'), '_', varargin{end}];
    vin{3} = varargin{1};
    vin{4} = varargin{end-1};
    vin{5} = guidata(varargin{1}.Peer);
    feval(vin{:});
    return;
elseif local_isInvokeHGCallback(gui_State, varargin{:})
    % UNTITLED('CALLBACK',hObject,eventData,handles,...)
    gui_Create = false;
else
    % UNTITLED(...)
    % create the GUI and hand varargin to the openingfcn
    gui_Create = true;
end
```

```
if ~gui_Create
    % In design time, we need to mark all components possibly
created in
    % the coming callback evaluation as non-serializable. This way,
they
    % will not be brought into GUIDE and not be saved in the figure
file
    % when running/saving the GUI from GUIDE.
    designEval = false;
    if (numargin>1 && ishghandle(varargin{2}))
        fig = varargin{2};
        while ~isempty(fig) && ~ishghandle(fig,'figure')
            fig = get(fig,'parent');
        end

        designEval = isappdata(0,'CreatingGUIDEFigure') ||
(isscalar(fig)&&isprop(fig,'GUIDEFigure'));
    end

    if designEval
        beforeChildren = findall(fig);
    end

    % evaluate the callback now
    varargin{1} = gui_State.gui_Callback;
    if nargout
        [varargout{1:nargout}] = feval(varargin{:});
    else
        feval(varargin{:});
    end

    % Set serializable of objects created in the above callback to
off in
    % design time. Need to check whether figure handle is still
valid in
```

```
    % case the figure is deleted during the callback dispatching.
    if designEval && ishghandle(fig)
        set(setdiff(findall(fig),beforeChildren),
'Serializable','off');
    end
else
    if gui_State.gui_Singleton
        gui_SingletonOpt = 'reuse';
    else
        gui_SingletonOpt = 'new';
    end


    % Check user passing 'visible' P/V pair first so that its value
can be
    % used by oepnfig to prevent flickering
    gui_Visible = 'auto';
    gui_VisibleInput = '';
    for index=1:2:length(varargin)
        if length(varargin) == index || ~ischar(varargin{index})
            break;
        end


        % Recognize 'visible' P/V pair
        len1 = min(length('visible'),length(varargin{index}));
        len2 = min(length('off'),length(varargin{index+1}));
        if ischar(varargin{index+1}) &&
strncmpi(varargin{index},'visible',len1) && len2 > 1
            if strncmpi(varargin{index+1},'off',len2)
                gui_Visible = 'invisible';
                gui_VisibleInput = 'off';
            elseif strncmpi(varargin{index+1},'on',len2)
                gui_Visible = 'visible';
                gui_VisibleInput = 'on';
            end
```

```
        end
    end


    % Open fig file with stored settings.  Note: This executes all
component
    % specific CreateFunctions with an empty HANDLES structure.



    % Do feval on layout code in m-file if it exists
    gui_Exported = ~isempty(gui_State.gui_LayoutFcn);
    % this application data is used to indicate the running mode of
a GUIDE
    % GUI to distinguish it from the design mode of the GUI in
GUIDE. it is
    % only used by actxproxy at this time.
    setappdata(0,genvarname(['OpenGuiWhenRunning_',
gui_State.gui_Name]),1);
    if gui_Exported
        gui_hFigure = feval(gui_State.gui_LayoutFcn,
gui_SingletonOpt);


        % make figure invisible here so that the visibility of
figure is
        % consistent in OpeningFcn in the exported GUI case
        if isempty(gui_VisibleInput)
            gui_VisibleInput = get(gui_hFigure,'Visible');
        end
        set(gui_hFigure,'Visible','off')


        % openfig (called by local_openfig below) does this for
guis without
        % the LayoutFcn. Be sure to do it here so guis show up on
screen.
        movegui(gui_hFigure,'onscreen');
    else
```

```
        gui_hFigure = local_openfig(gui_State.gui_Name,
gui_SingletonOpt, gui_Visible);

        % If the figure has InGUIInitialization it was not
completely created

        % on the last pass.  Delete this handle and try again.

        if isappdata(gui_hFigure, 'InGUIInitialization')

            delete(gui_hFigure);

            gui_hFigure = local_openfig(gui_State.gui_Name,
gui_SingletonOpt, gui_Visible);

        end

    end

    if isappdata(0, genvarname(['OpenGuiWhenRunning_',
gui_State.gui_Name]))

        rmappdata(0,genvarname(['OpenGuiWhenRunning_',
gui_State.gui_Name]));

    end


    % Set flag to indicate starting GUI initialization

    setappdata(gui_hFigure,'InGUIInitialization',1);


    % Fetch GUIDE Application options

    gui_Options = getappdata(gui_hFigure,'GUIDEOptions');

    % Singleton setting in the GUI MATLAB code file takes priority
if different

    gui_Options.singleton = gui_State.gui_Singleton;


    if ~isappdata(gui_hFigure,'GUIOnScreen')

        % Adjust background color

        if gui_Options.syscolorfig

            set(gui_hFigure,'Color',
get(0,'DefaultUicontrolBackgroundColor'));

        end


        % Generate HANDLES structure and store with GUIDATA. If
there is
```

```
        % user set GUI data already, keep that also.
        data = guidata(gui_hFigure);
        handles = guihandles(gui_hFigure);
        if ~isempty(handles)
            if isempty(data)
                data = handles;
            else
                names = fieldnames(handles);
                for k=1:length(names)
                    data.(char(names(k)))=handles.(char(names(k)));
                end
            end
        end
        guidata(gui_hFigure, data);
    end

    % Apply input P/V pairs other than 'visible'
    for index=1:2:length(varargin)
        if length(varargin) == index || ~ischar(varargin{index})
            break;
        end

        len1 = min(length('visible'),length(varargin{index}));
        if ~strncmpi(varargin{index},'visible',len1)
            try set(gui_hFigure, varargin{index},
varargin{index+1}), catch break, end
        end
    end

    % If handle visibility is set to 'callback', turn it on until
finished
    % with OpeningFcn
    gui_HandleVisibility = get(gui_hFigure,'HandleVisibility');
```

```
    if strcmp(gui_HandleVisibility, 'callback')
        set(gui_hFigure,'HandleVisibility', 'on');
    end


    feval(gui_State.gui_OpeningFcn, gui_hFigure, [],
guidata(gui_hFigure), varargin{:});


    if isscalar(gui_hFigure) && ishghandle(gui_hFigure)
        % Handle the default callbacks of predefined toolbar tools
in this
        % GUI, if any

guidemfile('restoreToolbarToolPredefinedCallback',gui_hFigure);


        % Update handle visibility
        set(gui_hFigure,'HandleVisibility', gui_HandleVisibility);


        % Call openfig again to pick up the saved visibility or
apply the
        % one passed in from the P/V pairs
        if ~gui_Exported
            gui_hFigure = local_openfig(gui_State.gui_Name,
'reuse',gui_Visible);
        elseif ~isempty(gui_VisibleInput)
            set(gui_hFigure,'Visible',gui_VisibleInput);
        end
        if strcmpi(get(gui_hFigure, 'Visible'), 'on')
            figure(gui_hFigure);


            if gui_Options.singleton
                setappdata(gui_hFigure,'GUIOnScreen', 1);
            end
        end
```

```
        % Done with GUI initialization
        if isappdata(gui_hFigure,'InGUIInitialization')
            rmappdata(gui_hFigure,'InGUIInitialization');
        end

        % If handle visibility is set to 'callback', turn it on
until
        % finished with OutputFcn
        gui_HandleVisibility = get(gui_hFigure,'HandleVisibility');
        if strcmp(gui_HandleVisibility, 'callback')
            set(gui_hFigure,'HandleVisibility', 'on');
        end
        gui_Handles = guidata(gui_hFigure);
    else
        gui_Handles = [];
    end

    if nargout
        [varargout{1:nargout}] = feval(gui_State.gui_OutputFcn,
gui_hFigure, [], gui_Handles);
    else
        feval(gui_State.gui_OutputFcn, gui_hFigure, [],
gui_Handles);
    end

    if isscalar(gui_hFigure) && ishghandle(gui_hFigure)
        set(gui_hFigure,'HandleVisibility', gui_HandleVisibility);
    end
end


function gui_hFigure = local_openfig(name, singleton, visible)


% openfig with three arguments was new from R13. Try to call that
first, if
```

```
% failed, try the old openfig.
if nargin('openfig') == 2
    % OPENFIG did not accept 3rd input argument until R13,
    % toggle default figure visible to prevent the figure
    % from showing up too soon.
    gui_OldDefaultVisible = get(0,'defaultFigureVisible');
    set(0,'defaultFigureVisible','off');
    gui_hFigure = matlab.hg.internal.openfigLegacy(name,
singleton);
    set(0,'defaultFigureVisible',gui_OldDefaultVisible);
else
    % Call version of openfig that accepts 'auto' option"
    gui_hFigure = matlab.hg.internal.openfigLegacy(name, singleton,
visible);
%     %workaround for CreateFcn not called to create ActiveX
%
peers=findobj(findall(allchild(gui_hFigure)),'type','uicontrol','st
yle','text');
%         for i=1:length(peers)
%             if isappdata(peers(i),'Control')
%                 actxproxy(peers(i));
%             end
%         end
end


function result = local_isInvokeActiveXCallback(gui_State,
varargin)


try
    result = ispc && iscom(varargin{1}) ...
             && isequal(varargin{1},gcbo);
catch
    result = false;
end
```

```
function result = local_isInvokeHGCallback(gui_State, varargin)


try
    fhandle = functions(gui_State.gui_Callback);
    result = ~isempty(findstr(gui_State.gui_Name,fhandle.file)) ||
...
             (ischar(varargin{1}) ...
             && isequal(ishghandle(varargin{2}), 1) ...
             && (~isempty(strfind(varargin{1},[get(varargin{2},
'Tag'), '_'])) || ...
                ~isempty(strfind(varargin{1}, '_CreateFcn'))) );
catch
    result = false;
end
```

ARDUINO code

```
/* Pump Regulator
  by: Ata Dönmez
*/


// Clockwise and counter-clockwise definitions.
// Depending on how you wired your motors, you may need to swap.
int num = 0;
int mode = 0;
int rat = 0;


#define FORWARD  0
#define REVERSE 1
```

```
// Motor definitions to make life easier:
#define MOTOR_A 0
#define MOTOR_B 1

// Pin Assignments //
//Default pins:
#define DIRA 2 // Direction control for motor A
#define PWMA 3  // PWM control (speed) for motor A
#define DIRB 4 // Direction control for motor B
#define PWMB 11 // PWM control (speed) for motor B

////Alternate pins:
//#define DIRA 8 // Direction control for motor A
//#define PWMA 9 // PWM control (speed) for motor A
//#define DIRB 7 // Direction control for motor B
//#define PWMB 10 // PWM control (speed) for motor B


void setup()
{
  setupArdumoto(); // Set all pins as outputs
}

char buf[3];
unsigned int i = 0;

void loop()
{
```

```
  if (Serial.available() > 0) {
    Serial.setTimeout(10);

    int len = Serial.readBytes(buf, 8);
    //incomingByte = Serial.read();
    //    //stream.readBytes(buffer, length)
    num = atoi(buf);
    if (num > 255) // saturate
      num = 255;
    if (num < 0)
      num = 0;
    //Serial.println(num);
    if (num == 0)
    {
      driveArdumoto(MOTOR_A, FORWARD, 0);
    }
    else
    {
      driveArdumoto(MOTOR_A, FORWARD, num); // Set motor A to REVERSE
at max
    }


  }
  //for (count=1;count<len;count++
  buf[0] = 0; buf[1] = 0; buf[2] = 0;
}


//}
```

```
// driveArdumoto drives 'motor' in 'dir' direction at 'spd' speed
void driveArdumoto(byte motor, byte dir, byte spd)
{
 if (spd > 0)
 {
  //Serial.println("HIGH");
  if (motor == MOTOR_A)
  {
   digitalWrite(DIRA, dir);
   analogWrite(PWMA, spd);

  }
  else if (motor == MOTOR_B)
  {
   digitalWrite(DIRB, dir);
   analogWrite(PWMB, spd);
  }
 }
 else
 {
  //Serial.println("LOW");
  digitalWrite(PWMA, LOW);
  digitalWrite(PWMB, LOW);
  digitalWrite(DIRA, LOW);
  digitalWrite(DIRB, LOW);
 }
}

// stopArdumoto makes a motor stop
```

```
void stopArdumoto(byte motor)
{
  driveArdumoto(motor, 0, 0);
}

// setupArdumoto initialize all pins
void setupArdumoto()
{
  Serial.begin(9600);
  // All pins should be setup as outputs:
  pinMode(PWMA, OUTPUT);
  pinMode(PWMB, OUTPUT);
  pinMode(DIRA, OUTPUT);
  pinMode(DIRB, OUTPUT);

  // Initialize all pins as low:
  digitalWrite(PWMA, LOW);
  digitalWrite(PWMB, LOW);
  digitalWrite(DIRA, LOW);
  digitalWrite(DIRB, LOW);
}
```

B. Calculation of d_{v10}, d_{v50} and d_{v90} Values From Frequency and Cumulative Curves

Malvern Mastersizer 3000 uses laser diffraction technique while performing the size analysis. Laser diffraction technique usually gives the results as volumetric size distribution curve. In Figure B.1, the volumetric size distribution is given for one of the experimental conditions which is when the dispersed phase is fed into the impeller zone and when the impeller shaft is positioned at e/T=0.2 and at an impeller tip speed of 2 m/s. In this thesis, d_{v10}, d_{v50} and d_{v90} diameter values were used to perform drop size distribution analysis. d_{v10}, d_{v50} and d_{v90} represent the maximum sample diameter below which 10%, 50% and 90% of the volume exists, respectively. d_{v50} is also known as median sample size by volume. d_{v10} and d_{v90} diameter values provide information about the extremes of the drop size distribution. These three diameter values were obtained from Malvern Mastersizer 3000. In order to mark the points where these diameter values correspond to in Figure B.1 or the volumetric size distribution curve, the volume density (%) values corresponding to these diameter values must be calculated. These volume density (%) values were found by interpolation. In Figure B.1, the green, blue and red arrows indicate the calculated d_{v10}, d_{v50} and d_{v90} diameter values and the scanned areas with green, blue and red lines show the area occupied by 10%, 50% and 90% of the sample volume, respectively.

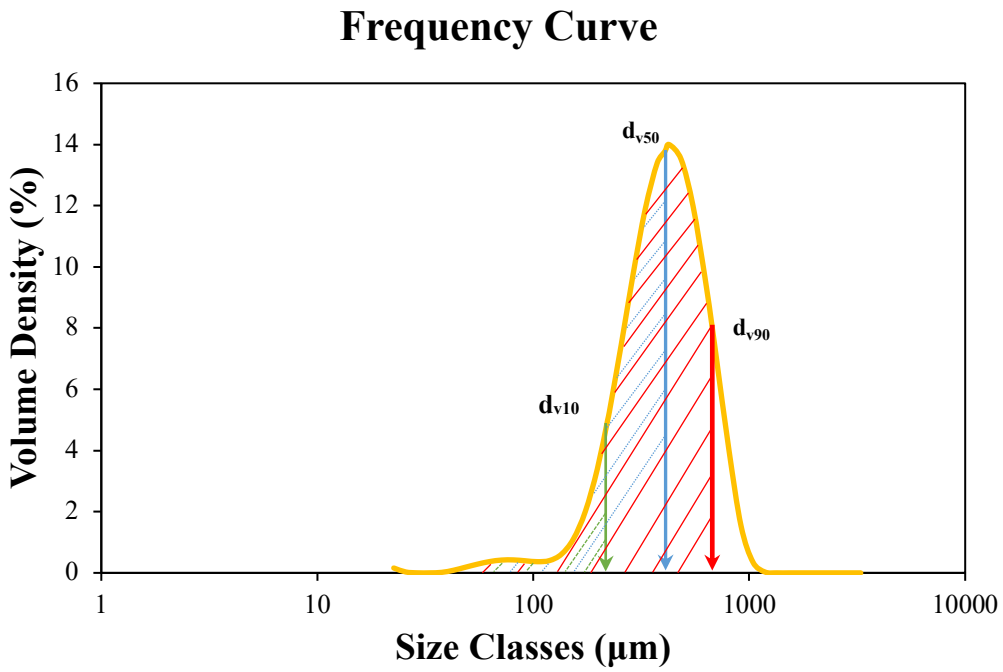

Figure B.1. Volumetric size distribution curve

It is important to monitor and examine these three diameter values in order to see if there is a considerable change in the width of distribution of drop size or polydispersity of a sample. The schematic representation of the width of distribution analysis on the volumetric size distribution curve is given in Figure B.2. For example, in this thesis, the effect of feeding conditions of the dispersed phase on the drop size and drop size distribution of Pickering emulsion is investigated. The width of distribution of drop size was determined by calculating the difference between d_{v90} and d_{v10} diameters for both feeding conditions of the dispersed phase. The difference between the d_{v90} and d_{v10} diameters gives us an information whether there are changes at the extremes of the width of distribution, which could be due to the presence of very small emulsion drops or the presence of very large emulsion drops. Figures in which these three diameter values are examined for different feeding conditions of the dispersed phase and different impeller shaft positions are given in Appendix C.

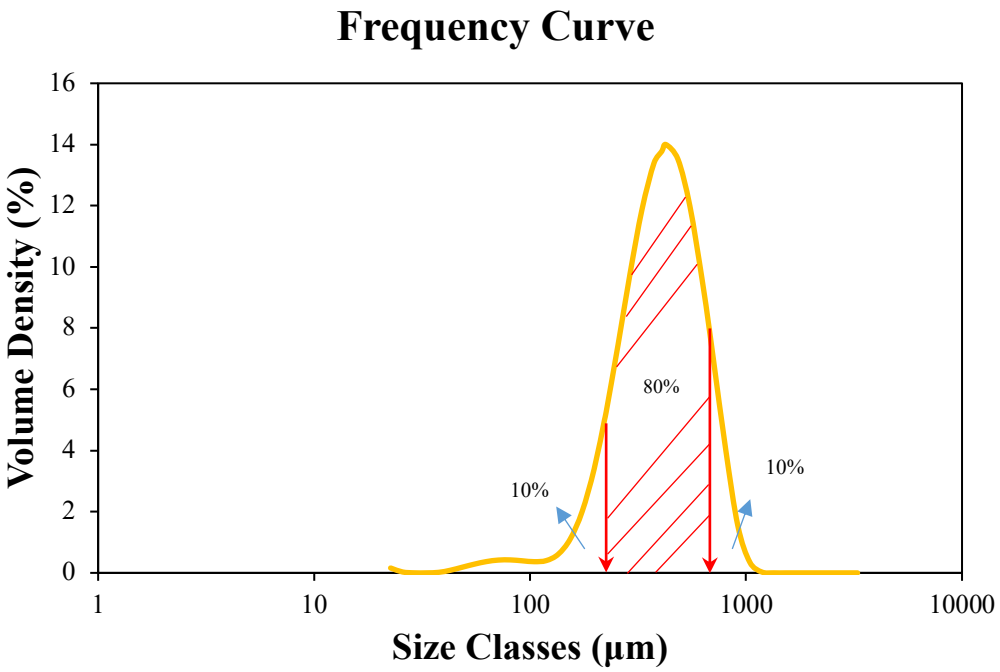

Figure B.2. Schematic representation of drop size distribution on volumetric size distribution curve

The d_{v10}, d_{v50} and d_{v90} values can also be found by using an undersize cumulative curve. The undersize cumulative curve of the same experimental condition can be obtained by using Malvern Mastersizer 3000 application software. The undersize cumulative curve for this same experimental condition is given in Figure B.3.

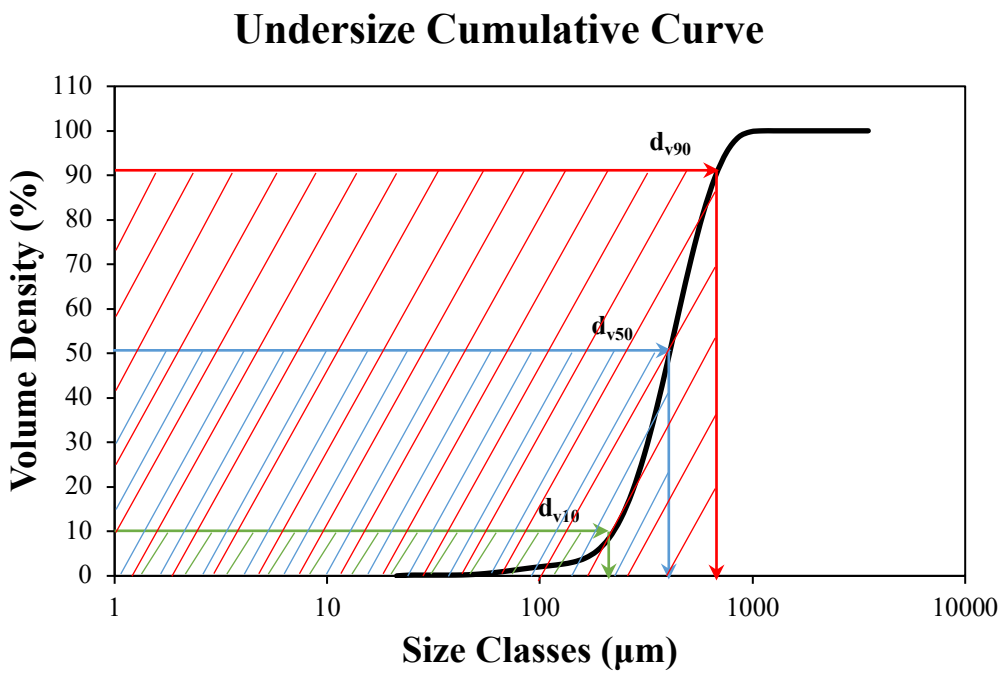

Figure B.3. Undersize cumulative curve

As can be seen from Figure B.3, d_{v10}, d_{v50} and d_{v90} values can be found by intersecting the corresponding volume density (%) with the size classes (µm). The values indicated by the green, blue, and red arrows in this curve are $\mathbf{d_{v10}}$, $\mathbf{d_{v50}}$, and $\mathbf{d_{v90}}$ and the scanned areas with green, blue and red lines show the area occupied by 10%, 50% and 90% of the sample volume, respectively.

Finally, it is worth noting that it is not possible to directly show the d_{v10}, d_{v50} and d_{v90} diameter values using the volumetric size distribution curve. In order to obtain these diameters, some calculations are required as mentioned above. However, d_{v10}, d_{v50} and d_{v90} can be shown directly using the undersize cumulative curve.

C. Effect of Feeding Condition and Position of the Impeller Shaft on the Width of Distribution

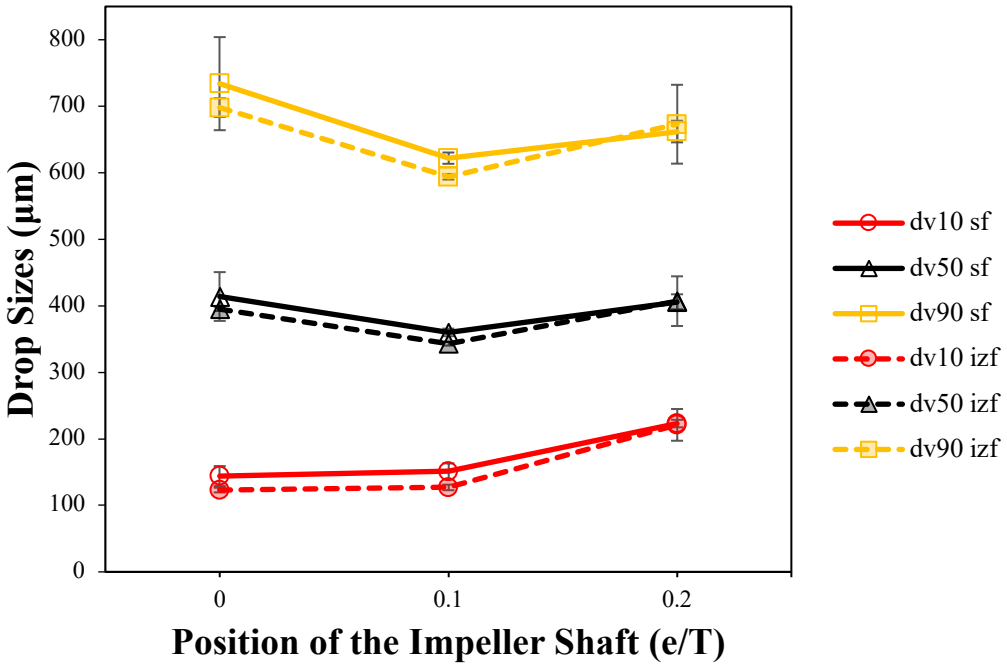

Figure C.1. The effect of feeding condition and positions of the impeller shaft on the width of distribution at an impeller tip speed of 1.85 m/s (sf and izf are the first letters of surface feeding and impeller zone feeding, respectively)

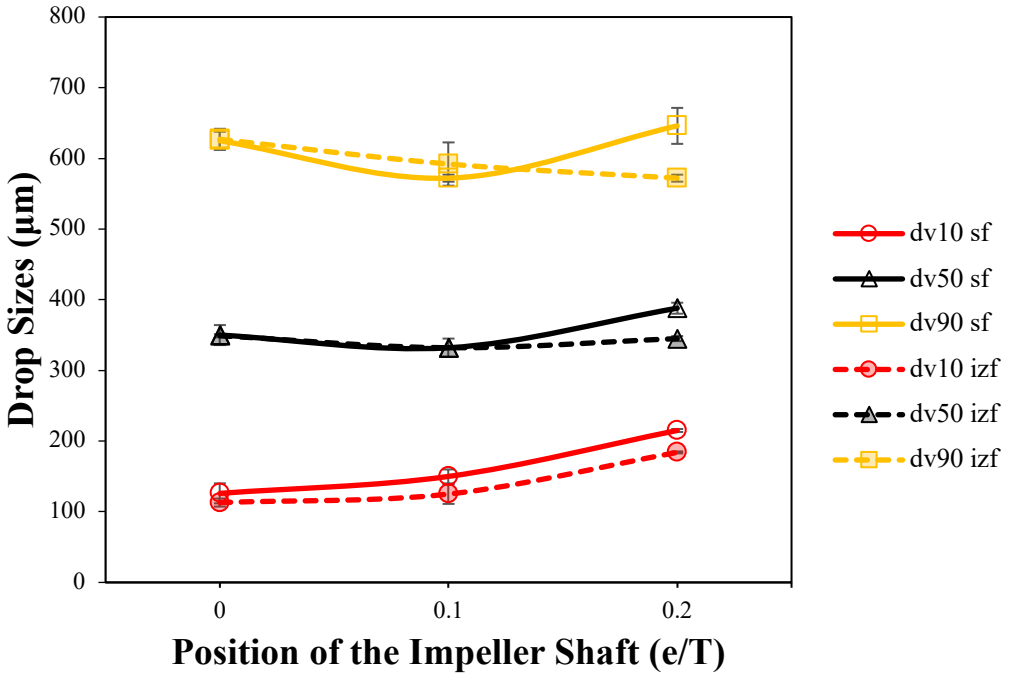

Figure C.2. The effect of feeding conditions and positions of the impeller on the width of distribution at an impeller tip speed of 2 m/s (sf and izf are the first letters of surface feeding and impeller zone feeding, respectively)

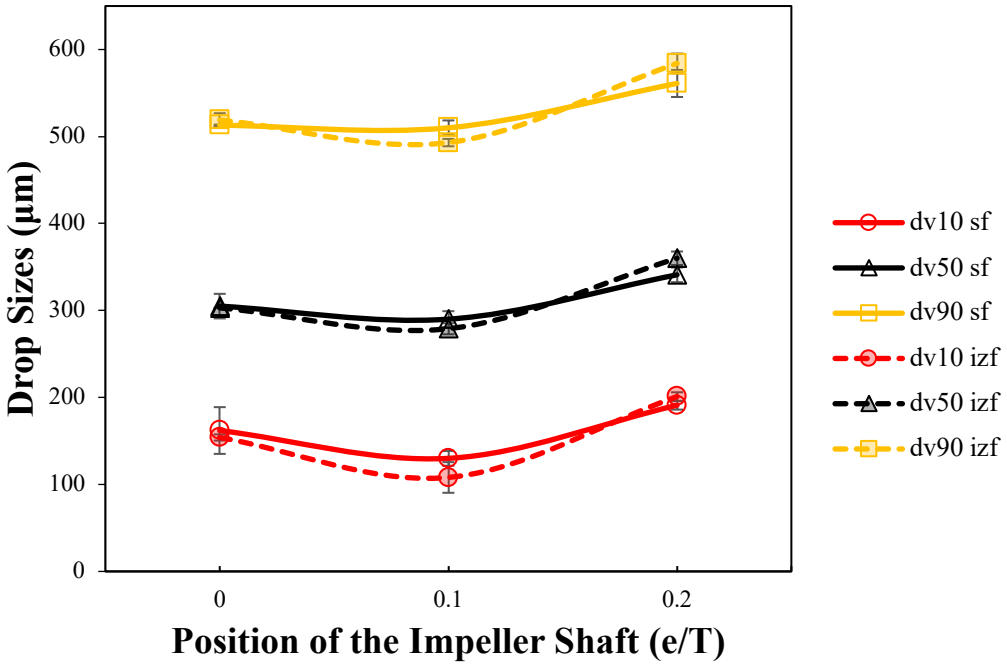

Figure C.3. The effect of feeding conditions and positions of the impeller on the width of distribution at an impeller tip speed of 2.32 m/s (sf and izf are the first letters of surface feeding and impeller zone feeding, respectively